The Messenger

No. 133 – September 2008

European ELT Phase B Progress
The Galactic Centre with VLT and APEX
VLTI of Active Galactic Nuclei
The Supernova Legacy Survey

Progress on the European Extremely Large Telescope

Jason Spyromilio, Fernando Comerón, Sandro D'Odorico, Markus Kissler-Patig
Roberto Gilmozzi
ESO

In December 2006 the ESO Council gave the go-ahead for the European Extremely Large Telescope (E-ELT) three-year Phase B study. The Baseline Reference Design (BRD) was presented to the ESO committees in 2006 and to the community at the Marseille meeting in December 2006. Phase B has been running for one and a half years and a progress report is presented covering science activities, telescope design, instrumentation, site selection and operations. The designs are maturing, in close synergy with industrial contracts, and the proposal for E-ELT construction is expected to be presented to the ESO Council in June 2010.

The decision by the ESO Council to fund the Phase B for the E-ELT at their meeting in December 2006, and the adopted baseline telescope design, were described in Gilmozzi & Spyromilio (2007). The meeting "Towards the European Extremely Large Telescope", which was held in Marseille immediately preceding the Council decision, was reported in the same issue of the Messenger (Hook, 2007; Monnet, 2007; Cuby, 2007). Now one and a half years later there has been much progress as well as evolution of the design of the telescope.

Science activities

Science activities for the E-ELT Phase B have now ramped up to full speed. Besides focussing on the Design Reference Mission (DRM), a small science office, under the guidance of and in close collaboration with the Science Working Group, is developing a Design Reference Science Plan (DRSP) and consolidating the top level requirements for the observatory. These activities are supported by the EU FP7 sponsored programme which has been funded (see Gilmozzi et al., 2008). Details about the science case, the science working group activities and the DRM can be found at *http://www.eso.org/sci/facilities/eelt/science*. A brief synopsis is given below.

The basic idea of the DRM is to be able to predict and monitor the ability of the telescope to effectively and efficiently address the challenges of the science cases. For this purpose, a number of key science cases proposed by the Science Working Group are being simulated in detail (see also Hook, 2007). For most science cases, simulations address key results to be achieved as a function telescope and instrument parameters. In some cases, the simulations will be performed end-to-end in order to provide additional feedback to the operations models.

A large amount of technical data is required for the simulations (such as atmospheric behaviour, telescope parameters and instrument models, as well as simulated adaptive optics point spread functions), and is made available to the public on the web pages under "Technical data for simulations" *(http://www.eso.org/sci/facilities/eelt/science/drm/tech_data/)*. A workshop was held in Garching on 20 and 21 May bringing together a number of the astronomers engaged in simulations for the DRM and/or instrument concept studies. The programme and presentations of this workshop can be found at *http://www.eso.org/sci/facilities/eelt/science/drm/workshop08/programme.html*.

While the DRM provides a detailed insight into the expected performance of the E-ELT, the DRSP is intended to explore the parameter space to be covered by the telescope and instruments. The DRSP will be a large collection of cases directly provided by the ESO community, and reflecting their interests. A web questionnaire is being made available from September 2008 on. This collection of cases will be analysed and will be used as one of the drivers for the telescope modes and instrument implementation plans.

Beyond the work on the science case, the E-ELT science office is currently consolidating the top level requirements for the observatory. Telescope and instrument requirements are being reviewed and justified in order to provide the necessary background for the decisions on the trade-offs to be made during the detailed design work on the telescope.

A number of workshops will be held in the near future to discuss the E-ELT science cases. In September, during the JENAM meeting in Vienna, there will be a major workshop "Science with the E-ELT" (see *http://www.eso.org/sci/facilities/eelt/science/meetings/jenam08/*). Two workshops are being prepared for next year. The first, in March 2009, is organised together with the ALMA, GMT and TMT projects (see announcement on page 65). The aim is to explore the synergies between ALMA and the up-coming giant optical and near-infrared telescopes. The second workshop (May 2009) will be dedicated to the DRM and DRSP work in the frame of the FP7 activities.

Telescope design

The design activities undertaken by industry as part of the Phase B, and their impact of the current version of the BRD, are described in the following sections. One significant evolution of the five-mirror design (see Gilmozzi & Spyromilio, 2007) has been the movement of the tertiary mirror from below the primary mirror to the same level. This change was made to improve the ventilation of the tertiary mirror. As a by-product the secondary mirror has become slightly smaller in diameter (now 6 m rather than 6.2 m). The adaptive quaternary mirror has increased slightly in diameter, thereby marginally improving its performance.

Industrial activities

Immediately after the approval by the ESO Council, a set of contracts were tendered to validate the BRD for the telescope and to explore the expertise in industry regarding the construction of such massive structures. The general policy has been to let two contracts to study a specific subsystem of the telescope, thus allowing different options to be explored whenever possible.

By May 2007 two contracts had been placed for the validation of the telescope main structure design as proposed by

ESO. The contracts included the study of the industrialisation of the concept, cost estimates and construction schedules. We encouraged the suppliers to consider variations on the design. Both these design contracts have now been concluded. The contractors considered variants on the ESO baseline and proposed alternatives that appear to perform better and are estimated to be cheaper to manufacture. The ESO design team has adopted these ideas and the new baseline telescope main structure appears significantly different to the original concept (see Gilmozzi & Spyromilio, 2007). Instead of four cradles supporting the primary mirror, only two are now seen as necessary to provide the required stiffness. By removing a significant fraction of the mass from below the telescope, the mount balances naturally, alleviating the necessity of significant additional mass in the upper parts of the telescope (see Figure 1). This change has increased the overall performance of the telescope and the first eigenfrequency of the structure is now around 2.6 Hz. The reduction in moving mass is also an overall cost saver, both in quantity of steel and in all the associated hardware.

The design for the telescope mount has been extensively analysed using Finite Element Models and fairly sophisticated control simulations (see Figure 2). Although the role of the mount may be simplified to “Keep the primary pointing at the right place on the sky, and the other mirrors at each other (sequentially)”, not only is this a non-trivial problem but the optimisation of the design can lead to significant cost savings in other subsystems. For example, the range of the actuators for the primary mirror is directly related to the extent to which the cell will deform as the telescope is inclined from the zenith towards the horizon.

Around the same time as the call for contracts for the telescope main structure, two contracts were placed for a preliminary design of the telescope dome. The companies that provided the best bids in response to the ESO tenders were new to telescope enclosure design, but brought their expertise in the design and construction of enormous buildings, and in particular sports stadia, to bear. The E-ELT dome will be of similar size to that of

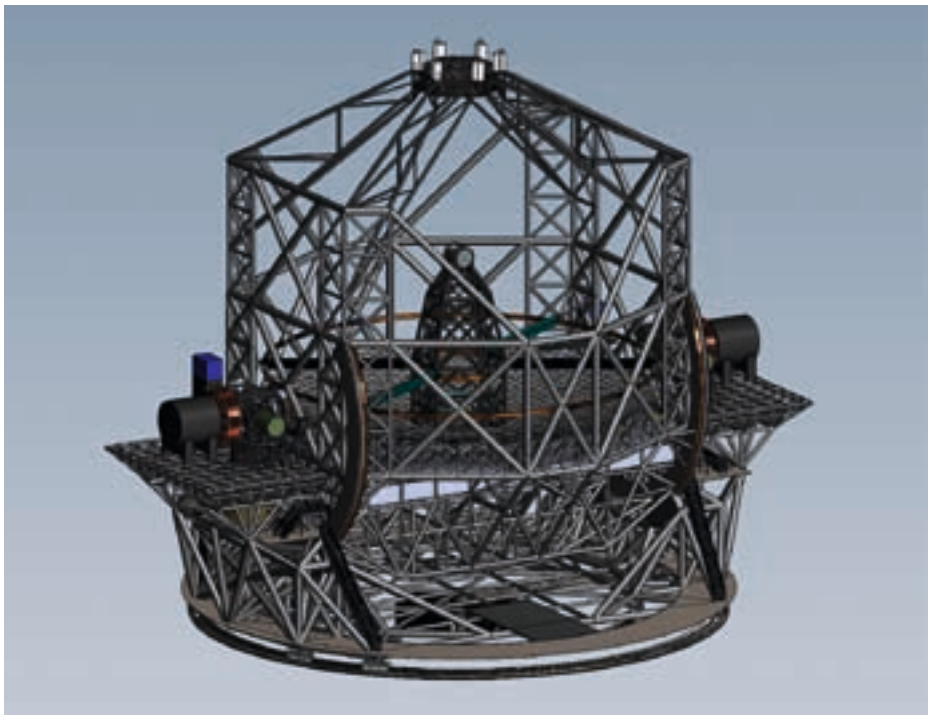

Figure 1 (above). A CAD rendering of the E-ELT Baseline Reference Design version 2 for the telescope and mount.

Figure 2 (below). A Finite Element Model of the E-ELT main structure is shown. The different coloured components encode different cross sections of the structural elements.

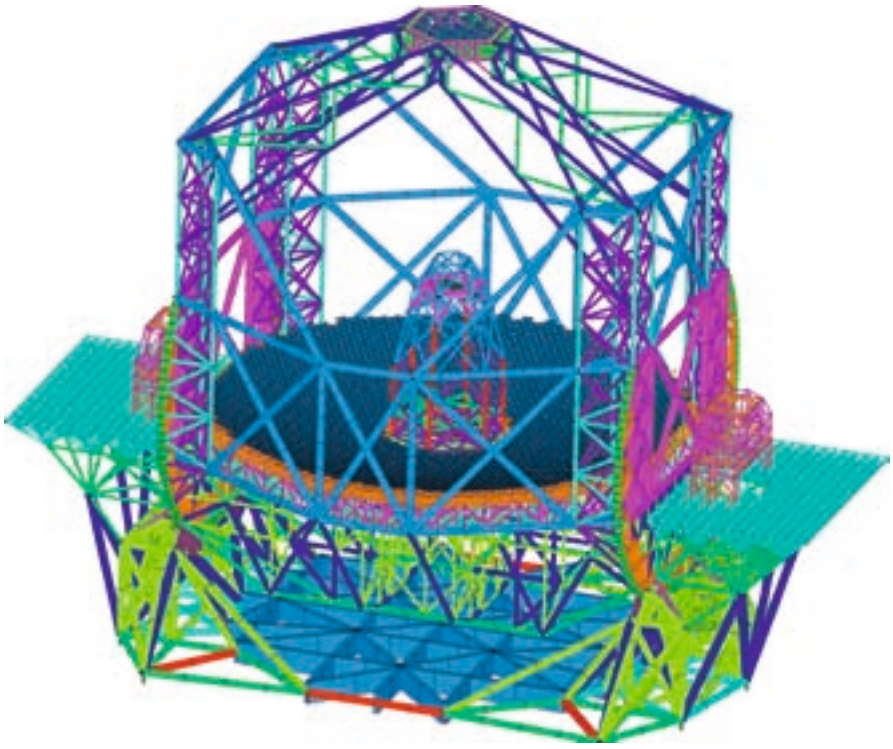

a football stadium, with a diameter at its base of order 100 m and a height of order 80 m. These contracts were particularly interesting to follow as the industrial expertise in this area is extensive, but also the requirements of a telescope dome are sometimes quite peculiar. Of the many challenges faced during the design of the dome, two stand out as having required ingenious solutions: the wind screen that shields the telescope from the effects of the wind; and the twenty-tonne crane that can access the entire volume of the dome. We are pleased to say that both designs proposed have elegant solutions for these two aspects. The two designs are similar to the extent that both assume a hemispherical dome but quite different in how the dome is supported and in the nature of the observing doors. One design proposes a single pair of large doors (see the image on the front cover), while the other proposes two sets of nested doors. Both suppliers have provided schedules for construction and the estimated costs for the dome. Figure 3 shows a cross-section through one of the E-ELT dome designs.

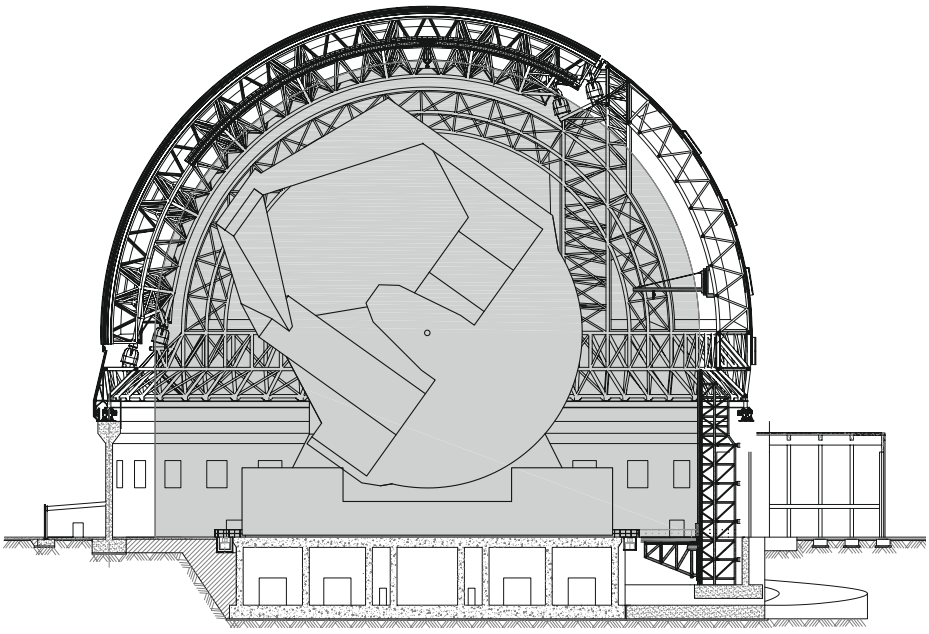

Figure 3 (above). A diametral cross section of one of the two concepts developed for the E-ELT dome.

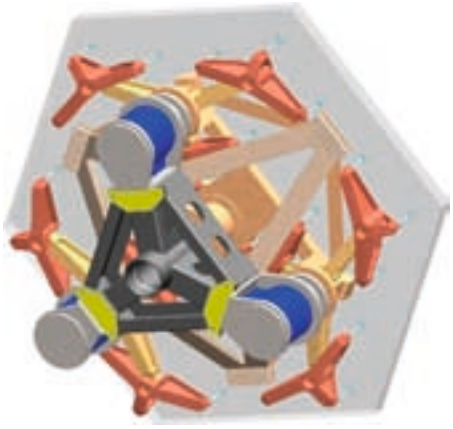

Figure 4 (left). A CAD figure of one of the mirror segment assemblies. The segment is shown on the 27 point wiffle tree; the three blue cylinders are the actuators for tip-tilt control.

Extensive investigation is being undertaken in the area of the impact of the wind on the telescope and the effect of the dome. Wind tunnel measurements have already started, computational fluid dynamical (CFD) simulations are ongoing and a campaign of fast sonic anemometer measurements was undertaken at Paranal.

A contract was placed in mid-2007 for the design of the primary mirror cell and the supporting elements. The support of the 984 1.45-m hexagonal mirror segments that form the primary mirror of the telescope is a critical component of the telescope design. The 50-mm thickness of the mirror segments is necessary to reduce the weight of the mirror. However, the thin segments are susceptible to deformation due to imperfections in their supports and the print-through of these supports onto the reflecting surface, which could limit the performance of the telescope. The mirror cell contractor analysed two types of support, one with 27 points and one with 18. The supporting principle is that the axial loads (i.e. in the direction through the segment) are taken with a wiffle tree structure, while the lateral loads are taken by a membrane implanted in the centre of the segment. The concept for the support structure has evolved significantly from the BRD. A moving frame carries the wiffle tree and the central membrane. The moving frame is moved in piston and tip-tilt by three actuators (see Figure 4). Additionally six motorised warping harnesses are foreseen to allow for the necessary corrections to the segment shape. A further restraint is designed to limit the clocking (i.e. rotation in the plane of the segment). The side of the segment not facing the sky is likely to be very complex as Figure 4 implies. The contract for the design has been concluded with ESO selecting the 27-point over the 18-point support. While the latter fulfilled the requirements for the extreme performance of the telescope, the former provided for a small but significant margin. In addition to the design of the segment support, we have also been testing the prototype edge sensors in a climatic chamber and continue to explore the actuator market.

In the third quarter of 2007, three large contracts for the adaptive optics system of the telescope were placed. Two of the contracts were for a preliminary design and prototyping of the adaptive quaternary mirror (M4; see Figure 5) and the third was for the design and 1:1 scale prototype of the electro-mechanical unit to support the fifth tip-tilt mirror (M5; see Figure 6) in the telescope optical train. All three contracts have gone through the

first preliminary design phase (Figures 5 and 6) and there is great interest in the prototyping activities. Real hardware is being built for these prototypes, including some very sophisticated actuators employing some of the biggest piezo-stacks currently available, tests of cooling circuits, etc. While the prime contractors leading the activities are well known companies in their areas of expertise, it is very reassuring that they have engaged other companies with differing expertise, such as in the areas of optics and/or complex opto-mechanical systems, to form powerful teams demonstrably able to address the challenges of the adaptive optics for the E-ELT.

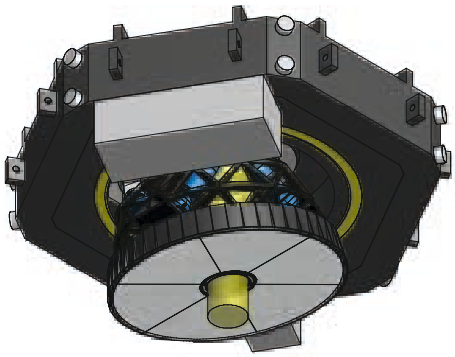

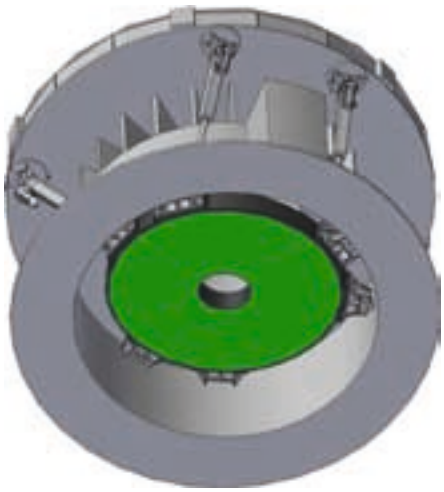

Figure 5 (above and right). Two preliminary designs for the M4 deformable mirror unit.

Two further large contracts were placed in late 2007. They entail the production of seven prototype segments for the primary mirror of the telescope. While seven segments, out of the 1148 that will need to be produced, may not sound very many, the contractors are required to demonstrate the industrialisation of the production process and test their mass production techniques on a variety of mirror substrates. Here again real hardware is being prepared for the manufacturing of the mirror segments. A new big polishing machine is under manufacture for the 1.45-m segments and the design of the test set-up used to determine the performance of the polishing is well advanced.

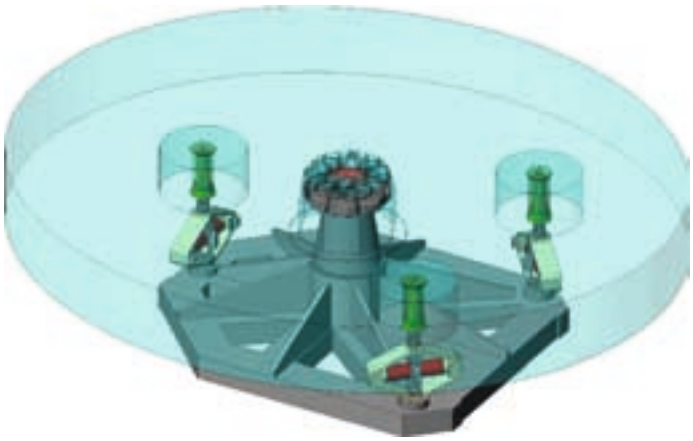

Figure 6 (left). The prototype design of the tip-tilt M5 mirror unit.

Figure 7 (below). CAD rendering of a Nasmyth platform populated with indicative instrument volumes and the prefocal unit.

In May 2008 a further significant contract was placed for the design study of the secondary mirror cell. The tendering process is already progressing well for the tertiary mirror cell and the pre-focal unit (adapter/rotator and M6 housing; see Figure 7). It is expected that contracts with industrial firms will be placed by the end of this year. A significant amount of work has been undertaken at ESO to understand the wavefront sensing needs of the telescope and to develop strategies for phasing the primary mirror, distributing the aberrations amongst the various mirrors, sensing lasers and natural guide stars. The progress has been significant and modern systems engineering processes and modelling languages have been employed to help.

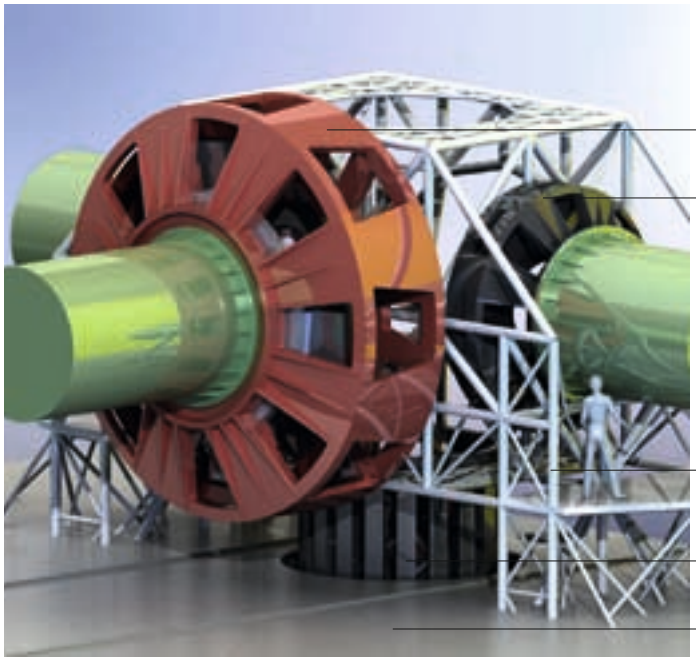

One significant modification, relative to the BRD version 1, in the area of the

adaptive optics instrumentation has been the merger of the two adapters at each Nasmyth focus into a single unit, and the reduction of the number of lasers necessary for the Ground Layer Adaptive Optics (GLAO) mode of the telescope from six to four (see Figure 8). The telescope will in any case be equipped with more than four lasers for the benefit of Laser Tomography Adaptive Optics (LTAO) and Multi-Conjugate Adaptive Optics (MCAO) instruments.

The effort in integrated modelling undertaken under the auspices of the FP6 study (see next section) has been further funded by the telescope project office. It is expected that great insight into the project will come through such efforts. Additionally many smaller, but no less significant, investigations are ongoing in areas such as the coating chambers for the mirrors, mirror segment replacement, general handling issues, etc. A detailed manpower estimate for technical operations is currently under review.

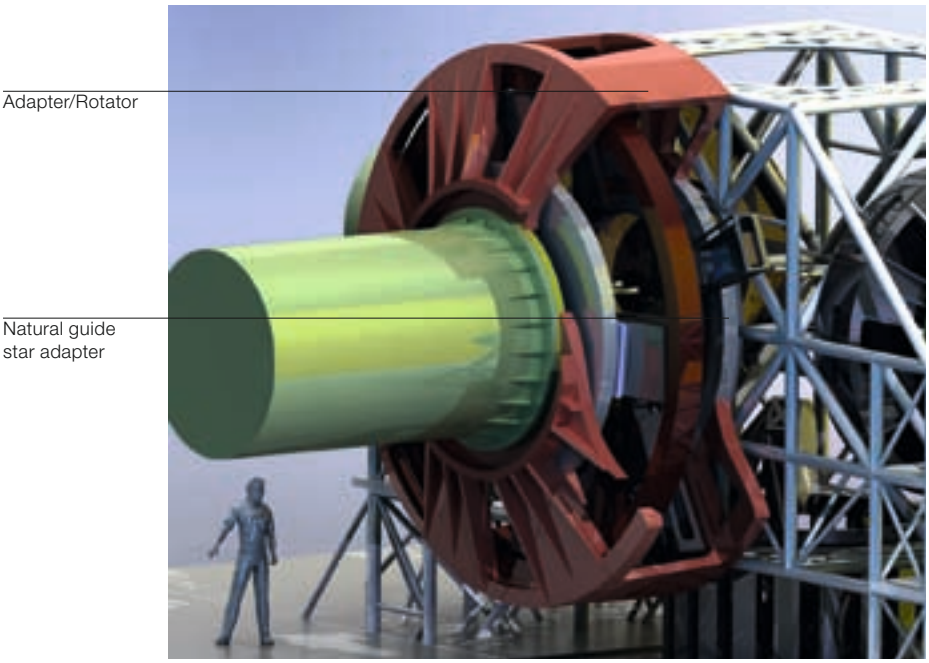

Figure 8 (above). Detail of the CAD model for the adaptor rotator housing for the Nasmyth focus showing the laser and natural guide star units.

Photo: H. H. Heyer, ESO

Figure 9. The ESO E-ELT team, arrayed behind a model of the E-ELT dome, during the Baseline Reference Design meeting held from 29 February to 4 March 2008 at ESO Headquarters.

Activities undertaken within the FP6 ELT Design Study

There has been good progress in the areas of study funded through the broad consortium of institutes and industrial partners within the EU FP6 ELT Design Study programme (see Gilmozzi & Spyromilio, 2007). The edge sensor work is providing excellent results. Testing of the inductive edge sensors in a climatic chamber is being undertaken and they are performing remarkably well. The actuators which have been developed are being produced for the Wind Evaluation Breadboard of the primary mirror segments, an activity that will begin at the end of the year.

Consolidation of the Phase B activities

With so many industrial studies continuing in parallel and together with the in-house work on a broad range of topics from interfaces, error budgets, alignment strategies, presetting sequences to mirror phasing plans and primary mirror segment exchanges, the project has established milestones that allow it to re-baseline the design in response to these inputs. The transition from BRD version 1 (i.e. that presented to the ESO Council and the committees and community at the end of 2006) to BRD version 2 took place at the end of February 2008.

The process of bringing together all the inputs generated a series of open issues that are being addressed in what we refer to as the 'consolidation phase'. We are progressing rapidly towards the baseline BRD version 3 that we expect to achieve by the end of this year. As the project advances we are also accreting more people from within ESO to work on various activities. Figure 9 shows the members of the team present at our BRD version 2 review, held in spring 2008.

Instrumentation

The E-ELT programme requires an early start on the instrumentation studies in order to confirm the scientific capabilities of the telescope, to identify those subsystems that need more research and development and to prove the feasibility of the instruments at an affordable cost and within the project schedule. In addition, the instrumentation studies at this phase of the project provide very useful feedback to the telescope design and the observatory infrastructure. An E-ELT Instrumentation Project Office has been established to work on the instrument studies and the telescope interface. A plan for instrument and post-focal adap-

Table 1. Instrument and AO Module Studies (as of August 2008).

Name	Instrument Type	Principal Investigator Institutes
EAGLE	Wide Field, Multi IFU NIR Spectrograph with MOAO	Jean-Gabriel Cuby, Laboratoire d'Astrophysique de Marseille (LAM); Observatoire Paris-Meudon (OPM), Laboratoire d'Etudes des Galaxies, Etoiles, Physique et Instrumentation (GEPI) and Laboratoire d'Etudes Spatiales et d'Instrumentation en Astrophysique (LESIA); Office National d'Etudes et Recherches Aérospatiale (ONERA); United Kingdom Astronomy Technology Centre (UK ATC); Durham University, Centre for Advanced Instrumentation
CODEX	High Resolution, High Stability Visual Spectrograph	Luca Pasquini, ESO; Istituto Nazionale di Astrofisica (INAF), Osservatori Trieste and Brera; Instituto de Astrofísica de Canarias (IAC); Institute of Astronomy, University of Cambridge; Observatoire Astronomique de l'Université de Genève
MICADO	Diffraction-limited NIR Camera	Reinhard Genzel, Max-Planck Institute for Extraterrestrial Physics (MPE); Max-Planck Institute for Astronomy (MPIA); INAF, Osservatorio Padova; Nederlandse Onderzoekschool Voor Astronomie (NOVA), Universities of Leiden and Groningen
EPICS	Planet Imager and Spectrograph with Extreme Adaptive Optics	Markus Kasper, ESO; Laboratoire d'Astrophysique de l'Observatoire de Grenoble (LAOG); LESIA; Université de Nice; LAM; ONERA; University of Oxford; INAF, Osservatorio Padova; ETH Zürich; NOVA, Universities of Amsterdam and Utrecht
HARMONI	Single Field, Wide Band Spectrograph	Niranjan Thatte, University of Oxford; Centre de Recherche Astrophysique, Lyon; Departamento de Astrofísica Molecular e Infraroja, Consejo Superior de Investigaciones Científicas, Madrid; IAC; UK ATC
METIS	Mid-infrared Imager and Spectrograph with AO	Bernhard Brandl, NOVA, University of Leiden; MPIA; Commissariat à l'Energie Atomique (CEA) Saclay, Direction des Sciences de la Matière (DSM)/Institut de Recherches sur les lois Fondamentales de l'Univers (IRFU)/Service d'Astrophysique (SAp); Katholieke Universiteit Leuven; UK ATC
OPTIMOS	Wide Field Visual MOS	tbd Negotiations under way with a Consortium of Science and Technology Facilities Council, Rutherford Appleton Laboratory; University of Oxford; LAM; INAF, Istituto di Astrofisica Spaziale e Fisica Cosmica, Milan; GEPI; NOVA, University of Amsterdam; INAF, Osservatori Trieste and Brera; Niels Bohr Institute, University of Copenhagen
SIMPLE	High Spectral Resolution NIR Spectrograph	Livia Origlia, INAF, Osservatorio Bologna; INAF, Osservatorio Arcetri; INAF, Osservatorio Roma; Uppsala Astronomical Observatory; Thüringer Landessternwarte; Pontificia Universidad Católica de Chile
MAORY	Multi Conjugate AO module	Emiliano Diolaiti, INAF, Osservatorio Bologna; INAF, Osservatorio Arcetri; INAF, Osservatorio Padua; University of Bologna; ONERA
tbd	Laser Tomography AO Module	Thierry Fusco, ONERA; GEPI and LESIA

tive optics studies, to be carried out in collaboration with institutes in the ESO community, was presented to the ESO Council in June 2007. The plan identified six instrument concepts, two post-focal AO modules (MCAO and LTAO) of high priority and two other instruments to be chosen after an open call to the community for additional concepts. By September 2008, all ten instrument consortia have been formed and the studies are under way (see Table 1). In two cases the consortia are led by ESO, two have been set up with a direct negotiation with external institutes and all the others have been selected after an open Call for Proposals. In this study phase, the instrumentation activities are supported by 2.4 Million Euros (of which ~ 85 % is committed to support external institutes involved in the studies) and 30 ESO FTEs. On the community side, 36 institutes in 10 ESO member states and one in Chile are contributing to the studies as part of the 10 consortia, with a combined effort over two years of more than one hundred FTEs.

All the studies are structured in two phases. During the first, the scientific requirements are defined and a trade-off between different concepts is made. After a review of the results by ESO, in the second phase a detailed study of the chosen concepts, including cost and construction schedule, is carried out. All studies are expected to deliver a report and to go through a final review in late 2009 or early 2010.

On the basis of these studies, ESO will include in the E-ELT proposal for construction an outline of the first generation of instruments and a plan on how to proceed with their construction. In parallel to launching these studies, the opto-mechanical interfaces with the telescope have been defined and incorporated in a document that has been made available to the instrument consortia (see Figure 10). As the studies of the telescope subsystems are taking place in parallel with those of the instruments, very useful exchanges are continuing to take place during this phase between the telescope and instrument teams to arrive at a common set of requirements.

Site selection

Several sites, both in the Northern and Southern hemispheres, are being characterised, in large part with the help of the community through the FP6 initiative. A Site Selection Advisory Committee has been appointed by the Director General to help ESO towards a decision. It is foreseen that site selection will occur at the end of 2009.

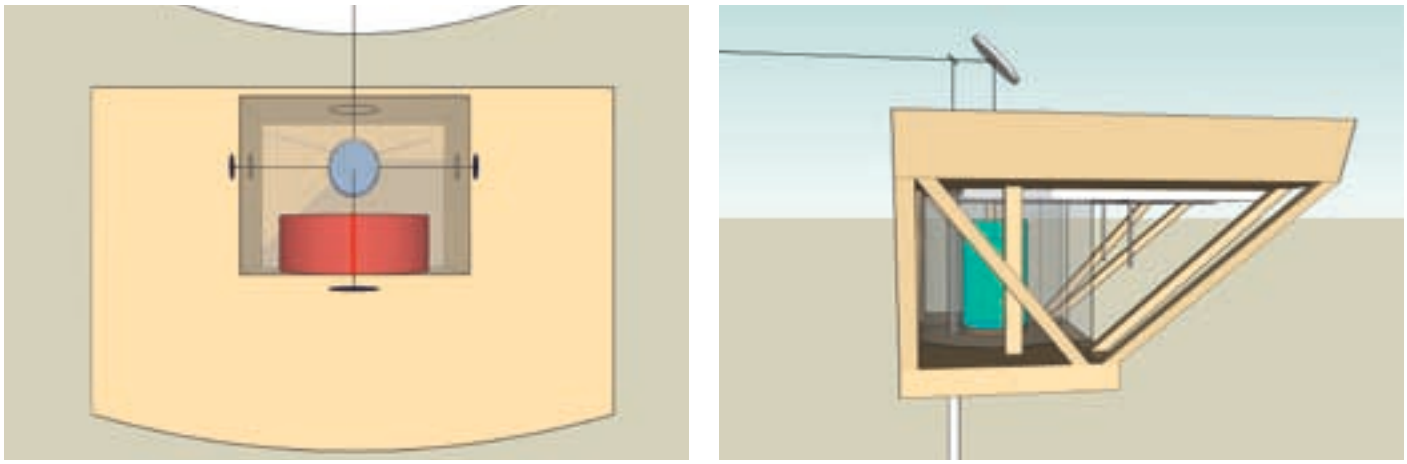

Figure 10. Figures taken from the E-ELT telescope interface document distributed to the instrument consortia, showing the layout of the Nasmyth platform with its four focal stations. **Left:** View from above (the dimensions of the platform are 24 by 15 m). **Right:** Side view showing the volume reserved for an instrument in the gravity-invariant focal station below the floor of the platform. This space is intended for large instruments that have to rotate during observations.

Operations

The science operations planning that is being developed during Phase B takes as a basis the current end-to-end model of the VLT, since the scientific requirements are similar to those currently encountered at the VLT. Specifically, as reflected in the DRM, the E-ELT will have to be able to execute a broad range of programmes using a variety of instruments and modes, many of them requiring performance of the telescope and instruments that can be achieved only under rare atmospheric conditions. The flexibility to schedule at short notice those programmes that can make best use of the prevailing conditions is thus a requirement for the efficient use of the facility.

The E-ELT design permits such flexibility. Several instruments, able to exploit different ranges of atmospheric conditions, will be either online or on standby at any given time. As specified in the top-level requirements and the telescope design, it will be possible to switch from one instrument to another with a moderate overhead of a few minutes, including the set-up of the post-focal adaptive optics module if needed. The telescope and dome will be able to preset from any position of the sky to any other, acquire the target field, and close the telescope adaptive optics loop on a similar timescale.

Service mode without real-time interaction between the users and the facility provides the greatest level of flexibility and is taken as the baseline observing mode for the E-ELT. However, it is anticipated that a fraction of programmes will require real-time interaction, allowing users to make decisions in the course of the observations at short notice. We expect to better quantify the fraction of time that the E-ELT will spend executing such classes of programmes as a result of the DRSP questionnaire described earlier. To satisfy this requirement, we are studying the implementation of new observing modes that allow users to interact with the facility in near-real time without being present in the control room, while retaining much of the scheduling flexibility necessary for the proper exploitation of the atmospheric conditions. Some specific implementation aspects of these modes have been studied in the FP6 activities on observatory operations.

We have produced estimates of the typical and peak data rates expected from each instrument based on their Phase A study specifications, in order to quantify the capabilities needed from the communications infrastructure between the observatory and the outside. E-ELT operations planning assumes that support to science operations will be provided by geographically distributed groups, who will be exchanging data on a short timescale over fast data distribution channels.

Preliminary estimates of the science operations staffing needs, in terms of number and qualifications, have been produced. The estimate is based on factors such as the breakdown of tasks to be carried out in end-to-end operations, the complexity of the systems being operated, the personnel working schedule, the location of each operations group, and the synergies with the operation of other facilities. It may be noted in this regard that significant cost savings in operations are achieved by having operations groups sharing the E-ELT support tasks and infrastructure with the support to other ESO facilities, particularly in the areas of user support, data processing, and archive operations.

Prospect

The E-ELT Phase B was funded for 57.2 Million Euro, including manpower. The majority of these funds have already been committed and technically the project is advancing well. We are on schedule to produce the construction proposal in time for the June 2010 ESO Council meeting.

References

Cuby, J.-G. 2007, The Messenger, 127, 25
Gilmozzi, R. & Spyromilio, J. 2007, The Messenger, 127, 11
Gilmozzi, R., Monnet, G. & Robinson, M. 2008, The Messenger, 132, 48
Hook, I. 2007, The Messenger, 127, 20
Monnet, G. 2007, The Messenger, 127, 24

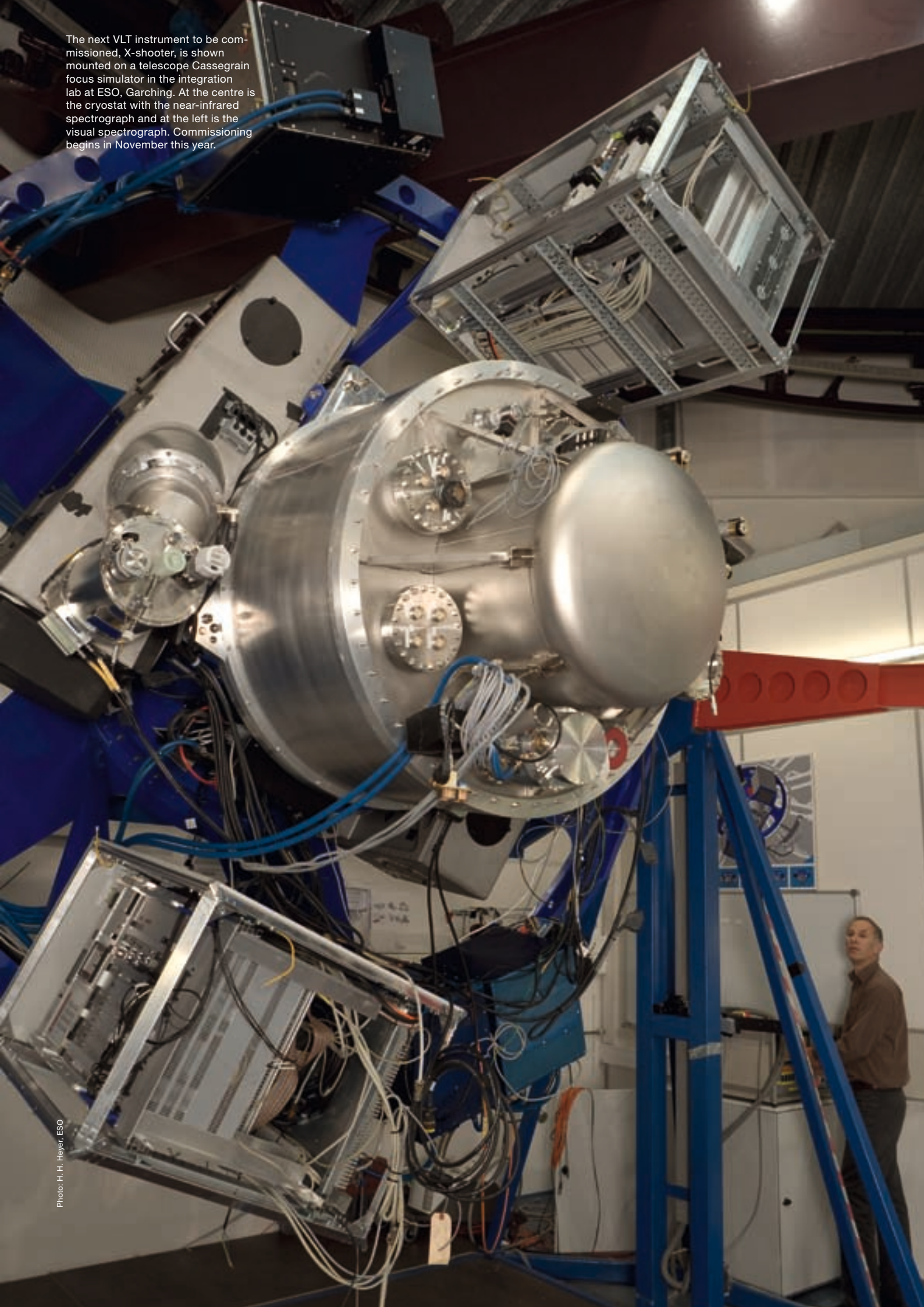

The next VLT instrument to be commissioned, X-shooter, is shown mounted on a telescope Cassegrain focus simulator in the integration lab at ESO, Garching. At the centre is the cryostat with the near-infrared spectrograph and at the left is the visual spectrograph. Commissioning begins in November this year.

Photo: H. H. Heyer, ESO

E-ELT and the Cosmic Expansion History – A Far Stretch?

Jochen Liske[1]
Andrea Grazian[2]
Eros Vanzella[3]
Miroslava Dessauges[4]
Matteo Viel[3,5]
Luca Pasquini[1]
Martin Haehnelt[5]
Stefano Cristiani[3]
Francesco Pepe[4]
Piercarlo Bonifacio[6,3]
François Bouchy[7,8]
Sandro D'Odorico[1]
Valentina D'Odorico[3]
Sergei Levshakov[9]
Christoph Lovis[4]
Michel Mayor[4]
Paolo Molaro[3]
Lauro Moscardini[10,11]
Michael Murphy[12]
Didier Queloz[4]
Stephane Udry[4]
Tommy Wiklind[13,14]
Shay Zucker[15]

[1] ESO
[2] INAF – Osservatorio Astronomico di Roma, Italy
[3] INAF – Osservatorio Astronomico di Trieste, Italy
[4] Observatoire de Genève, Switzerland
[5] Institute of Astronomy, University of Cambridge, United Kingdom
[6] Cosmological Impact of the First STars (CIFIST) Marie Curie Excellence Team, GEPI, Observatoire de Paris, Centre National de la Recherche Scientifique (CNRS), France
[7] Laboratoire d'Astrophysique de Marseille, France
[8] Observatoire de Haute-Provence, France
[9] Ioffe Physico-Technical Institute, St. Petersburg, Russian Federation
[10] Università di Bologna, Italy
[11] INFN – National Institute for Nuclear Physics, Sezione di Bologna, Italy
[12] Swinburne University of Technology, Melbourne, Australia
[13] Space Telescope Science Institute, Baltimore, USA
[14] Affiliated with the Space Sciences Department of the European Space Agency
[15] Tel Aviv University, Israel

The redshifts of all cosmologically distant sources are expected to experience a small, systematic drift as a function of time due to the evolution of the Universe's expansion rate. Here, we briefly review the motivation for measuring this effect and summarise our reasons for believing that the E-ELT will be the first telescope to detect it.

Accelerated expansion

1998 was a remarkable year for astronomy. Not only did the VLT see first light, but it was also the year in which two research groups independently announced a result that would profoundly change cosmology (again), if not all of physics: the measured distances to remote type Ia supernovae seemed to indicate that the expansion of the Universe was accelerating (Riess et al., 1998; Perlmutter et al., 1999)!

Since its discovery by Hubble in 1929 it had been assumed – more or less as a matter of course – that the universal expansion was forever being slowed down by the gravitational pull exerted by all of the matter in the Universe. Without any proof to the contrary, this was indeed a rather sensible assumption, because an accelerating expansion has quite fundamental consequences: it requires new physics.

Most of the models that have been put forward to explain the acceleration can be assigned to one of two categories. The first class of models assumes that General Relativity is indeed the correct theory of gravity, and accounts for the observed acceleration by postulating that, in the latter half of the Universe's history, its mass-energy was dominated by an unusual form of energy – unusual in that it has *negative* pressure. In its simplest incarnation this so-called dark energy is the cosmological constant Λ, but numerous other – some quite exotic – possibilities have been suggested (e.g. quintessence, phantom energy, Chaplygin gas), which all differ in the details of their equation of state and evolution. A feature that is common to all of these variants, however, is that it has so far proven very difficult to underpin any form of dark energy with a viable *physical theory*, i.e. to understand its origin and nature within the standard model of (particle) physics.

Instead of introducing a new mass-energy component, the models of the second type seek to explain the acceleration by replacing General Relativity with a different theory of gravity. Again, there are many ways in which the field equations can be modified in order to reproduce the late-time accelerated expansion, without spoiling the standard theory's success in explaining early structure formation. In this case the challenge is to physically motivate the more complicated structure of the field equations.

Whatever the correct explanation for the acceleration will turn out to be, it is clear that it will have far-reaching implications. That is why cosmologists have taken such an intense interest in exploring different ways of measuring the expansion history of the Universe.

Observing the expansion history

Observables that depend on the expansion history include distances and the linear growth of density perturbations; so SN Ia surveys, weak lensing (Heavens, 2003) and baryon acoustic oscillations (BAO) in the galaxy power spectrum (Seo & Eisenstein, 2003) are all generally considered to be excellent probes of the acceleration.

In practice, however, extracting information on the expansion history from weak lensing and BAO requires a prior on the spatial curvature, a detailed understanding of the linear growth of density perturbations and hence a specific cosmological model. Given the uncertain state of affairs regarding the source of the acceleration, these are conceptually undesirable features and the importance of taking a cosmographic, model-independent approach to determining the expansion history is evident. Using SN Ia to measure luminosity distances as a function of redshift is conceptually the simplest experiment and hence appears to be the most useful in this respect. The caveats are that distance is 'only' related to the expansion history through an integral over redshift and that one still requires a prior on spatial curvature.

Sandage (1962) first discussed an effect that suggests an extremely direct measurement of the expansion history. He showed that the evolution of the Hubble expansion causes the redshifts of distant objects partaking in the Hubble flow to change slowly with time. Just as the redshift, z, is in itself evidence of the expansion, so is the change in redshift ($\dot{z} = (1 + z)H_0 - H(z)$), evidence of its de- or acceleration between the epoch z and today, where H is the Hubble parameter and H_0 its present-day value. This equation implies that it is remarkably simple (at least in principle) to determine the expansion history: one simply has to monitor the redshifts of a number of cosmologically distant sources over several years.

This simple equation has two remarkable features. The first is the stunning simplicity of its derivation. For this equation to be valid all one needs to assume is that the Universe is homogeneous and isotropic on large scales, and that gravity can be described by a metric theory. That's it. One does not need to know or assume anything about the geometry of the Universe or the growth of structure. One does not even need to assume a specific theory of gravity. The redshift drift is an entirely direct and model-independent measure of the expansion history of the Universe which does not require any cosmological assumptions or priors whatsoever.

The other remarkable feature of the equation is that it involves observations of the *same* objects at *different* epochs (albeit separated only by a few years or decades). Other cosmological observations, such as those of SN Ia, weak lensing and BAO also probe different epochs but use different objects at each epoch. In other words, these observations seek to deduce the evolution of the expansion by mapping out our present-day past light-cone. In contrast, the redshift drift directly measures the evolution by comparing our past light-cones *at different times*. In this sense the redshift drift method is qualitatively different from all other cosmological observations, offering a truly independent and unique approach to the exploration of the expansion history of the Universe.

Measuring the redshift drift with E-ELT

The trouble with the redshift drift is that it is exceedingly small. From Figure 1 we see that at $z = 4$ the redshift drift is of the order of 10^{-9} or 6 cm/s per decade! Putting meaningful data points onto Figure 1 will clearly require an extremely stable and well-calibrated spectrograph as well as a lot of photons. Let us assume that the first requirement has been met, i.e. that we are in possession of a spectrograph capable of delivering radial velocity measurements that are only limited by photon-noise down to the cm/s level. In this best possible (but by no means unrealistic) scenario, how well can we expect the E-ELT to measure the redshift drift, and hence constrain the cosmic expansion history?

First of all, we need to define where we want to measure the redshift drift. There are several reasons to believe that the so-called Lyman-α forest is the most suitable target, as first suggested by Loeb (1998). These HI absorption lines are seen in the spectra of all QSOs and arise in the intervening intergalactic medium. Using hydrodynamical simulations we have explicitly shown that the peculiar motions of the gas responsible for the absorption are far too small to interfere with a redshift drift measurement (Liske et al., 2008). Similarly, other gas properties, such as the density, temperature or ionisation state, also evolve too slowly to cause any headaches. Furthermore, QSOs exist over a wide redshift range, they are the brightest objects at any redshift, and each QSO spectrum displays hundreds of lines. These are all very desirable features.

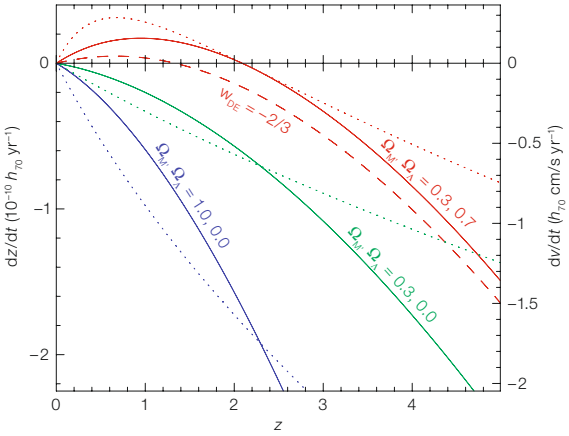

Figure 1. The solid lines and left axis show the redshift drift $\dot{z}$ as a function of redshift for standard relativistic cosmology and various combinations of Ω_M and Ω_Λ as indicated. The dotted lines and right axis show the same in velocity units. The dashed line shows $\dot{z}$ for the case of an alternative dark energy model with a different equation of state parameter w_{DE} (and Ω_M, Ω_{DE} = 0.3, 0.7).

The next question is how the properties of the Lyman-α forest (the number and sharpness of the absorption features), and the signal-to-noise (S/N) at which it is recorded, translate to the accuracy, σ_v, with which one can determine a radial velocity shift. In order to obtain this translation we have performed extensive Monte Carlo simulations of Lyman-α forest spectra. Mindful of the forest's evolution with redshift, we have derived a quantitative relation between the σ_v of the Lyman-α forest on the one hand, and the spectral S/N and the background QSO's redshift on the other hand (Liske et al., 2008).

Now in a photon-noise limited experiment the S/N only depends on the flux density of the source, the size of the telescope (D), the total combined telescope/instrument throughput (ε) and the integration time (t_{int}). Unfortunately, the photon flux from QSOs is not a free parameter that can be varied at will. In Figure 2 we show the fluxes and redshifts of all known high-z QSOs. Assuming values for D, ε and t_{int} we can calculate the expected S/N for any given N_{phot}. Combining this with a given z_{QSO} and using the relation derived above, we can calculate the value of σ_v that would be achieved if *all* of the time t_{int} were invested into observing a single QSO with the given values of N_{phot} and z_{QSO}. The background colour image and solid contours in Figure 2 show the result of this calculation, where we have assumed D = 42 m, ε = 0.25, and t_{int} = 2 000 h. Note that t_{int} denotes the total integration time, summed over all epochs.

We can see that, although challenging, a reasonable measurement of the redshift drift appears to be possible with a 42-m telescope. The best object gives σ_v = 1.8 cm/s and there exist 18 QSOs that are bright enough and/or lie at a high enough redshift to put them at σ_v < 4 cm/s.

Figure 2 tells us which QSO delivers the best accuracy and is hence the most suitable for a redshift drift experiment. However, for many practical reasons it will be desirable to include more than just the best object in the experiment. Doing so comes at a penalty though: the more objects that are included into the experiment the worse the final result will be because some of the fixed amount of observing time will have to be redistributed from the 'best' object to the less suited ones.

The dependence of the full experiment's final, overall σ_v on the telescope diameter, system throughput, total integration time and number of QSOs is shown in Figure 3. We can see that an overall accuracy of 2–3 cm/s is well within reach of the E-ELT, even when 20 or so objects are targeted for the experiment. However, the figure also shows that for a 30-m telescope it would be very time consuming indeed to achieve an accuracy better than 3 cm/s.

To further illustrate what can be achieved we show in Figure 4 three different simulations of the redshift drift experiment. The blue dots show the results that can be expected from monitoring the 20 best QSOs over a 20-year period, investing a total of 4 000 h of observing time. By construction these points represent the most precise measurement of $\dot{z}$ that is possible with a set of 20 QSOs and the given set-up. However, since many of the selected QSOs lie near the redshift where $\dot{z}$ = 0 this experiment does not actually result in a positive detection of the effect. If we want to detect the effect with the highest possible significance we need to choose a different set of QSOs. The yellow squares show the result of selecting the 10 best QSOs according to this criterion.

However, neither of these datasets is particularly well suited to proving the existence of accelerated expansion, i.e. of a region where $\dot{z} > 0$. Ideally, this would be achieved by obtaining a $\dot{z}$ measurement at $z \approx 0.7$ – were it not for the atmosphere that restricts observations of the Lyman-α forest to $z > 1.7$. The best thing to do is to combine a measurement at the lowest possible redshift with a second measurement at the highest possible redshift, thereby gaining the best possible constraint on the slope of $\dot{z}(z)$. The brown triangles in Figure 4 show the result of a simulation using appropriately selected QSOs: clearly, given these data one could confidently conclude that $\dot{z}$ must turn positive at $z \approx 2$ for *any* reasonably well-behaved functional form of $\dot{z}(z)$, i.e. *regardless of the cosmological model*. Thus we find that a redshift drift experiment on

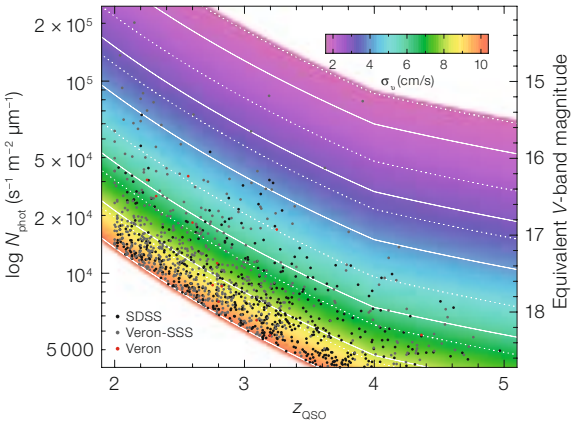

Figure 2. The dots show the known, bright, high-redshift QSO population as a function of redshift and estimated photon flux. The right-hand vertical axis shows the photon flux converted to a corresponding Johnson *V*-band magnitude. The background colour image and solid contours show the value of σ_v that can be achieved for a given photon flux and redshift, assuming D = 42 m, ε = 0.25, and t_{int} = 2 000 h. The contour levels are at σ_v = 2, 3, 4, 6, 8 and 10 cm/s. The dotted contours show the same as the solid ones, but for D = 35 m or, equivalently, for ε = 0.17 or t_{int} = 1389 h.

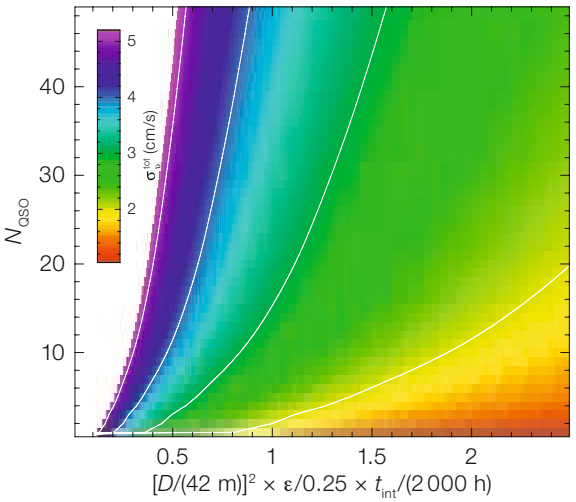

Figure 3. The colour image and the contours show the final, overall value of σ_v achieved by targeting the N_{QSO} best objects and by employing a given combination of telescope size, efficiency and total integration time. The contour levels are at σ_v^{tot} = 2, 3, 4 and 5 cm/s.

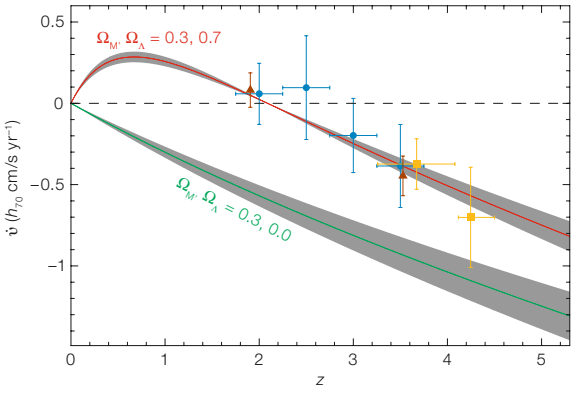

Figure 4. The three sets of 'data' points show simulations of three different implementations of the redshift drift experiment. In each case we have assumed D = 42 m, ε = 0.25, t_{int} = 4 000 h and a total experiment duration of 20 years. Blue dots: best overall σ_v, N_{QSO} = 20 (binned into four redshift bins). Yellow squares: most significant redshift drift detection, N_{QSO} = 10 (in two redshift bins). Brown triangles: best constraint on Ω_Λ, N_{QSO} = 2. The solid lines show the expected redshift drift for different parameters as indicated. The grey shaded areas result from varying H_0 by ± 8 km/s Mpc^{-1}.

the E-ELT will indeed be capable of providing unequivocal proof of the existence of past acceleration.

So will these constraints be able to compete with those coming from SN Ia, weak lensing or BAO measurements in 2037? No, they will not. However, the statistical significance of its constraints is not the only criterion by which to judge the value of a cosmological experiment. As we have seen, measuring the expansion history using $\dot{z}$ is not only entirely independent of all other cosmological observations, it is fundamentally different from them – indeed unique. Moreover, it does not assume spatial flatness or require any other cosmological or astrophysical assumptions whatsoever. In fact, it does not even rely on any specific theory of gravity being correct. Instead, it can provide us with the most direct and inescapable evidence of acceleration possible. In that sense the redshift drift will not only be highly competitive, it will have the edge. Even in 2037.

References

Heavens, A. 2003, MNRAS, 343, 1327
Liske, J., et al. 2008, MNRAS, 386, 1192
Loeb, A. 1998, ApJ, 499, L111
Perlmutter, S., et al. 1999, ApJ, 517, 565
Riess, A. G., et al. 1998, AJ, 116, 1009
Sandage, A. 1962, ApJ, 136, 319
Seo, H.-J. & Eisenstein, D. J. 2003, ApJ, 598, 720

Photo: H. H. Heyer, ESO

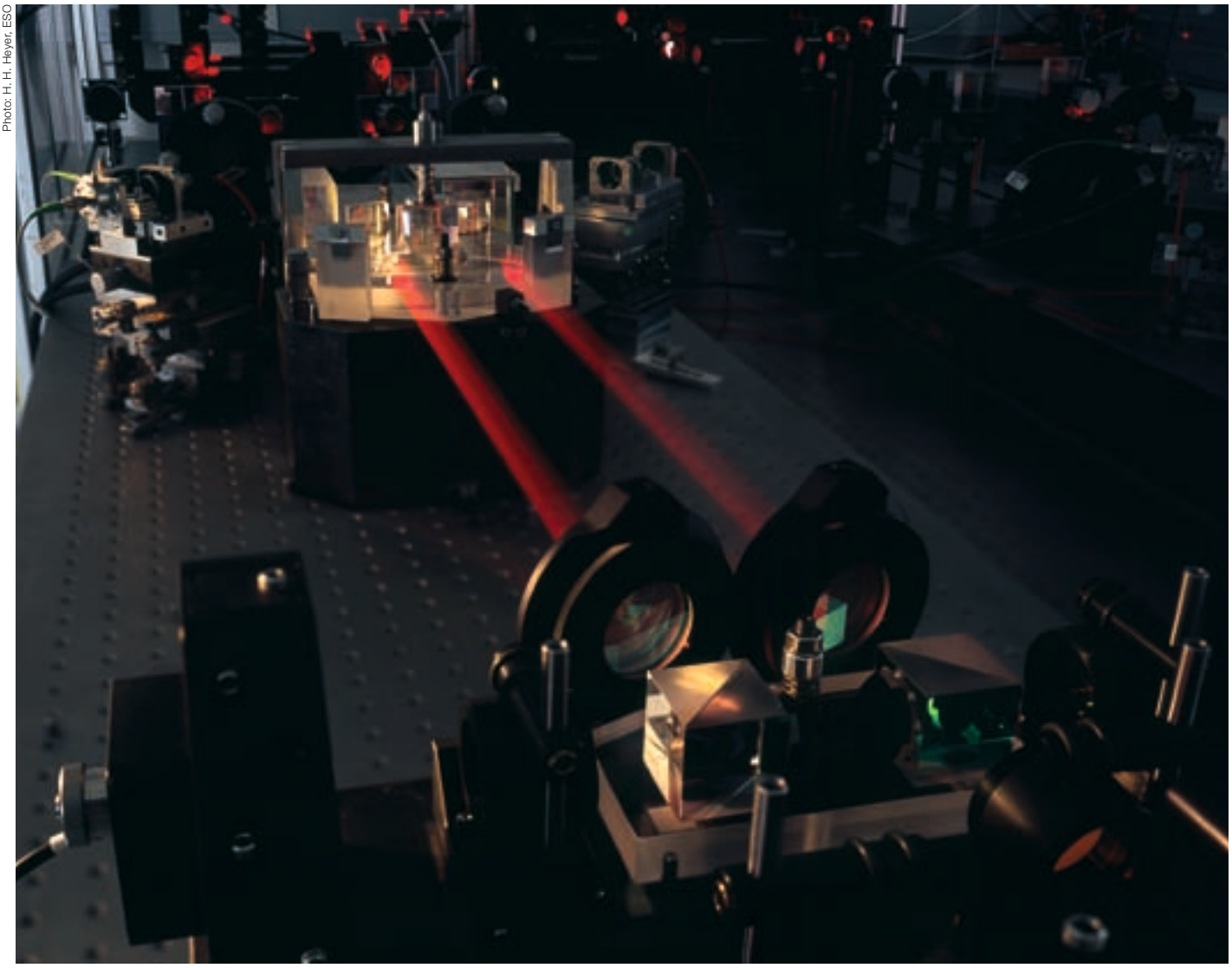

The VLTI PRIMA instrument is shown during testing in Garching. The two combined beams of the PRIMA fringe sensor unit (FSU) B are seen, in red metrology laserlight, joining the FSU's beam combiner in the background to the fibre injection optics. The second FSU is seen to the right. The PRIMA hardware was shipped to Paranal in July 2008 and underwent assembly, integration and verification in August. On-sky commissioning will begin in Period 82, and when complete the facility is expected to provide improvements in VLTI sensitivity, along with astrometry to better than 100 microarcseconds.

The Quest for Near-infrared Calibration Sources for E-ELT Instruments

Maria Aldenius[1]
Florian Kerber[1]
Paul Bristow[1]
Gillian Nave[2]
Yuri Ralchenko[2]
Craig J. Sansonetti[2]

[1] ESO
[2] National Institute of Standards and Technology, Gaithersburg, Maryland, USA

Extremely Large Telescopes (ELTs) and most of their instrumentation will be optimised for operation in the Near-InfraRed (NIR) because of the wavelength dependent performance of adaptive optics. Few established sources for wavelength calibration exist in this wavelength domain. A project is described which aims to provide the basic data to select the best calibration sources for NIR instruments at the European ELT (E-ELT) as a function of wavelength range and spectral resolution. This work directly supports the Phase A studies of E-ELT instruments; in addition its results will be highly valuable for future use in analysis of NIR science observations.

Since the focus of astronomy and laboratory atomic physics has been on ultraviolet and visible wavelengths for more than 100 years, a wealth of reliable atomic data exists in this wavelength range. In contrast, existing data for most elements are sparse at Near-InfraRed (NIR) wavelengths and a better knowledge of the spectral properties is clearly needed for both the analysis of astronomical spectra and for selecting possible calibration sources. No comprehensive database of NIR spectra is available. The European Southern Observatory (ESO) and the US National Institute of Standards and Technology (NIST) are collaborating on a project to provide the necessary basic data to help select the best calibration sources for the European Extremely Large Telescope (E-ELT) instruments. About 20 different hollow cathode lamps are chosen for this study. We are investigating their spectral and operational properties through laboratory measurements using a Fourier Transform (FT) spectrometer at ESO. The most interesting sources will then be studied at atomic physics laboratories in order to produce accurate wavelength standards and calibration reference data directly applicable to operations of E-ELT instruments.

Requirements of E-ELT spectrographs

Instruments at ELTs will cover a variety of wavelength regions and spectral resolutions. The projected large size of E-ELT instruments will make it possible to deliver excellent calibration by combining optimised sets of calibration lamps, provided such lamps can be identified in advance.

Recent developments indicate that frequency-based systems such as the laser frequency comb (Araujo-Hauck et al., 2007) may provide wavelength calibration of unprecedented accuracy and stability for future high-resolution spectrographs such as CODEX. At lower resolution, and for instruments with less stringent calibration requirements, classical calibration sources such as hollow cathode lamps (HCLs) are expected to remain the preferred choice for many ELT instruments.

Currently, conceptual designs for six instruments suitable for the E-ELT are being made, with another two designs to start soon. Our project will directly support these studies by providing information on possible calibration sources for a given spectrograph. Figure 1 shows the parameter space of the suite of spectrographs currently under study. The values used in the diagram are very preliminary since both wavelength range and spectral resolution are parameters that will be optimised during the conceptual design, based on the proposed science and technical feasibility. Nevertheless, it is obvious that the emphasis of E-ELT spectrographs will be in the NIR, and covering a large range of spectral resolution.

Hollow cathode lamps and their selection

Gas discharge sources such as hollow cathode lamps have been used as sources for wavelength calibration of astronomical spectrographs for many decades. HCLs are mass-produced for a commercial market and more than fifty elements are readily available from manufacturers. However, few have been studied for use in astronomy. The successful characterisation of a Th-Ar HCL (Kerber et al., 2008) – a joint ESO/NIST project – for CRIRES has improved the calibration of NIR high-resolution spectrographs; while at lower resolution improved data for the noble gases have made it possible to model and quantitatively predict the IR performance of the calibration system for X-shooter (Kerber et al., 2007).

Ideally, existing databases of atomic spectra based on laboratory measurements would make it straightforward to select good calibration sources. The NIST Atomic Spectra Database (ASD) (Ralchenko et al., 2008) is probably the most extensive database of experimental data, and NIST is continually expanding the data volume by adding critically compiled data from various sources. For the NIR, the most recent comprehensive compilation of many elements dates back 30 years (Outred, 1978). A careful analysis has demonstrated that it is currently

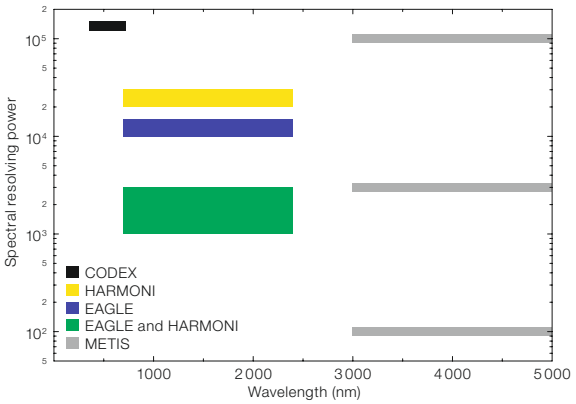

Figure 1. Parameter space covered by some of the projected E-ELT spectrographs. The numbers are preliminary since both wavelength range and spectral resolving power will be optimised during the initial design.

Metal	Al	Ti	Cr	Fe	Ni	Ge	Se	Zr	Ce	Ce	Dy	Ho	Tm	Hf
Atomic no.	13	22	24	26	28	32	34	40	58	58	66	67	69	72
Work function (eV)	4.28	4.33	4.5	4.7	5.15	5	5.9	4.05	2.84	2.84	–	–	–	3.9
First ionisation potential (eV)	5.99	6.29	6.77	7.90	7.64	7.90	9.75	6.84	5.54	5.54	5.94	6.02	6.18	6.65
Gas	Ne	Ne	Ne	Ne	Ne	Ne	Ne	Ne	Ne	Ar	Ne	Ne	Ne	Ar

Table 1. Hollow cathode lamps selected so far for investigation of their properties.

not possible to select calibration sources in the NIR based on the existing databases, since these are not adequately populated with spectral data for many of the relevant elements.

Since HCLs are commercially available for more than 50 elements, it would be very convenient if their spectra could be predicted with some accuracy based on first principles. Unfortunately, reasonable accuracy can only be achieved with very considerable effort. We have used the freely available code by R. D. Cowan (Cowan, 1981) that calculates atomic energy levels, transition rates and spectra. For a more detailed description see Aldenius et al., 2008.

While the Cowan code can produce good results for many atomic systems, especially the light elements, the calculation of spectra for heavier species is greatly exacerbated by strong correlation effects resulting from a large number of overlapping low-excited configurations. Such correlations are especially important for atoms with open *d*- and *f*-shells that have rich NIR spectra of importance to the present work. A proper *ab initio* account of correlation effects would have to include an exceedingly large number of configurations. Any attempt to survey 20 or more elements in this manner would incur long-term computational efforts, and hence such an approach is impractical for our project.

In the absence of good line data or reliable calculations, we restricted ourselves to using some very basic and practical considerations to guide our selection of elements for procuring HCLs for laboratory measurements.

In the process of choosing suitable lamps, the properties of different metals have been considered in terms of e.g. availability, possible line structure, and possibility to produce a number of observable spectral lines in the wavelength region of interest. For calibration of high-resolution spectrographs, we have chosen elements dominated by even isotopes, as hyperfine structure in odd isotopes may produce asymmetric spectral lines. For the calibration of low-resolution spectrographs, the line strengths are more important and any line structure will be negligible compared to instrument profiles. Theoretical calculations have also been made, in order to estimate the possible number of spectral lines. At the present time, 14 different lamps have been selected (see Table 1).

Fourier Transform spectrometry

Spectra of the HCLs are being recorded with the commercial Fourier Transform (FT) spectrometer at ESO. This type of spectrometer is mainly used for industrial applications using absorption spectroscopy, but it also provides a port for external sources. In order to duplicate the optical path used for internal sources, the light from the external source is collimated using an elliptical and a parabolic mirror (see Figure 2). Spectra are recorded in the spectral range between 3 000 cm^{-1} and 14 000 cm^{-1} (3.3 µm to 0.7 µm). For each lamp the spectrum is recorded at six different operating currents (4, 6, 8, 10, 12 and 14 mA) with a resolution of 0.125 cm^{-1}. Between 128 and 1200 scans (1 h to 10 h) are co-added for each spectrum in order to increase the signal-to-noise of all lines. In order to further investigate the spectral properties of the lamps, spectra are also recorded with lower resolution (1, 4 and 8 cm^{-1}).

The spectral lines are identified using available compilations, databases, individual publications, and comparisons to Ritz wave numbers, that is wave numbers calculated from the difference in energy between published energy level values. Gaussian profiles are fitted to all observable spectral lines and the integrated intensity is studied as a function of lamp operating current. For each spectral line the ratio of the intensity of the line to the intensity of the same line in the 10-mA spectrum is calculated. The ratios are then averaged for all lines of the corresponding species at each current, showing a distinct difference between the behaviour of the gas and the metal lines. The average behaviour of line intensities as a function of current is displayed in Figure 3 where only resolved lines present at all currents are included.

This distinctive behaviour, which can be qualitatively explained in terms of the sputtering effect in HCLs (Kerber et al., 2006), provides a useful tool in distinguishing between gas and metal lines

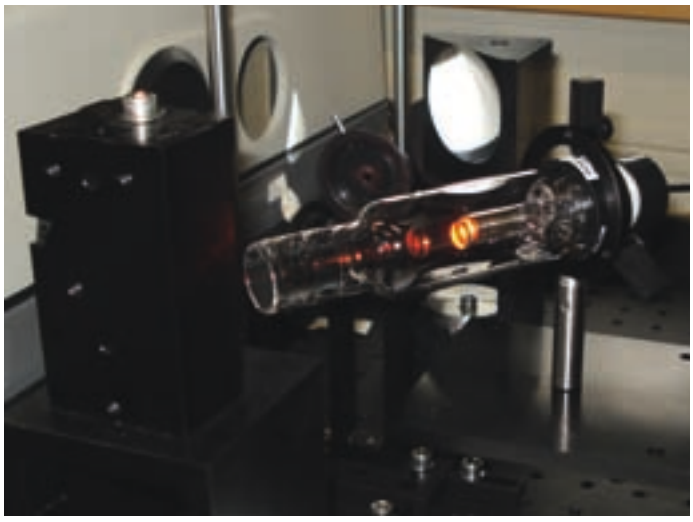

Figure 2. Set-up of a hollow cathode lamp and the Fourier Transform spectrometer.

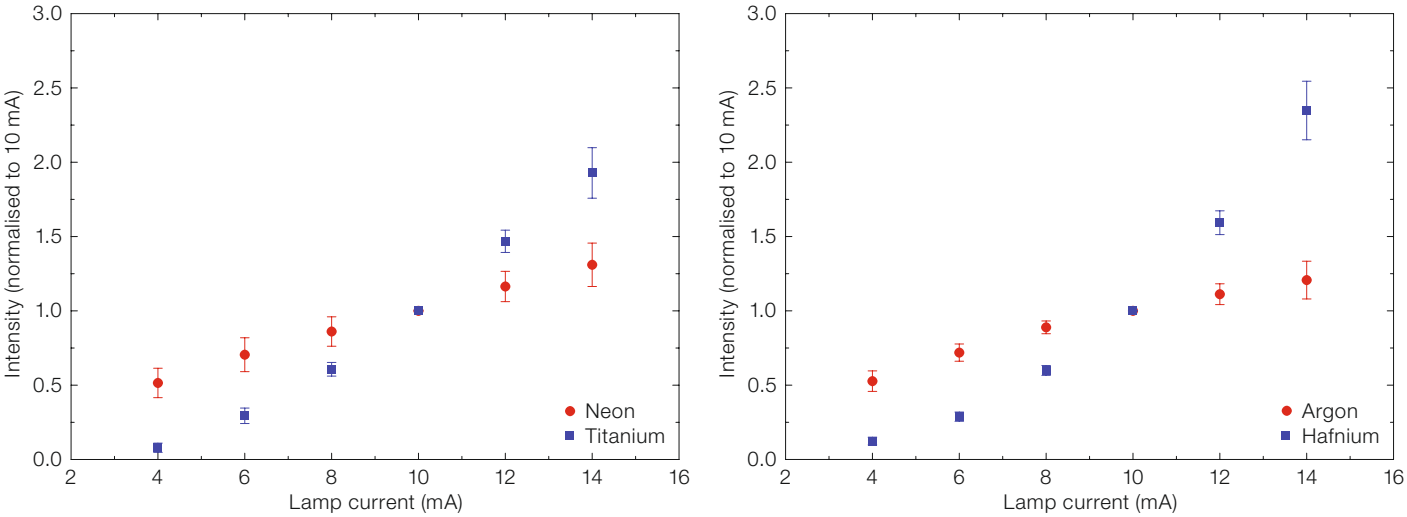

Figure 3. Line intensities as a function of operating current in the Ti-Ne and Hf-Ar HCLs. The intensities are normalised to the intensity at 10 mA and average values are calculated for identified lines from the carrier gas and the metal respectively. The error bars are statistical uncertainties and represent one standard deviation.

when trying to identify the presently unidentified lines in the spectra. In addition to line identification, the results of the investigations of current dependence should also provide important information on how to optimise the operation of the calibration lamp.

Results and outlook

Five lamps have to date been thoroughly analysed resulting in solid knowledge about the number of lines available and their intensity ratios. Also the behaviour of line intensities as a function of lamp current has been well established. In general the spectra are dominated by lines from the carrier gas, but many metal lines are present as well. A small spectral region for the Ce-Ne, Zr-Ne and Ti-Ne lamps is displayed in Figure 4. The three lamps have the same carrier gas and the spectra are therefore similar, but significant differences are evident. Different metals produce lines in different spectral regions and lamps can thus be used in combination in order to optimise their utility.

Our laboratory project to conduct a preliminary survey of about 20 elements with a small commercial FT spectrometer forms the basis for developing a more robust understanding of the NIR spectra of elements suitable as wavelength calibration sources. We focus our effort on the needs of currently planned spectrographs for the E-ELT, which will require good calibration sources for various resolutions across the NIR range. In a second phase we plan to establish the best qualified elements as wavelength standards by conducting dedicated laboratory measurements with high-precision FT spectrometers at qualified atomic spectroscopy laboratories.

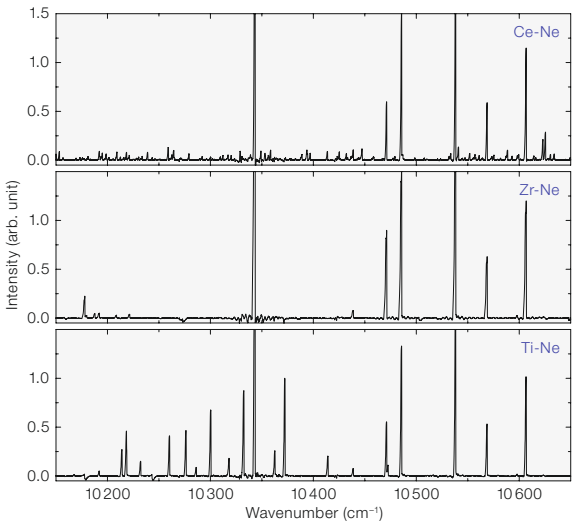

Figure 4. Observed spectra of the Ce-Ne, Zr-Ne and Ti-Ne lamps at operating current 10 mA in a small wave number range (0.99 μm to 0.94 μm). The spectra are dominated by lines from Ne (the lines common to all spectra), but metal lines contribute to significant differences.

References

Aldenius, M., et al. 2008, Proc. SPIE, 7014, 70145U, in press
Araujo-Hauck, C., et al. 2007, The Messenger, 129, 24
Cowan, R. D. 1981, *The Theory of Atomic Structure and Spectra,* (Berkley: University of California Press), *ftp://aphysics.lanl.gov/pub/cowan*
Kerber, F., Saitta, F. & Bristow, P. 2007, The Messenger, 129, 21
Kerber, F., et al. 2006, Proc. SPIE, 6269, 626942
Kerber, F., Nave, G. & Sansonetti, C. J. 2008, ApJS, in press
Outred, M. 1978, J. of Phys. Chem. Ref. Data, 7, 1
Ralchenko, Y., et al. 2008, NIST Atomic Spectra Database version 3.1.5, (National Institute of Standards and Technology, Gaithersburg, Maryland), *http://physics.nist.gov/asd3*

Detector Upgrade for FLAMES: GIRAFFE Gets Red Eyes

Claudio Melo, Luca Pasquini, Mark Downing, Sebastian Deiries, Dominique Naef, Reinhard Hanuschik, Ralf Palsa, Roberto Castillo, Eduardo Peña, Eduardo Bendek, Mark Gieles
ESO

In May 2008, a new CCD, called Carreras, was installed in the GIRAFFE spectrograph to replace Bruce, the old detector. Carreras is more sensitive to wavelengths redward of 700 nm. The main characteristics and results obtained in the commissioning of Carreras are reported.

FLAMES is the multi-object, intermediate and high resolution fibre facility of the VLT. Mounted at the Nasmyth A platform of UT2 it offers a rather large corrected field of view (25 arcmin diameter) and consists of several fibre modes (see Pasquini et al., 2002 for details). Most of the FLAMES fibre modes feed GIRAFFE, a medium-high resolution spectrograph (R = 6000–33 000) for the entire visible range (370–950 nm).

Shortly after the beginning of operations, we started to look for a new detector for GIRAFFE to boost the instrument's red quantum efficiency (QE) capabilities, while still retaining very good blue response. We aimed also at reducing the strong fringing present in the red spectral range. It has taken some time for devices to become available which meet our strong requirements. The solution finally offered by e2v was a custom two-layer AR (Anti-Reflection) coated Deep Depletion CCD (CCD44-82). This device was made in a new e2v AR coating plant and delivered to ESO in mid-2007 with a performance that matches predictions.

Carreras

The new detector Carreras (e2v serial number 06383-13-01) is a CCD44-82 2 k × 4 k. It is electrically and mechanically identical to the existing detector (Bruce), thus making the upgrade a simple plug-in replacement. Bruce is a standard silicon (nominal thickness 16 µm) CCD44-82 and has a single layer AR coating optimised for the blue. Carreras (the new detector) is a Deep Depletion device (nominal thickness 40 µm) that has a special custom two-layer coating (HfO/SiO2) optimised for broadband QE response over the wavelength range of 370–950 nm.

The upgrade was performed by assembling a new cryostat and installing Carreras. Carreras was fully characterised in this new system. The GIRAFFE detector head and cryostat were then shipped from Paranal to ESO Garching to enable the field lens to be swapped into the new system.

Read-out modes

For scientific applications (in service mode) it was decided to retain the 225 kpx, 1 × 1, low-gain (read-out noise 4.3 electrons (e^-)) as the default mode. The improvement in signal-to-noise (S/N) ratio of the 225 kpx, 1 × 1, high-gain (read-out noise 3.1 e^-) with respect to the low-gain is negligible as soon as the counts go over 110 e^- (S/N ratio 7.5, assuming that the signal is extracted over six pixels). Since this mode has a much higher dynamical range, we decided to keep it as the standard one.

Other interesting modes such as the ultra-fast read-out 625 kpx, 1 × 1, low-gain and the 50 kpx, 1 × 1, high-gain (with a read-out noise of only 2 e^-) were commissioned and can be offered in visitor mode for instance. The low read-out noise in the 50 kpx, 1 × 1, high-gain mode, along with the improvements in the QE and the reduction of the fringing (see below), make this mode very appealing for studies of faint objects, especially if coupled with the binning 1 × 2. The available read-out modes of Carreras are summarised in Table 1.

Cosmetics and linearity

As far as cosmetics are concerned, Carreras is a very good detector. The master bias shows no hot pixels. Similarly, the master dark (1-h-long) shows only one bad pixel. Image flats show 62 dark pixels (i.e., pixels with less than 50 % of the local mean). As expected, the cosmic hit rate is higher for Carreras than for Bruce because Carreras has over twice the thickness. The cosmic hit event rate measured in Paranal is 3.14 ± 0.18 events/min/cm^2. Translated into pixels, 20 000 pixels out of a total of 2 k × 4 k (or 0.25 %) are affected by cosmic ray hits for a 1-h dark.

The linearity of both the left and right amplifiers was measured to be better than ± 0.5 % in the main default scientific mode (225 kpx, 1 × 1, low-gain).

Fringing

In addition to the QE improvement, Carreras was expected to have much lower fringing due to its increased thickness and reduced reflectivity at red wavelengths. The reduction of the fringing amplitude is immediately seen by looking at the raw flat frames taken with the L881.7 wavelength setting (Figure 1). The improvement is impressively shown in Figure 2, where flat-field spectra of fibre flats are compared. Flats collected with Bruce (black line) have a fringing level of 30 % with respect to the continuum. This level is reduced to about 5 % with Carreras.

QE improvement

The QE curves for both detectors were measured in Garching. The QE ratio is shown in Figure 3. Flats taken prior to the dismounting of Bruce from GIRAFFE

Mode	Read-out speed (kHz)	Dynamics* (Ke^-/pixel)	Conversion factor (e^-/ADU)	Read-out noise (e^-)	Read-out time (s)
1	50 kpx, 1 × 1, high	45	0.69 ± 0.1	2.2 ± 0.1	190
2	225 kpx, 1 × 1, low	142	2.35 ± 0.1	4.3 ± 0.1	43
3	625 kpx, 1 × 1, low	142	2.4 ± 0.1	5.2 ± 0.1	24

Table 1. Summary of performance of the scientific read-out modes.

* Limit of the 16 bit Analogue to Digital Converter (ADC).

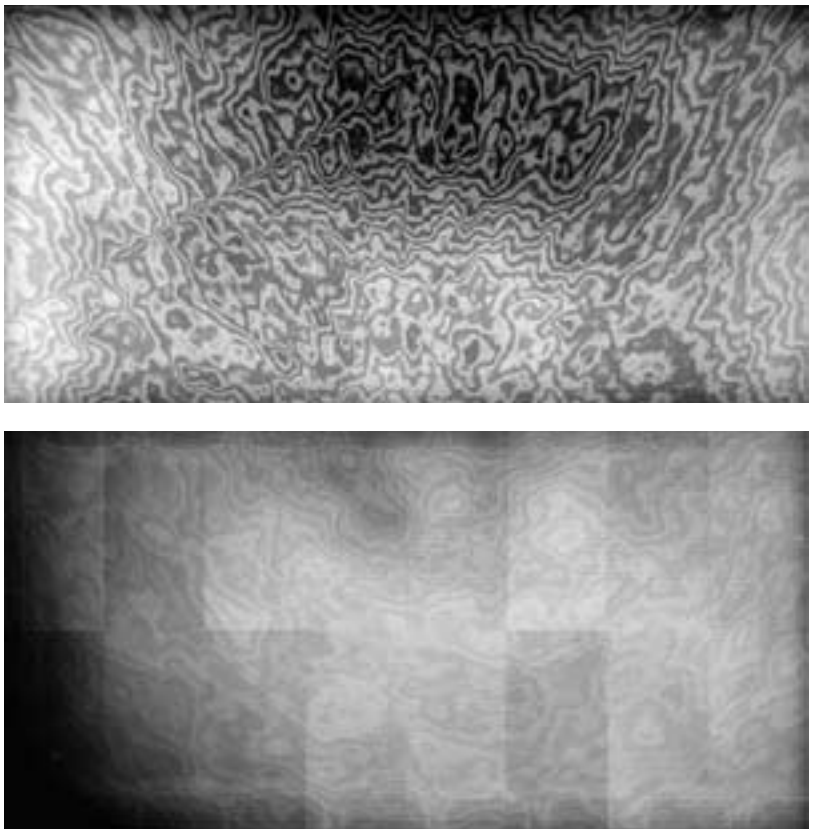

Figure 1. Comparison of flat-field images (~ 25 000 e^-) at wavelength 900 nm with 5 nm bandwidth. **Top:** Previous CCD Bruce. **Bottom:** New CCD Carreras. Carreras is a much thicker device (40 µm versus 16 µm) and thus has much less fringing.

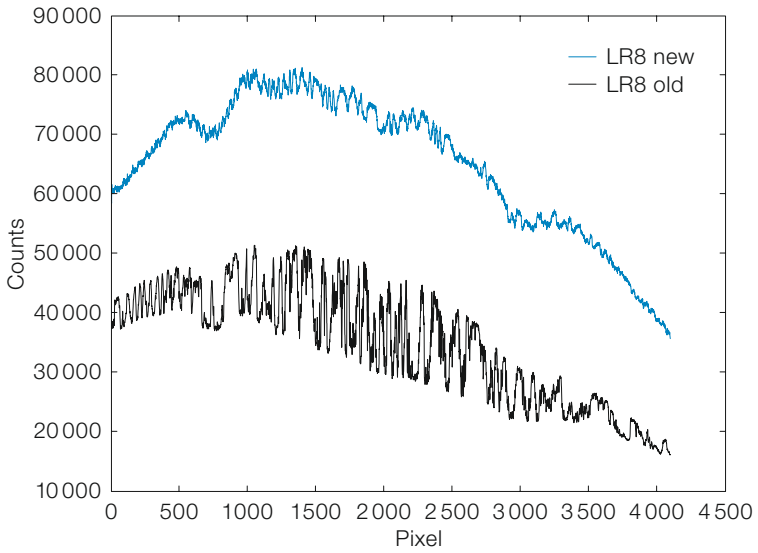

Figure 2. Extracted fibre flats for LR8 (881.7 nm) set-up taken with the same exposure time. Blue line is for the flat-field obtained with Carreras whereas the black line is the flat-field collected with Bruce.

were used to validate this curve. For the recent flats found in the ESO archive, the agreement of the observation with the lab prediction is very good in the red regime as shown in Figure 3, but slightly below the expectations for the blue settings.

Data reduction

During the commissioning, calibrations were taken for all set-ups in all five slit systems (two Medusa, two IFU and one Argus) in order to re-adjust the exposure times. These first flats and arcs allowed us to check whether the present default parameters are good enough to allow the pipeline to find and trace the fibres and compute the wavelength solution. We were happy to see that the pipeline with the default parameters could reduce all wavelength settings blueward of 650 nm.

A first trial was made to reduce a flat and an arc spectrum with the Geneva pipeline (Blecha et al., 2000; Royer et al., 2002).

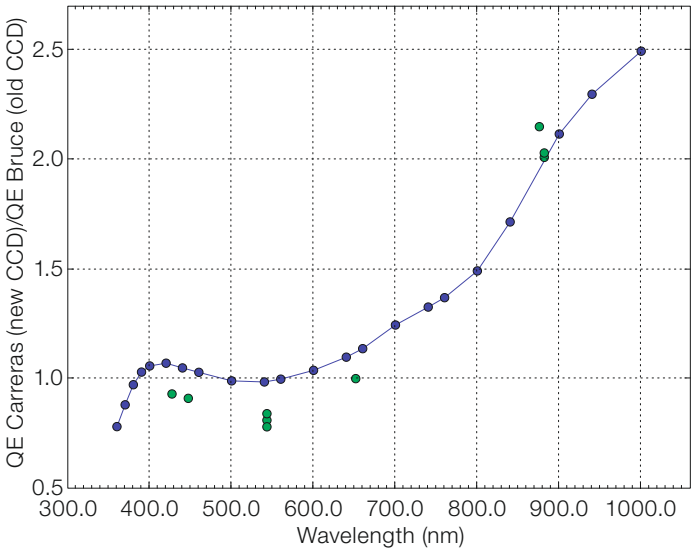

Figure 3. Quantum Efficiency ratio (Carreras/Bruce; new/old detector). The blue line shows the laboratory measurements. The green circles are the QE ratio measured using archive flat-field frames.

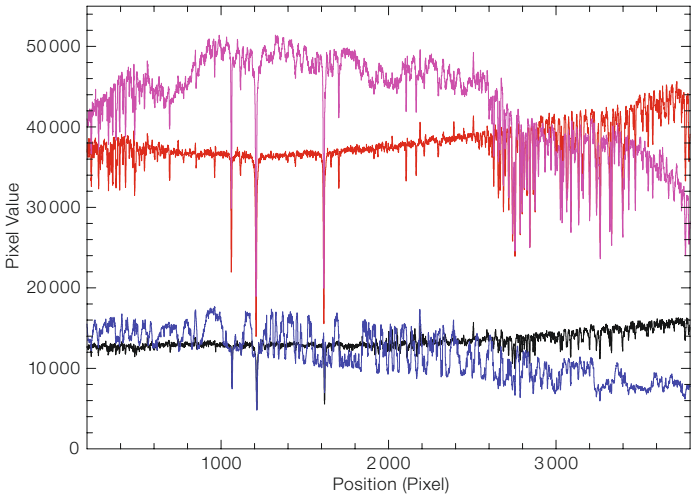

Figure 4. 10-min LR8 observations (low-resolution grating centred on 881.7 nm) for a V = 13.5 star in the globular cluster M15 (NGC 7078) observed with the old CCD Bruce (black and blue lines) and the new one Carreras (red and cyan lines). The blue (old observations) and the cyan (new observations) plots are the extracted spectra without flat-field correction, whereas the black (old observations) and the red (new observations) are spectra for which flat-field corrections were made.

The reduction took place without problems. This implies that those using this pipeline will probably be able to do so in the future. The static calibration database was prepared and installed at Paranal Observatory. A release of the new calibration database will be made public soon. Quality Control pages are available, fed by the QC parameters produced by the pipeline[1].

Science tests – Calcium triplet region

An important aspect for a full understanding of galactic evolution is the metallicity distribution function of the stellar population with time. There is an empirically developed, simply calibrated method available which allows an efficient estimate of metallicity ([Fe/H]) for individual red giant branch (RGB) stars using the strength of the CaII triplet (CaT) lines at 849.8 nm, 854.2 nm and 866.2 nm. This method was pioneered for use on individual stars by Armandroff & da Costa (1991). It has the advantage that the lines are broad enough to be accurately measured with moderate spectral resolution (e.g. Cole et al., 2004). Since RGB stars are bright, this method can be successfully used to observe stars in other galaxies. As mentioned in section 1, the improvement of the QE and the drastic reduction of the fringing provided by Carreras are extremely interesting for studies using set-ups redder than 700 nm.

In Figure 4 we show 10-min LR8 set-up observations (low-resolution grating centred on 881.7 nm) for a V = 13.5 star in the globular cluster M15 (NGC 7078) observed with the old CCD (black and blue lines) and the new one (red and cyan lines). The blue (old observations) and the cyan (new observations) plots are the extracted spectra without flat-fielding whereas the black (old observations) and the red (new observations) are spectra for which flat-field correction was made.

From Figure 4 we can see that the difference in signal is almost a factor of three. The measured S/N ratios are 220 for the red spectrum and 60 for the black one, respectively. Even if the newer observations were taken in better seeing conditions (0.7 versus 1.1 arcsec) and after the M1 recoating, the impressive S/N improvement (higher than what was expected from photon noise only) is due to the QE enhancement and also (largely) to a much better fringing correction.

[1] Health Check pages can be accessed at *http://www.eso.org/observing/dfo/quality/GIRAFFE/reports/HEALTH/trend_report_BIAS_HC.html*.

Acknowledgements

We are indebted to Vanessa Hill, Carine Babusiaux and Giuseppina Battaglia who kindly provided us with their own data collected with Bruce. We also thank Samantha Milligan who helped us to improve the text.

References

Pasquini, L., et al. 2002, The Messenger, 110, 1
Battaglia, G., et al. 2008, MNRAS, 383, 183
Blecha, A., et al. 2000, Proc. SPIE, 4008, 467
Royer, F., et al. 2002, Proc. SPIE, 4847, 184
Armandroff, T. E. & Da Costa, G. S. 1991, AJ, 101, 1329
Cole, A. A., et al. 2004, MNRAS, 347, 367

Colour-composite of the spiral galaxy M83 (NGC 5236) formed from *B*, *V*, *R* and *H-alpha* filter images taken with the WFI on the ESO/MPG 2.2-m telescope (see ESO Press Photo 25/08). Image credit: Davide De Martin.

Behind the Scenes of the Discovery of Two Extrasolar Planets: ESO Large Programme 666

Dante Minniti[1,2]
Claudio Melo[3]
Dominique Naef[3]
Andrzej Udalski[4,5]
Frédéric Pont[6]
Claire Moutou[7]
Nuno Santos[8]
Didier Queloz[6]
Tsevi Mazeh[9]
Michel Gillon[6]
Michel Mayor[6]
Stephane Udry[6]
Rodrigo Diaz[10]
Sergio Hoyer[11]
Sebastian Ramirez[1]
Grzegorz Pietrzynski[4,12]
Wolfgang Gieren[12]
Maria Teresa Ruiz[11]
Manuela Zoccali[1]
Omer Tamuz[9]
Abi Shporer[9]
Marcin Kubiak[4,5]
Igor Soszynski[4,5]
Olaf Szewczyk[4,5]
Michal Szymanski[4,5]
Krzysztof Ulaczyk[4,5]
Lukasz Wyrzykowski[5,13]

[1] Departamento de Astronomía y Astrofísica, Pontificia Universidad Católica de Chile, Santiago, Chile
[2] Specola Vaticana, Città del Vaticano, Italy
[3] ESO
[4] Warsaw University Observatory, Poland
[5] The OGLE Team
[6] Observatoire de Genève, Sauverny, Switzerland
[7] Laboratoire d'Astrophysique de Marseille, France
[8] Centro de Astrofísica, Universidade do Porto, Portugal
[9] School of Physics and Astronomy, R. and B. Sackler Faculty of Exact Sciences, Tel Aviv University, Israel
[10] Instituto de Astronomía y Física del Espacio, Buenos Aires, Argentina
[11] Departmento de Astronomía, Universidad de Chile, Santiago, Chile
[12] Departamento de Astronomía, Universidad de Concepción, Chile
[13] Institute of Astronomy, University of Cambridge, United Kingdom

This is the story of the Large Programme 666, dedicated to discover sub-stellar objects (extrasolar planets and brown dwarfs), and to measure their masses, radii, and mean densities. We hunt selected OGLE transit candidates using spectroscopy and photometry in the 'twilight zone', stretching the limits of what is nowadays possible with the VLT.

The programme

Transiting extrasolar planets are essential to our understanding of planetary structure, formation and evolution outside the Solar System. The observation of transits and secondary eclipses gives access to such quantities as a planet's true mass, radius, density, surface temperature and atmospheric spectrum.

The OGLE search for transiting planets and low-mass stellar companions has been the first photometric transit survey to yield results. Follow-up of existing OGLE low-amplitude transit candidates prior to our Large Programme has uncovered five extrasolar planets and has yielded the measurement of their radii and therefore their densities. Despite these successes, many important points remain to be understood: how hot Jupiters form, how they evolve, what is the frequency of hot Jupiters, why the density range of hot Jupiters is so large, etc. The main difficulty in answering these questions is the limited number of transiting planets detected so far.

Our Large Programme 177.C-0666 (LP666 for short) proposed to enlarge this sample of confirmed OGLE extrasolar planets, and also to populate the mass-radius diagram for low-mass objects, including planets, brown dwarfs and late M-type stars. 177 transiting candidates from the OGLE survey had been published when we started this LP666, and as part of this programme three new OGLE seasons produced 62 new candidates.

We used VLT+FLAMES to obtain radial velocity orbits in order to measure the mass of all interesting OGLE transiting candidates, and also VLT+UVES and VLT+FORS to measure their precise radius from high-resolution spectroscopy of the primary and high-definition transit light curves.

The telescopes and instruments

We use the Very Large Telescope UT2 in order to measure radial velocities, and UT1 and 2 for photometry in order to measure the transits. Most of the spectroscopic observations required real-time decisions to be taken and therefore were made in visitor mode, whereas photometry collected at precise transit times was carried out in service mode by expert mountain personnel.

The spectroscopic runs were done with FLAMES in GIRAFFE mode which allows simultaneously more than 100 stars to be observed at resolutions ranging from about 5 000 to 20 000. At the same time, the other seven to eight fibres feed UVES at the other Nasmyth focus of the telescope, collecting spectra with a resolution of 50 000. Both GIRAFFE and UVES allow us to acquire spectra of a comparison lamp simultaneously with the target observations. The lamp spectrum is used afterwards to correct spectrograph shifts. This is essential in order to be able to measure radial velocity with a precision of a few m/s. Accurate radial velocity measurements require high-resolution spectra, for this reason we placed the best candidates in the UVES fibres in order to measure more accurate velocities. The photometric runs were acquired with FORS1 or FORS2, yielding milli-magnitude photometry and a high-quality light curve, essential to derive accurate physical parameters for the transiting planets.

The team preparations

Three teams were competing for the same resources: the OGLE team, the Geneva team, and the Chilean team. The idea arose of working together and the final details were discussed at the workshop in Haute-Provence "10 years of 51 Peg". In preparation for this Large Programme, we had to re-examine the OGLE database to check old candidates and improve the ephemeris, and to run the OGLE pipelines to select new candidates. Our teams have put together their respective spectroscopic and photometric databases in order to select the most promising candidates, but it was not easy to decide which were these best candidates, and this was extensively dis-

cussed by many team members. The spectroscopic run of February 2006 by the Swiss team was used to cull some candidates. The photometric run of the last period of March 2006 of the Chilean team was used to observe some of these most promising candidates. We finally started the planet hunting for this Large Programme in April 2006 with many promising candidates.

The first step is to acquire radial-velocity information for the most promising OGLE planetary transit candidates, and to identify real transiting planets among them. This requires five to eight radial velocity points with UVES in good observing conditions. As the OGLE candidates are disposed in a few square degrees of the sky, a few of them (typically two to five targets) can be observed simultaneously using the FLAMES configuration. The weather conditions of this first run were rather poor, with five clouded nights and three clear nights. As our targets are faint and we need < 100 m/s radial velocity accuracy, the clouded nights were of very limited use, despite the occasional gaps in the clouds.

This Large Programme had another component, many hours of service observations on FORS to obtain high-accuracy measurements of the transits of the planets that we expected to discover. In fact, the results of these initial runs suggested three possible planets, but because of bad weather we could not reach solid conclusions on these objects. Due to the bad weather, it was more important at this initial stage to recover some of the spectroscopic time that was lost. We therefore requested to ESO to swap some of our photometric time for spectroscopic time in service mode, a request that was kindly (and quickly) approved.

The candidates

We measured and analysed the various candidates found during the OGLE season III, from OGLE-TR-138 to OGLE-TR-177. This was done using new data from the present LP666 in combination with data already in hand. A detailed publication for these candidates is in preparation. This paper would be a large effort, like the previous papers by Pont et al. (2005) for Carina, and Bouchy et al. (2005) for the Galactic Bulge. In addition, the flexibility of the OGLE telescope has allowed us to obtain the candidates needed, producing a new set of candidates for this LP666, which we have followed-up during periods P78–P82. These were selected carefully among periodic low-amplitude transits observed with the Warsaw telescope during the last seasons: season IV from candidates OGLE-TR-178 to TR-200; and season V from candidates OGLE-TR-201 to TR-219. These are listed in Table 1. New candidates from season VI (up to OGLE-TR-238) are still being analysed.

The spectroscopic runs had two goals: (1) to sort out the non-planetary candidates; and (2) to measure an orbital motion for the planetary candidates. The need to discard as quickly as possible the impostors required that data reduction and radial velocity measurement had to be done in real time. This was achieved by a combination of the FLAMES/UVES pipeline and our own code. The previous nights results were analysed by our team

Object	Period	*I*	Depth	Status
OGLE-TR-178	2.97115	16.56	0.016	faint target, not observed
OGLE-TR-179	12.67106	15.13	0.034	flat CCF
OGLE-TR-180	1.99601	16.74	0.012	faint target, not observed
OGLE-TR-181	2.3896	16.29	0.01	fast rotator (synch.?)
OGLE-TR-182	3.98105	15.86	0.01	transiting planet
OGLE-TR-183	4.78217	15.32	0.015	fast rotator (synch.?)
OGLE-TR-184	4.92005	15.57	0.015	fast rotator (synch.?)
OGLE-TR-185	2.78427	16.72	0.035	fast rotator (synch.?)
OGLE-TR-186	14.81481	16.54	0.054	faint target, not observed
OGLE-TR-187	3.45686	14.07	0.008	double-lined spectroscopic binary (SB2)
OGLE-TR-188	6.87663	16.38	0.031	blend of two line systems
OGLE-TR-189	1.73937	15.03	0.006	not observed
OGLE-TR-190	9.38262	16.06	0.043	not observed
OGLE-TR-191	2.51946	15.57	0.007	fast rotator (synch.?)
OGLE-TR-192	5.42388	14.41	0.008	flat CCF
OGLE-TR-193	2.95081	14.99	0.008	not observed
OGLE-TR-194	1.59492	14.69	0.006	flat CCF
OGLE-TR-195	3.62174	14.19	0.006	not obseved
OGLE-TR-196	2.1554	15.57	0.012	fast rotator (synch.?)
OGLE-TR-197	2.40587	14.59	0.019	flat CCF
OGLE-TR-198	13.63141	15.44	0.018	not observed
OGLE-TR-199	8.8347	14.88	0.017	single-lined spectroscopic binary (SB1)
OGLE-TR-200	6.48845	15.63	0.023	not observed
OGLE-TR-201	2.368	15.6	0.016	fast rotator
OGLE-TR-202	1.6545	13.6	0.017	not observed
OGLE-TR-203	3.3456	15.6	0.014	not observed
OGLE-TR-204	3.1097	14.8	0.026	SB2
OGLE-TR-205	1.7501	16	0.015	not observed
OGLE-TR-206	3.2658	13.8	0.006	no variation
OGLE-TR-207	4.817	14.3	0.021	SB2
OGLE-TR-208	4.5025	15.3	0.022	SB2
OGLE-TR-209	2.2056	15	0.022	no variation
OGLE-TR-210	2.2427	15.2	0.032	fast rotator
OGLE-TR-211	3.6772	14.3	0.008	planet
OGLE-TR-212	2.2234	16.3	0.016	blend?
OGLE-TR-213	6.5746	15.3	0.036	SB2
OGLE-TR-214	3.601	16.5	0.023	SB1
OGLE-TR-215	4.9237	14.8	0.016	no variation
OGLE-TR-216	1.9763	14.6	0.011	blend?
OGLE-TR-217	5.7208	16.1	0.037	no CCF
OGLE-TR-218	2.2488	14.5	0.02	fast rotator
OGLE-TR-219	9.7466	15.1	0.032	SB2

Table 1. List of targets selected for follow-up from OGLE seasons IV and V. The photometric period, *I*-band magnitude and transit depth are based on the OGLE data. The last column is our final assessment of the status of the OGLE transit candidates after the spectroscopic follow-up with FLAMES.

members in Europe. Based on their feedback, FLAMES configuration files were updated or simply discarded. We will here discuss the first two confirmed planets, but along this work we have analysed about 100 OGLE candidates (from OGLE-TR-138 to OGLE-TR-238), including several new ones that were selected for this programme from OGLE seasons IV, V and VI.

The non-planets

A vast number of candidates are produced by OGLE, which needed to be confirmed spectroscopically and photometrically. Therefore, a large part of the work we did was dedicated to eliminate non-planetary candidates from the OGLE selection.

The shape of the cross correlation function (CCF) can be efficiently used for bad candidate detection and rejection. Figure 1 represents the CCFs obtained for some new P78–P80 targets for which we were able to conclude, after a single FLAMES observation, that a follow-up was useless. All these data were obtained in the February 2007 run, when five new fields were started. Only one contained a good candidate out of 10 new objects; that is OGLE-TR-235, shown in Figure 2. From the photometric point of view, the light curve produced by OGLE was always compatible with a planet. That is one of the reasons why a follow-up is mandatory (the other important reason being the need to determine an accurate planetary mass, of course).

Following the procedure described in the papers, we have discarded several candidates. For example, we analysed 42 new OGLE candidates, finding two planets plus the following:

– obvious or suspected single- or double-lined spectroscopic binaries (blend, binary with high-mass companion): 11 candidates;
– broad CCF (synchronised, fast rotator): 9 candidates;
– no CCF dip detected, no radial velocity (false detections, faint candidates): 8 candidates;
– too faint candidates, outside the field (not observed): 11 candidates;
– others: 3 candidates.

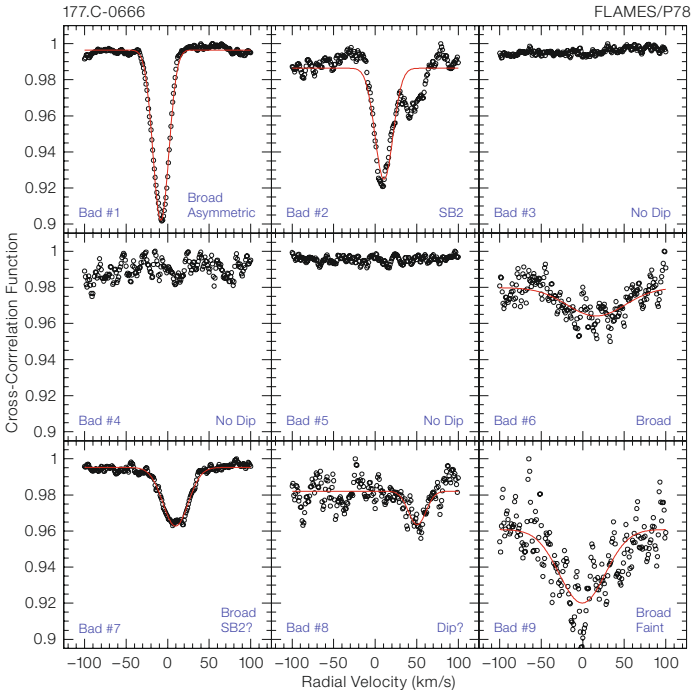

Figure 1. The cross-correlation functions (CCF) from the spectra of the different candidates shown as an example of all the typical bad CCF cases.

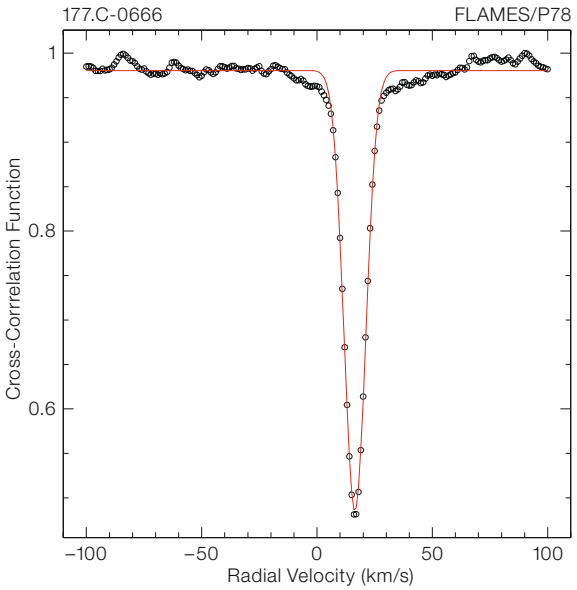

Figure 2. The CCF of a good candidate (OGLE-TR-235).

FLAMES has been very efficient in identifying bad candidates. It is not an exaggeration to say that FLAMES-UVES is in a league of its own for follow-up of faint transit candidates, such as the ones discovered by OGLE. We have observed the complete sample of all accessible new OGLE candidates. We note that all the data acquired with FLAMES-UVES are fully reduced already. We have so far concentrated on looking for the best planetary candidates and measuring their parameters. In the near future we would go back and sift through the whole dataset, looking for low-mass companions (M-dwarfs and brown-dwarfs), fitting the best parameters. We expect some more interesting results, other than the few new planets that we have found, which are still being analysed, along with hundreds of eclipsing binary stars, for which we have radial velocities.

The first planet OGLE-TR-182-b

After the first year, we had discarded several candidates, but we also had tentative orbits for three planet candidates. These good ones, however, did not have enough velocities to exclude random radial velocity fluctuations as the cause of the orbital signal. In addition, the ephemeris was not confirmed by the photometry: there was a slight discrepancy, which required collection of more data to resolve. Then we started the year 2007, full of hopes about these three objects. Below we tell the story of the first two.

The masses and radii of the stars were not accurately measured, and therefore we could not estimate precisely the masses and radii of our good planet candidates. We again asked ESO to allow a change in strategy, swapping a few hours of FORS time into UVES time in order to get high S/N echelle spectra of a couple of stars to confirm that they are main-sequence stars and to measure their parameters (temperature, gravity, luminosity, and chemical abundances). ESO kindly and quickly approved our change, which allowed us to measure the stellar mass, M = 1.14 +/– 0.05 $M_{\odot}$, and radius, R = 1.14 + 0.23 – 0.06 $R_{\odot}$.

The main effort has been devoted to obtaining the ephemeris, which for the two most promising candidates has proven to be difficult. In one case we suspect that we missed the transit because it was observed during the flat bottom portion before the observations ended, and in another case we just caught the ingress, but we observed a full transit on 19 June 2007 (Figure 3).

Finally, we succeeded in confirming candidate OGLE-TR-182-b as a planet, in a paper that also contains analysis of OGLE-TR-178 to TR-200 (Pont et al., 2008). In Figure 4 we show the fit to the OGLE-TR-182 radial velocities obtained with P = 3.9789 days. This object was very difficult to confirm because the period is almost a multiple of one day. Table 2 summarises the derived parameters.

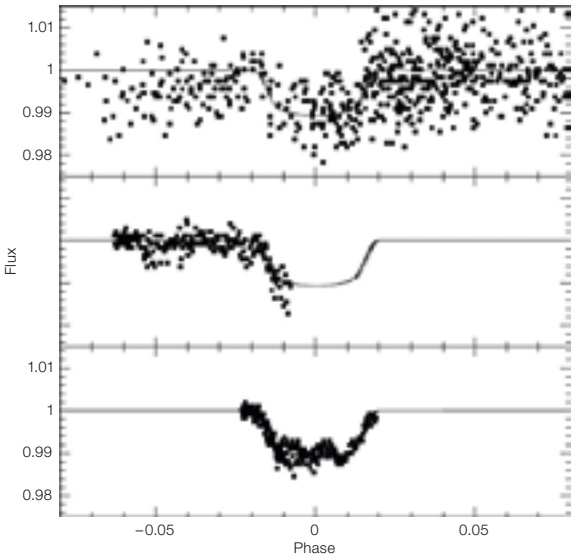

Figure 3. Transit light curves for OGLE-TR-182 from OGLE (top panel), and FORS1 for the nights of 6 June (middle panel), and 9 June 2007 (bottom panel).

Planet ID	OGLE-TR-182-b	OGLE-TR-211-b
Period (days)	3.97910 +/– 0.00001	3.67724 +/– 0.00003
Transit epoch (JD)	2454270.572 +/– 0.002	2453428.334 +/– 0.003
RV semi-amplitude (m/s)	120 +/– 17	82 +/– 16
Semi-major axis (AU)	0.051 +/– 0.001	0.051 +/– 0.001
Radius ratio with primary	0.102 +/– 0.004	0.085 +/– 0.004
Orbital inclination angle	85.7 +/– 0.3	> 82.7
Planet Radius (R_J)	1.13 (+ 0.4 – 0.06)	1.36 (+ 0.18 – 0.09)
Planet Mass (M_J)	1.01 +/– 0.15	1.03 +/– 0.20

Table 2. Measured parameters for the new planets.

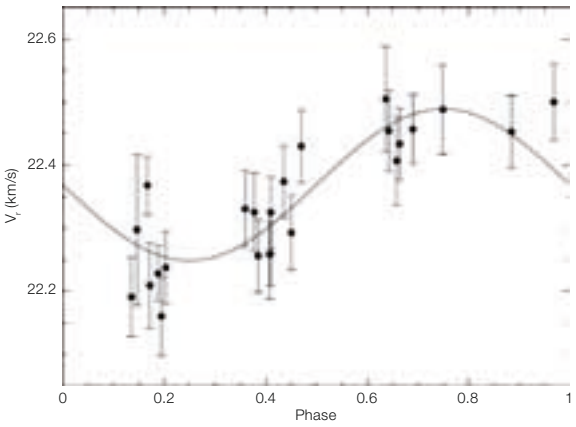

Figure 4. Radial velocity curve for OGLE-TR-182 measured with FLAMES, phased with the photometric transit signal.

The second planet OGLE-TR-211-b

The second planet was not easier to confirm, but we managed to conclude that OGLE-TR-211 is also a planet, in a paper that contains the analysis of candidates OGLE-TR-201 to OGLE-TR-219 (Udalski et al., 2008). Again, we used UVES to determine the stellar parameters: mass M = 1.33 +/– 0.05 $M_{\odot}$, and radius R = 1.64 + 0.21 – 0.07 $M_{\odot}$. Figure 5 shows the FLAMES orbital fit for OGLE-TR-211 obtained with a radial velocity amplitude of 82 m/s and period P = 3.67718 days. It can be seen that the velocity curve is very well sampled, from which we measure a planetary mass of M = 1.0 $M_{Jupiter}$.

The photometric transit measured with FORS (Figure 6) gives a radius of R = 1.36 R_J (see Table 2). This radius is about 20 % larger than the typical radius of

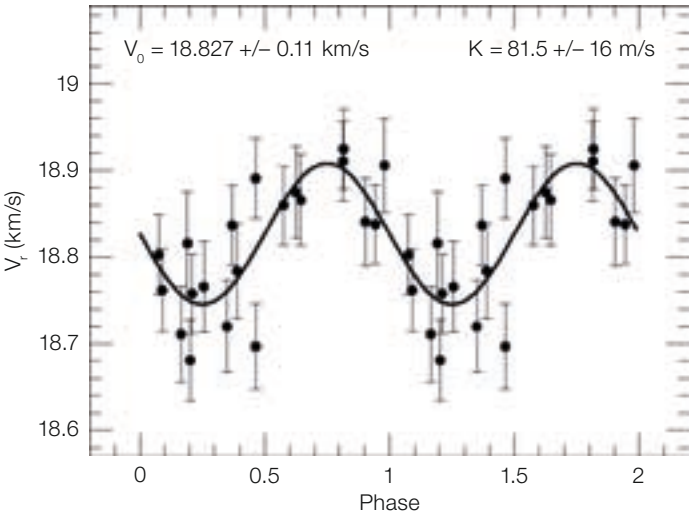

Figure 5. Radial velocity curve for OGLE-TR-211 measured with FLAMES.

hot Jupiters with similar masses. Indeed, this new planet seems to be one of the rare examples of an inflated hot Jupiter, with an unusually low mean density, like HD 209458b. In this case there is some evidence that the velocity of the centre of the mass of the star-planet orbit is changing. Also, slight variations of transit times lead us to suspect that there may be another massive planet in the system that may be perturbing the orbit, but only future observations can confirm if this is real (e.g. due to a companion in the system), or to an instrumental artefact.

Lessons learned

We discovered two new planets! We can now tell with certainty that they are gaseous planets like Jupiter and Saturn, and not rocky like Earth or Venus, nor mostly liquid like Uranus or Neptune. Transiting planets are the only way to get information about their internal structure (and therefore mechanism of formation). Despite the scarce number of such planets, the number starts to be large enough to reveal interesting features. For example, it seems that in order to explain the observed radii, one needs to add a certain quantity of metals in the form of a solid core. It turns out that the mass of this solid core is proportional to the metallicity of the parent star. This trend supports the mode of formation via core accretion (Guillot et al., 2006). However it seems that metallicity is not the only parameter controlling the size of these giant planets, since there are inflated planets around metal rich stars (Torres et al., 2008). The issue is clearly not settled and, in this sense, every new planet counts.

The question can be asked if it isn't more efficient to have a space mission like COROT that focuses on brighter targets? Aside from the obvious answer that a space mission is much more risky and expensive, the LP666 programme, and the observations carried out prior to it, helped the whole team to gain enormously in experience. The team learned how to obtain milli-magnitude photometry, and more importantly, to understand the systematics involved in these kinds of observations (e.g. the red-noise – Pont, 2006). This understanding led to a better (more realistic) prediction of the space mission yields.

In terms of spectroscopic follow-up we learned how to identify the signatures of impostors in an efficient way, and that the candidates that cannot be observed spectroscopically will remain candidates. In particular, we pushed to the limit the FLAMES radial velocity capabilities, and after careful characterisation of these radial velocities, found a precision around 30–50 m/s. More recently, we understood why these two (or three) planets required so much time to be confirmed. They lay in a place that we called the *Twilight Zone* (Pont et al., 2008). When both the photometric and spectroscopic signals are marginal, many more observations are necessary until reasonable certainty can be achieved about the presence of a planetary companion. The uncertainties on the light curve make it difficult to phase the radial velocity data. The high radial velocity uncertainties hinder the identification of an orbital motion with the correct period, and the elimination of eclipsing binary blend scenarios. The OGLE survey is the first to explore this 'twilight zone' in real conditions, since other ground-based surveys target brighter stars, for which very precise radial velocities can be obtained, so that the significance of the radial velocity signal can be established relatively easily. All this *savoir-faire* is already being used in the COROT mission, and would again be useful when the KEPLER mission flies.

References

Bouchy, F., et al. 2005, A&A, 431, 1105
Guillot, T., et al. 2006, A&A, 453, L21
Pont, F. 2006, MNRAS, 373, 231
Pont, F., et al. 2005, A&A, 438, 1123
Pont, F., et al. 2008, A&A, in press
Torres, G., et al. 2008, ApJ, 677, 1324
Udalski, A., et al. 2008, A&A, 482, 299

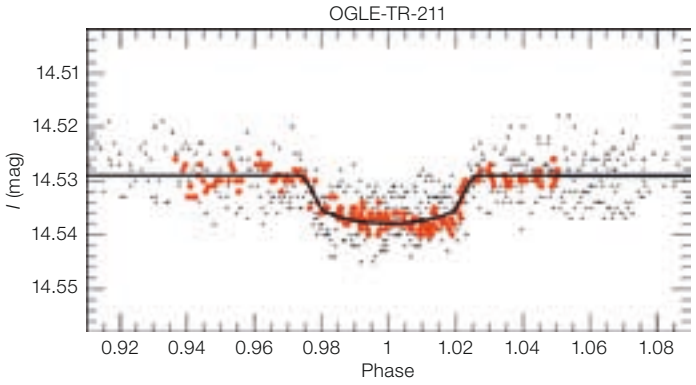

Figure 6. Light curve of the transit of OGLE-TR-211 measured with FORS2.

Probing Sagittarius A* and its Environment at the Galactic Centre: VLT and APEX Working in Synergy

Andreas Eckart[1,2]
Rainer Schödel[3]
Macarena García-Marín[1]
Gunther Witzel[1]
Axel Weiss[2]
Frederick Baganoff[4]
Mark R. Morris[5]
Thomas Bertram[1]
Michal Dovčiak[6]
Dennis Downes[7]
Wolfgang Duschl[8,9]
Vladimír Karas[6]
Sabine König[1]
Thomas Krichbaum[2]
Melanie Krips[10]
Devaky Kunneriath[1,2]
Ru-Sen Lu[2,1]
Sera Markoff[11]
Jon Mauerhan[5]
Leo Meyer[5]
Jihane Moultaka[12]
Koraljka Mužić[1]
Francisco Najarro[13]
Jörg-Uwe Pott[5,17]
Karl Schuster[7]
Loránt Sjouwerman[14]
Christian Straubmeier[1]
Clemens Thum[7]
Stuart Vogel[15]
Helmut Wiesemeyer[16]
Mohammad Zamaninasab[1,2]
Anton Zensus[2]

[1] University of Cologne, Cologne, Germany
[2] Max-Planck-Institut für Radioastronomie, Bonn, Germany
[3] Instituto de Astrofísica de Andalucía, Granada, Spain
[4] Centre for Space Research, Massachusetts Institute of Technology, Cambridge, USA
[5] Department of Physics and Astronomy, University of California, Los Angeles, USA
[6] Astronomical Institute, Academy of Sciences, Prague, Czech Republic
[7] Institut de Radio Astronomie Millimétrique, St. Martin d'Heres, France
[8] Institut für Theoretische Physik und Astrophysik, Christian-Albrechts-Universität, Kiel, Germany
[9] Steward Observatory, The University of Arizona, Tucson, USA
[10] Harvard-Smithsonian Centre for Astrophysics, Cambridge, USA
[11] Astronomical Institute "Anton Pannekoek", University of Amsterdam, the Netherlands
[12] LATT, Université de Toulouse, CNRS, Toulouse, France
[13] DAMIR, Instituto de Estructura de la Materia, Consejo Superior de Investigaciones Científicas, Madrid, Spain
[14] National Radio Astronomy Observatory, Socorro, USA
[15] Department of Astronomy, University of Maryland, College Park, USA
[16] IRAM, Granada, Spain
[17] W. M. Keck Observatory, CARA, Kamuela, USA

On 3 June 2008 an international team of researchers observed one of the brightest near-infrared flares close to SgrA*, the black hole at the centre of the Milky Way. For the very first time the flare emission was detected in infrared light, with one of the VLT telescopes, and time delayed in sub-millimetre radiation with the APEX telescope. Recent simultaneous X-ray and infrared flares from SgrA* have been detected and can be explained by spots on relativistic orbits around the central, accreting supermassive black hole. The observations of flares now also show some evidence for time evolution of the spot properties. The investigation of dusty stars and filaments in the central stellar cluster also indicates the presence of a wind from the central region – possibly with a contribution from SgrA* itself.

At the centre of the Milky Way, at a distance of only about 8 kpc, stellar orbits have convincingly proven the existence of a supermassive black hole (SMBH) of mass ~ 3.7×10^6 $M_\odot$ at the position of the compact radio, infrared, and X-ray source Sagittarius A* (SgrA*; see Eckart et al., 2002; Schödel et al., 2002; Eisenhauer et al., 2003; Ghez et al., 2005; and following publications). Additional strong evidence for an SMBH at the position of SgrA* comes from the observation of rapid flare activity both in the X-ray and near-infrared (NIR) wavelength domain (Baganoff et al., 2001; Genzel et al., 2003; Ghez et al., 2004; Eckart et al., 2006).

On account of its proximity, SgrA* provides us with a unique opportunity to understand the physics and possibly the evolution of SMBHs in the nuclei of galaxies. Variability at radio through sub-millimetre (sub-mm) wavelengths has been studied extensively, showing that variations occur on timescales from hours to years (e.g. Mauerhan et al., 2005; Eckart et al., 2006a; Yusef-Zadeh et al., 2008; Marrone et al., 2008). Several flares have provided evidence for decaying mm and sub-mm emission following NIR/X-ray flares.

The combined APEX/VLT measurements

The sub-mm regime is of special interest for simultaneous flare measurements. Here synchrotron source components that radiate also in the infrared domain become optically thick, and represent the dominant reservoir of photons that are then scattered to the X-ray domain through the inverse Compton process. Substantial progress was made during a global observing session on SgrA* in May/June 2008. On 3 June, for the first time, observations of the Galactic Centre were performed with ESO telescopes operating in the NIR and sub-mm wavelength domains, that resulted in the simultaneous successful detection of strongly variable emission. Such a clear detection with ESO telescopes at both wavelengths had not been achieved in several previous attempts. It was made possible through a special effort by the APEX/ONSALA staff to have the LABOCA bolometer ready for triggering.

At an angular resolution of 100 milliarcseconds, *K*- and *L'*-band (2.2 µm and 3.8 µm respectively) images were taken with the NAOS/CONICA adaptive optics assisted imager at VLT UT4 (Yepun). The calibrated images were deconvolved using a Lucy-Richardson algorithm. Sub-millimetre data were taken with LABOCA on APEX. The Atacama Pathfinder Experiment (APEX) is a new-technology 12-m telescope, based on an ALMA (Atacama Large Millimeter Array) prototype antenna, and operating at the Llano de Chajnantor at an altitude of 5105 m. APEX is a collaboration between the Max-Planck-Institut für Radioastronomie, the Onsala Space Observatory and ESO.

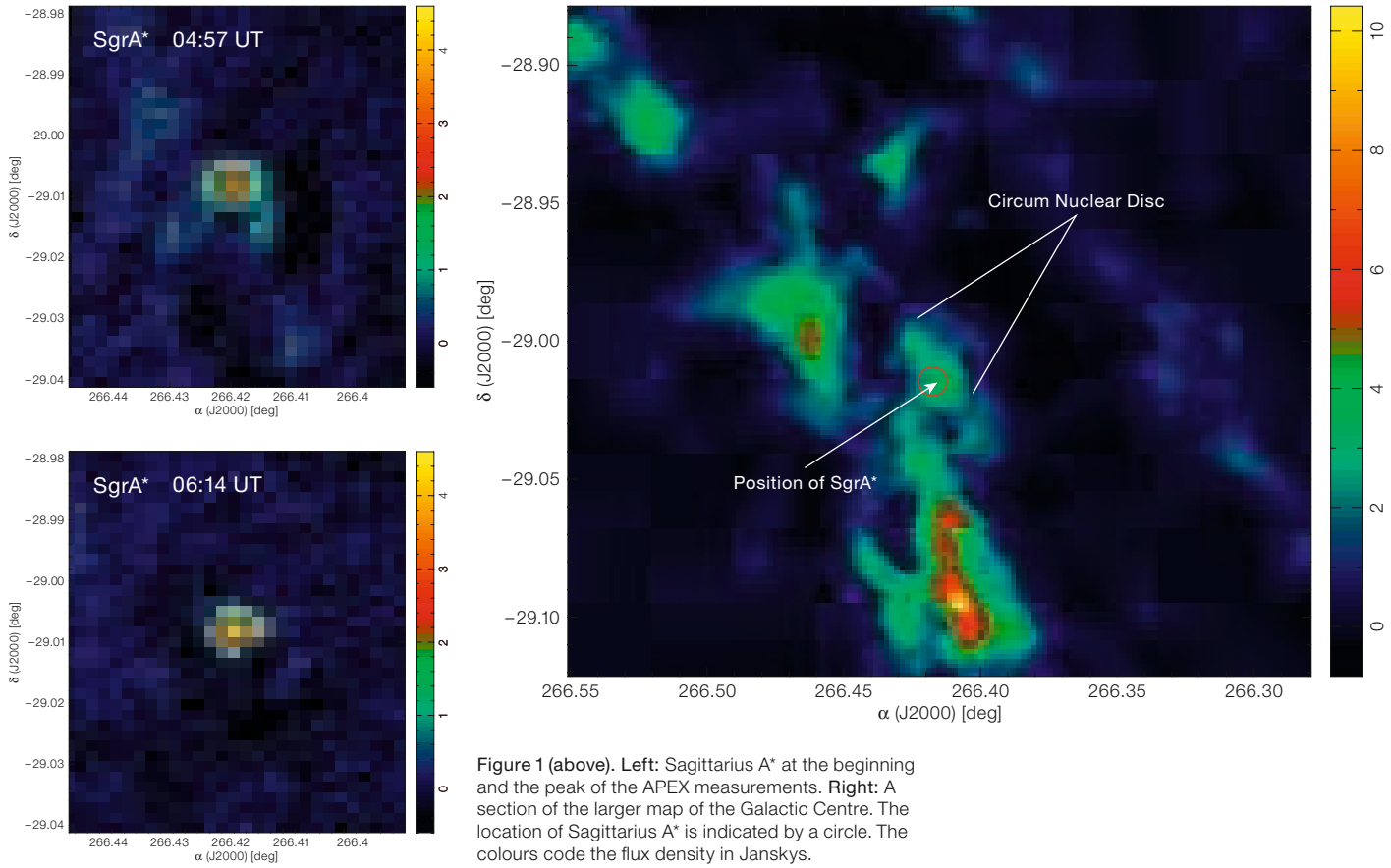

Figure 1 (above). Left: Sagittarius A* at the beginning and the peak of the APEX measurements. **Right:** A section of the larger map of the Galactic Centre. The location of Sagittarius A* is indicated by a circle. The colours code the flux density in Janskys.

The radiation collected by the APEX telescope is directed to the LArge BOlometer CAmera (LABOCA) in the Cassegrain cabin. LABOCA consists of an array of 295 composite bolometers, which are cooled to a temperature of less than 0.3 K, and are very sensitive to continuum radiation (see Siringo et al., 2007). With a total bandwidth of about 60 GHz the system is optimised for the 345 GHz atmospheric window. The final relative calibration was obtained by comparison to and subtraction of a high signal-to-noise reference map in which SgrA* was subtracted out and therefore effectively set in an off state (see Figure 1 right). The resulting light curves are shown in Figure 2. Each data point of the sub-mm light curve was derived from a full 48′ × 25′ fully sampled map obtained with the 19.2″ APEX beam.

The combined *K*- and *L*′-band data (Figure 2) show violently variable emission with at least four prominent flare events (I–IV). The sub-mm data start with a low flux density at the time of the first NIR flare. The gap in the sub-mm data occurred during culmination of SgrA*, when the source rises above the elevation limit (80°) for observations with APEX. A preliminary model fit to the variable sub-mm emission is shown in comparison to the data in Figure 2. We attribute the time difference between the NIR and sub-mm flares to an adiabatic expansion of synchrotron source components with an expansion speed of about 0.5 % of the speed of light (1500 km/s). With a spectral index between the sub-mm and the

Figure 2 (right). The near-infrared (top) and sub-mm (bottom) light curve of Sagittarius A*. The data points are represented by vertical red bars (with ±1σ error bars) with a black connecting line between them. The dashed line represents a smoothed version of the data (after application of a seven point sliding average for all data points except the first). The model – as described in the text – is shown as a thick solid line. To select the intra-day variable part of the sub-mm data, a flux density of 3.25 Jy has been subtracted. This amount is attributed to more extended (many Schwarzschild radii) source components.

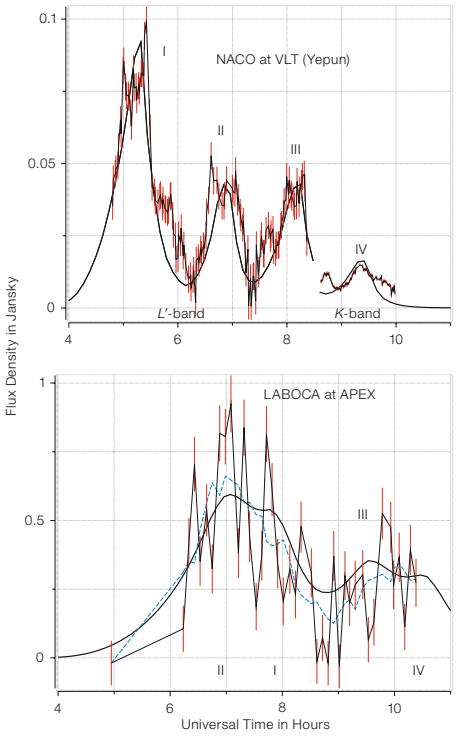

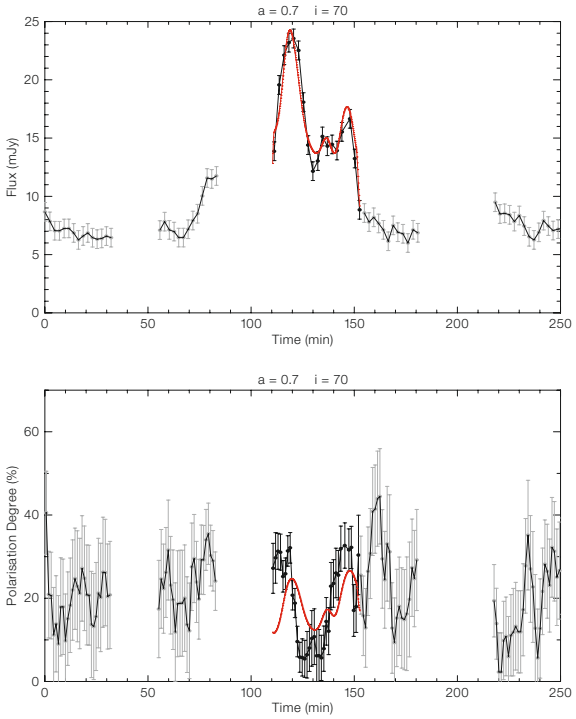

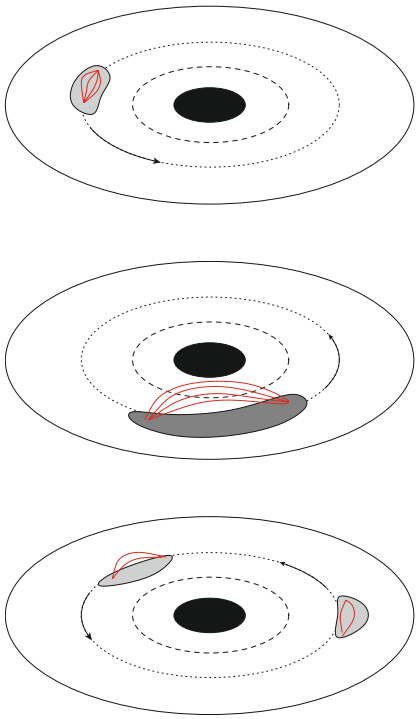

Figure 3. **Left:** Fit of the 2006 flare data with an evolving spot model. We show the total flux and degree of polarisation for a single spot during two revolutions for a perpendicular E-field configuration (for details see Eckart et al., 2008). **Right:** Sketch of an expanding hot spot within an inclined temporary accretion disc of SgrA*. The black centre indicates the event horizon of the massive black hole; the solid line the outer edge of the accretion disc. The long dashed line marks the inner last stable orbit. The dotted line represents a random reference orbit to show the effect of differential rotation of an extended emission region. The red solid line across the grey shaded extended spots depict the magnetic field lines that, through magneto-hydrodynamical instabilities, provide a coupling between disc sections at different radii.

infrared of about $-0.8 \leq \alpha \leq -1.4$, we find that the flares are associated with source components that have sizes of the order of one Schwarzschild radius and spectra that peak around 1–3 THz with flux densities of a few Janskys. In the sub-mm domain the flares blend with each other. Models with significantly different expansion speeds or source sizes fail to represent either the extent or the shape of the observed flare features. These data show that the VLT/APEX combination is especially well suited for very long simultaneous light curves between the NIR and the sub-mm domain.

The adiabatic expansion results in a time difference between the peaks in the VLT and APEX light curves of about 1.5 to 2 hours. This compares well with the values obtained in a global, multi-wavelength observing campaign by our team in 2007. Two bright NIR flares were traced by CARMA (Combined Array for Research in mm-wave Astronomy; 100 GHz) in the US, ATCA (Australia Telescope Compact Array; 86 GHz) in Australia, and the MAMBO bolometer at the IRAM 30-m in Spain (230 GHz; first results given by Kunneriath et al., 2008). This light curve complements our parallel 13, 7, and 3 mm VLBA run (Lu et al., 2008).

Simultaneous multi-wavelength observations indicate the presence of adiabatically expanding source components with a delay between the X-ray and sub-mm flares of about 100 minutes (Eckart et al., 2006a; Yusef-Zadeh et al., 2008; Marrone et al., 2008). From modelling the mm-radio flares at individual frequencies, Yusef-Zadeh et al. (2008) invoke expansion velocities in the range from v_{exp} = 0.003 – 0.1 c, which is small compared to the expected relativistic sound speed in orbital velocity in the vicinity of the SMBH. The low expansion velocities suggest that the expanding gas cannot escape from SgrA* or must have a large bulk motion (Yusef-Zadeh et al., 2008). Therefore the adiabatically expanding source components either have a bulk motion larger than v_{exp} or the expanding material contributes to a corona or disc, confined to the immediate surroundings of SgrA*.

Polarised emission from an accretion disc?

X-ray and polarised infrared emission of flares allow an even deeper insight into the processes that show some of their dominant signatures in the sub-mm domain. Recent NIR polarisation measurements have revealed that the emission of SgrA* is significantly polarised during flares. It consists of a non- or weakly-polarised main flare with highly polarised sub-flares (Eckart et al., 2006a; Meyer et al., 2007 and references therein). These are the first NIR polarimetric observations of a source clearly operating in the strong-gravity regime. Therefore they are important to test general relativity models of accreting SMBHs. In several cases the flare activity suggests a quasi-periodicity of ~ 20 min. By simultaneous fitting of the light curve fluctuations and the time-variable polarisation angle, we show that the data can be successfully modelled with a simple relativistic hot spot/ring model. In this model the broad NIR flares (~ 100 minutes duration) of SgrA* are due to a sound wave that travels around the SMBH once. The sub-flares, superimposed on the broad flare, are then caused by the Doppler-boosted spot emission, which is thought to be due to transiently heated and accelerated electrons of a plasma component. Recent investigations of infrared light curves show that significant contributions due to a red noise process (i.e. larger amplitudes towards lower frequencies) are likely as well (Do et al., 2008; Meyer et al., 2008).

In the presence of an extended disc structure, such a contribution can also be modelled through multiple components with properties following power spectrum distributions (Eckart et al., 2008; and below). The spots would then be the brightest contributors to the overall flux density. Scenarios in which spiral wave structures contribute to the observed variability are also under discussion (e.g. Karas et al., 2007).

VLT and Chandra provide indications for spot evolution

The May 2007 polarimetric NIR measurements showed a flare event with the highest sub-flare contrast observed until now. In the relativistic disc model these data provide direct evidence for a spot expansion and its shearing due to differential rotation (Figure 3). An expansion by only 30 % will lower the Synchrotron-Self-Compton (SSC) X-ray flux significantly. Therefore this scenario may explain the July 2004 flare (Eckart et al., 2006a) and possibly also the 17 July 2006 flare reported by Hornstein et al. (2007). In these events a strong NIR/X-ray flare was followed by a weaker NIR flare with no X-ray activity.

In summary, a combination of a temporary accretion disc with a short jet can explain most of the properties associated with infrared/X-ray SgrA* light curves (Eckart et al., 2008). The close correlation between the NIR and X-ray flares can be explained by combining relativistic amplification curves with a simple SSC mechanism. This explanation allows a zeroth order interpretation within a time-dependent flare emission model. We use a synchrotron model with an optically thin spectral index of $0.4 \leq \alpha \leq 1.3$ and relativistic electrons with boosting factor $\gamma_e \sim 10^3$. The source component flux densities are represented by a power spectrum $N(S) \propto S_m^{\alpha_S}$ with α_S close to –1. Such a multi-component model explains possible quasi-periodic sub-flare structure at infrared wavelengths, and shows that with adequate sensitivity and time resolution they should be detectable in the X-ray domain as well.

Further simultaneous radio/sub-mm data, NIR *K*- and *L*-band measurements in combination with X-ray observations should lead to a set of light curves that will allow us to prove the proposed model and to discriminate between the individual higher and lower energy flare events. Here Chandra's high angular resolution is ideally suited to separate the thermal non-variable bremsstrahlung from the non-thermal variable part of the SgrA* X-ray flux density for weak flares.

Indications for an outflow from Sagittarius A*?

Well within the central stellar cluster (Schödel et al., 2007), *L'*-band (3.8 μm) images of the Galactic Centre show a large number of long and thin filaments in the mini-spiral, located west of the mini-cavity and along the inner edge of the Northern Arm (Figure 4). Mužić et al. (2007) present the first proper motion measurements of these filaments and show that the shape and motion of the filaments do not agree with a purely Keplerian motion of the gas in the potential of the SMBH. The authors argue that the properties of the filaments are probably related to an outflow from a disc of young mass-losing stars or (in part) from the SMBH itself. In addition Mužić et al. (2007) also present the proper motions of two cometary shaped dusty sources close (in projection) to SgrA* (Figure 4). The proper motion of the stars X7 and X3 are at large angles to its V-shape. Therefore these dust shells indicate an interaction with a fast wind in the Galactic Centre ISM. The V-shapes of both sources are pointed towards the position of SgrA* and therefore represent the most direct indication for a wind from SgrA*. The wind responsible for the V-shape of the sources may in fact be the same wind that was claimed to be responsible for the formation of the mini-cavity in the mini-spiral.

Further evidence for young stars in the central cluster

The presence and formation of stars in the central parsec is a long standing problem. Only half an arcsecond north of IRS 13E there is a complex of extremely red sources, called IRS 13N. Their nature is still unclear. Based on the analysis of their colours, they may either be dust-embedded sources, older than a few Myrs, or extremely young objects with ages less than 1 Myr. Mužić et al. (2008) pre-sent the first proper motion measurements of IRS 13N members and give proper motions of four of IRS 13E stars resolved in NACO *L'*-band images. They show that six of seven resolved northern sources show a common proper motion, thus revealing a new comoving group of stars in the central half a parsec of the Milky Way. The common proper motions of the IRS 13E and IRS 13N clusters are also significantly different. By fitting the positional data for those stars onto Keplerian orbits, assuming SgrA* as the centre of the orbit, Mužić et al. (2008) could demonstrate that the IRS 13N association also indicates a dynamically

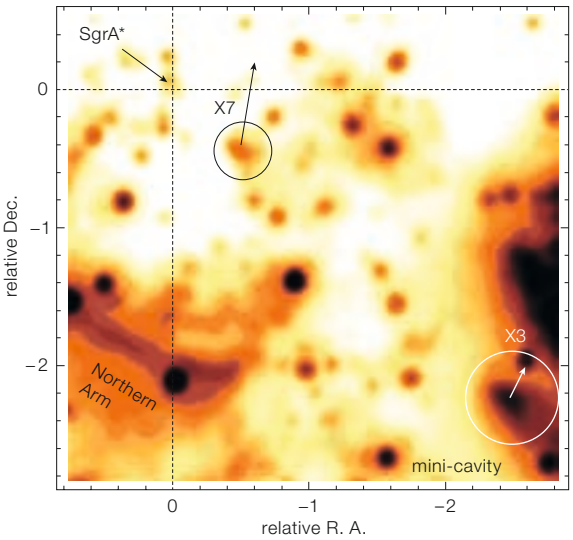

Figure 4. A 3.8″ × 3.8″ section of an *L'*-band image showing SgrA* and the two cometary shaped sources X3 and X7, which have proper motions of 155 ± 30 km/s and 463 ± 30 km/s respectively. The V-shaped dust shells indicate an interaction with a strong wind in the local Galactic Centre ISM. The V-shapes of both sources are pointed toward the position of SgrA*, suggesting that the wind originates in the immediate surroundings of SgrA*.

young system of stars and therefore is in favour of the very young star hypothesis.

New VLTI results in the central stellar cluster

In addition to the MIDI VLTI results on IRS 3 (Pott et al., 2008a), Pott et al. (2008b) now present the first spectro-interferometry on IRS 7, which is a prime reference source for Galactic Centre observations at the highest angular resolution. The VLTI-AMBER and MIDI instruments were used to spatially resolve IRS 7 and to measure the wavelength dependence of the visibility using the low spectral resolution mode ($\lambda/\Delta\lambda \sim 30$) and projected baseline lengths of about 50 m. The observations resulted in an angular resolution of about 9 mas (74 AU) and 45 mas (370 AU) for the NIR and MIR, respectively. The first *K*-band fringe detection of a star in the central parsec suggests that IRS 7 is possibly marginally resolved at 2 μm. At 10 μm wavelength, IRS 7 is strongly resolved with a visibility of approximately 20 % of the total flux density. This would imply that the photosphere of the supergiant is enshrouded by a molecular and dusty envelope.

References

Baganoff, F. K., et al. 2001, Nature, 413, 45
Do, T., et al. 2008, JPhCS, accepted and ApJ, submitted
Eckart, A., et al. 2008, A&A, 479, 625
Eckart, A., et al. 2006, A&A, 450, 535
Eckart, A., et al. 2002, MNRAS, 331, 917
Eisenhauer, F. 2003, ApJ, 597, L121
Genzel, R., et al. 2003, Nature, 425, 934
Ghez, A. M., et al. 2004, ApJ, 601, 159
Ghez, A. M., et al. 2005, ApJ, 620, 744
Karas, V., et al. 2007, Proceedings of the Workshop on Black Holes and Neutron Stars, eds. S. Hledik & Z. Stuchlik, 99 (astro-ph0709.3836)
Kunneriath, D., et al. 2008, JPhCS, accepted
Hornstein, S. D., et al. 2007, ApJ, 667, 900
Lu, R.-S., et al. 2008, JPhCS, accepted
Marrone, D. P., et al. 2008, ApJ, in press (arXiv0712.2877M)
Mauerhan, J. C., et al. 2005, ApJ, 623, L25
Meyer, L., et al. 2007, A&A, 473, 707
Meyer, L., et al. 2008, ApJ, submitted
Mužić, K., et al. 2008, A&A, 482, 173
Mužić, K., et al. 2007, A&A, 469, 993
Pott, J.-U., et al. 2008a, A&A, 480, 115
Pott, J.-U., et al. 2008b, A&A, in press (arXiv:0805.4408)
Schödel, R., et al. 2002, Nature, 419, 694
Schödel, R., et al. 2007, A&A, 469, 125
Siringo, G., et al. 2007, The Messenger, 129, 2
Yusef-Zadeh, F., et al. 2008, ApJ, accepted (arXiv0712.2882Y)

False colour near-infrared image of the central parsec of the Milky Way as obtained from data taken in the *H*, *Ks*, and *L'* filters with the VLT adaptive optics camera system NACO in 2004. Red sources are brighter at longer wavelengths. The image is dominated by the bright stars of the central star cluster and the diffuse emission of the dusty mini-spiral. Image credit: Rainer Schödel and Andreas Eckart.

Stellar Populations of Bulges of Disc Galaxies in Clusters

Lorenzo Morelli[1,5]
Emanuela Pompei[2]
Alessandro Pizzella[1]
Jairo Méndez-Abreu[1,3]
Enrico Maria Corsini[1]
Lodovico Coccato[4]
Roberto Saglia[4]
Marc Sarzi[6]
Francesco Bertola[1]

[1] Dipartimento di Astronomia, Università di Padova, Italy
[2] ESO
[3] INAF-Osservatorio Astronomico di Padova, Italy
[4] Max-Planck-Institut für Extraterrestrische Physik, Garching, Germany
[5] Department of Astronomy, Pontificia Universidad Católica de Chile, Santiago, Chile
[6] Centre for Astrophysics Research, University of Hertfordshire, Hatfield, United Kingdom

Photometry and long-slit spectroscopy are presented for 14 S0 and spiral galaxies of the Fornax, Eridanus and Pegasus clusters and the NGC 7582 group. The age, metallicity and α/Fe enhancement of the stellar population in the centres and their gradients are obtained using stellar population models with variable element abundance ratios. Most of the sample bulges display solar α/Fe enhancement, no gradient in age, and a negative gradient of metallicity. One of the bulges, that of NGC 1292, is a pseudobulge and the properties of its stellar population are consistent with a slow build-up within a scenario of secular evolution.

The relative importance of dissipative collapse (Gilmore & Wyse, 1998), major and minor merging events (Aguerri, Balcells & Peletier, 2001), and redistribution of disc material due to the presence of a bar or environmental effects (Kormendy & Kennicutt, 2004) drives the variety of observed properties in bulges. The bulges of lenticulars and early-type spirals are similar to low-luminosity elliptical galaxies and their photometric and kinematic properties satisfy the same fundamental plane (FP) correlation found for ellipticals. The surface-brightness radial profile of large bulges is well described by the de Vaucouleurs law, although this law can be drastically changed taking into account the small-scale inner structures, smoothed by the seeing in ground-based observations. Some bulges are rotationally-flattened oblate spheroids with little or no anisotropy. But, the intrinsic shape of a large fraction of early-type bulges is triaxial, as shown by the isophotal misalignment with respect to their host discs and non-circular gas motions. The bulk of their stellar population formed between redshifts 3 and 5 (~ 12 Gyr ago) over a short timescale. The enrichment of the interstellar medium is strongly related to the time delay between type II and type Ia supernovae, which contributed most of the α elements and iron, respectively.

On the contrary, the bulges of late-type spiral galaxies are reminiscent of discs. They are flat components with exponential surface brightness radial profiles and rotate as fast as discs. Moreover, the stellar population in late-type bulges is younger than in early-type bulges. They appear to have lower metallicity and lower α/Fe enhancement with respect to early-type galaxies.

In the current paradigm, early-type bulges were formed by rapid collapse and merging events, while late-type bulges have been slowly assembled by internal and environmental secular processes (Kormendy & Kennicutt, 2004). But many questions are still open. For instance, the monolithic collapse scenario cannot explain the presence in bulges of kinematically-decoupled components. Moreover, the environment plays a role in defining the properties of galaxies. Recent studies of early-type galaxies in different environments have shown that age, metallicity, and α/Fe enhancement are more correlated with the total mass of the galaxy than local environment.

To investigate the formation and evolution of bulges, there are two possible approaches: going back in redshift and looking at the evolution of galaxies through cosmic time; or analysing nearby galaxies in detail to understand the properties of their stellar population in terms of the dominant mechanism at the epochs of star formation and mass assembly. We present a photometric and spectroscopic study of the bulge-dominated region of a sample of spiral galaxies in clusters. Our aim is to estimate the age and metallicity of the stellar population and the efficiency and timescale of the last episode of star formation in order to disentangle early rapid assembly from late slow growth of bulges.

Sample, photometry, and spectroscopy

In order to simplify the interpretation of the results, we selected a sample of disc galaxies, which do not show any morphological signature of having undergone a recent interaction event. All the observed galaxies are classified as non-barred or weakly barred galaxies. They are bright ($B_T \leq 13.5$) and nearby (D < 50 Mpc) lenticulars and spirals with a low-to-intermediate inclination ($i \leq 65^\circ$). Twelve of them were identified as members of the Fornax, Eridanus and Pegasus clusters and a further two are members of the NGC 7582 group.

The photometric and spectroscopic observations of the sample galaxies were carried out in three runs at ESO La Silla in 2002 (run 1), 2003 (run 2) and 2005 (run 3). We imaged the galaxies with the Bessel *R*-band filter. In runs 1 and 2 spectra were taken at the 3.6-m telescope with EFOSC2; in run 3 spectra were obtained with EMMI on the NTT in red medium-dispersion mode.

In order to derive the photometric parameters of the bulge and disc, we fitted iteratively a model of the surface brightness to the pixels of the galaxy image using a non-linear least-squares minimisation. We adopted the technique for photometric decomposition developed in GASP2D by Méndez-Abreu et al. (2008, see Figure 1). We measured the stellar kinematics from the galaxy absorption features present in the wavelength range and centred on the Mg line triplet at 5 200 Å by applying the Fourier correlation quotient method (Bender et al., 1994). We also measured the Mg, Fe, and H_β line-strength indices from the flux-calibrated spectra. We indicate the average iron index with <Fe> = (Fe5270 + Fe5335)/2, and the magnesium-iron index with [MgFe]′ = Mg_b (0.72 × Fe5270 + 0.28 × Fe5335) (see Fig-

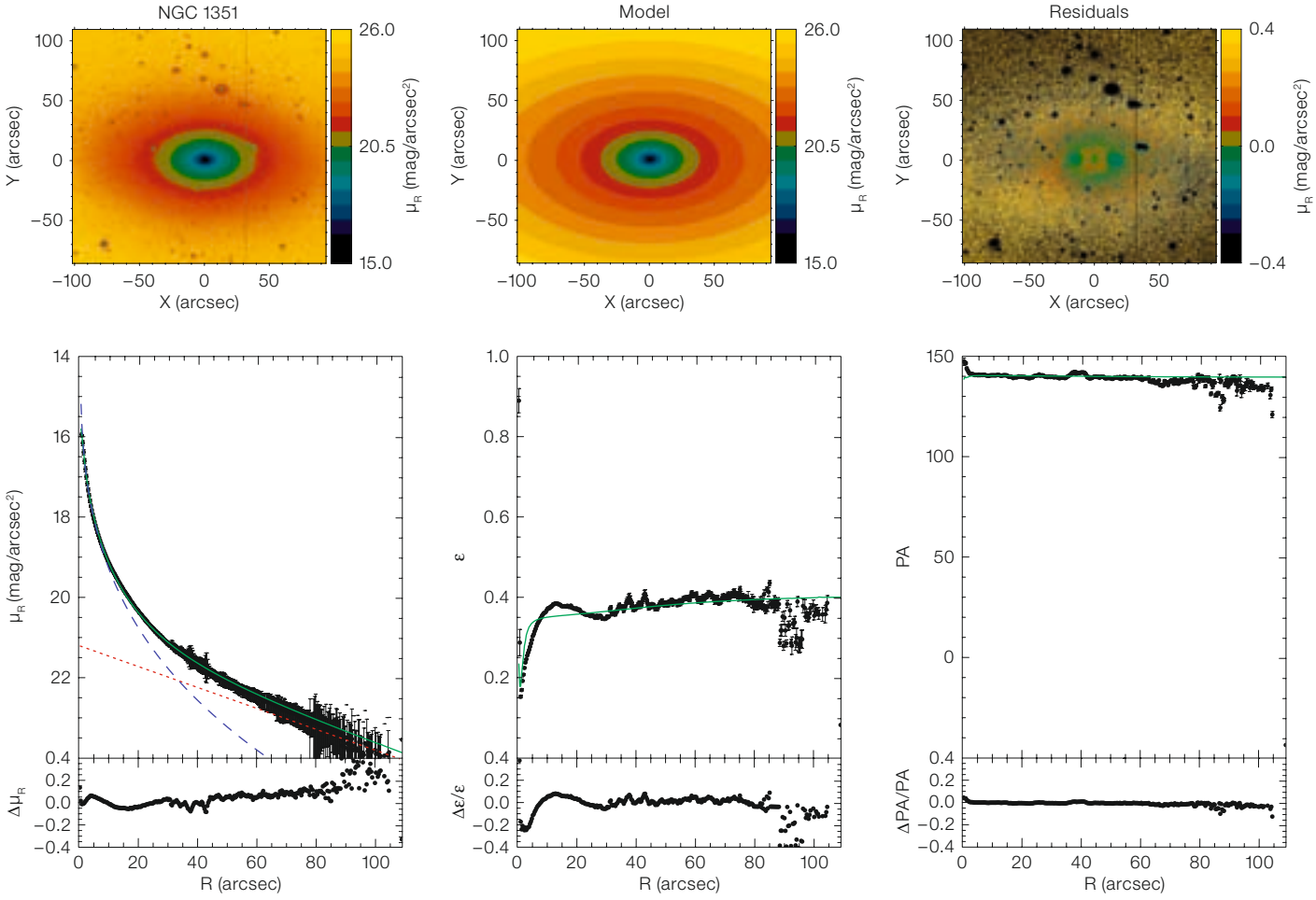

Figure 1 (above). Two-dimensional photometric decomposition of a sample galaxy, NGC 1351. **Upper panels (from left to right):** Map of the observed, modelled and residual (observed-modelled) surface-brightness distribution of the galaxy. **Lower panels (from left to right):** Ellipse-averaged radial profile of surface-brightness, position angle, and ellipticity measured in the observed (dots with error-bars) and modelled image (solid line). Residuals on the observed model are shown in the bottom plots.

ure 2). The H_β line-strength index was measured from the resulting H_β absorption line, after the emission line was subtracted from the observed spectrum.

Age, metallicity, and α/Fe enhancement: central values

From the central line-strength indices we derived the mean ages, total metallicities and total α/Fe enhancements of the stellar populations in the centre of the

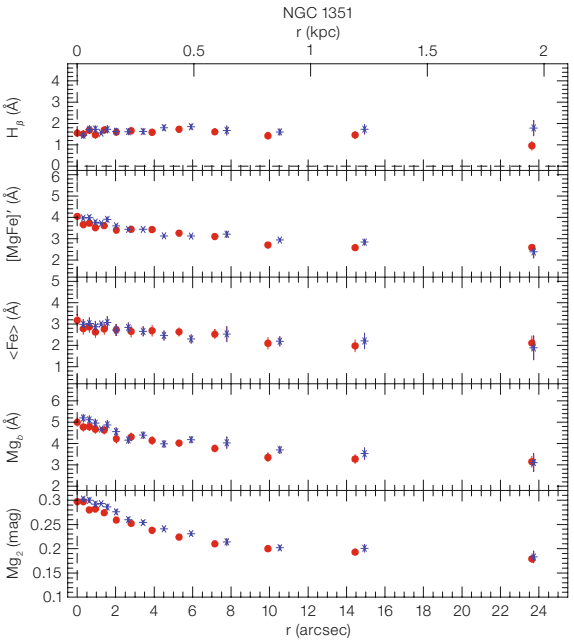

Figure 2. The line-strength indices measured along the major axes of one of the sample galaxies, NGC 1351. **From top to bottom:** East-west folded radial profiles of H_β, [MgFe]′, <Fe>, Mg_b, and Mg_2. Asterisks and dots refer to the two sides (east/west) of the galaxy.

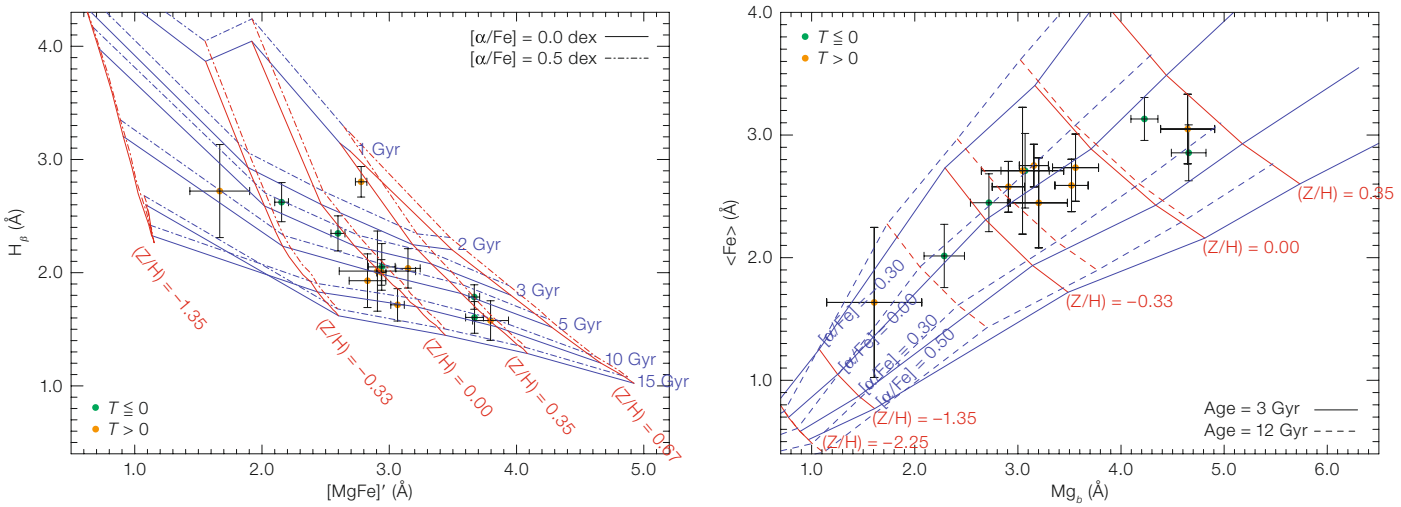

Figure 3 (above). The distribution of the central values of H_β and [MgFe]′ indices (left panel) and <Fe> and Mg_b indices (right panel) averaged over 0.3 r_e for the 15 sample galaxies. Points are coloured according to their RC3 galaxy type. The lines indicate the models by Thomas et al. (2003). **Left panel:** The age–metallicity grids are plotted with two different α/Fe enhancements: [α/Fe] = 0.0 dex (continuous lines) and [α/Fe] = 0.5 dex (dashed lines). **Right panel:** The [α/Fe]–metallicity grids are plotted with two different ages: 3 Gyr (continuous lines) and 12 Gyr (dashed lines).

sample bulges by using the stellar population models of Thomas et al. (2003) shown in Figure 3. These models predict the values of the line-strength indices for a single stellar population as function of the age, metallicity, and [α/Fe] ratios.

Three classes of objects were identified, according to their age and metallicity (Figure 4). The young bulges are scattered about an average age of 2 Gyr with hints of star formation, as shown by the presence of the H_β emission line in their spectra. The intermediate-age bulges span the age range between 4 and 8 Gyr. They are characterised by solar metallicity. Finally, the old bulges have high metallicity and a narrow distribution in age around 10 Gyr.

Although the correlations are not statistically very strong, the elliptical and S0 galaxies ($T < 0$, where T is the numerical RC3 galaxy type) have bulges older and more metal-rich than the spirals ($T > 0$) in the central region. Most of the sample bulges display solar α/Fe enhancements with the median of the distribution at [α/Fe] = 0.07 dex (Figure 4, right panel).

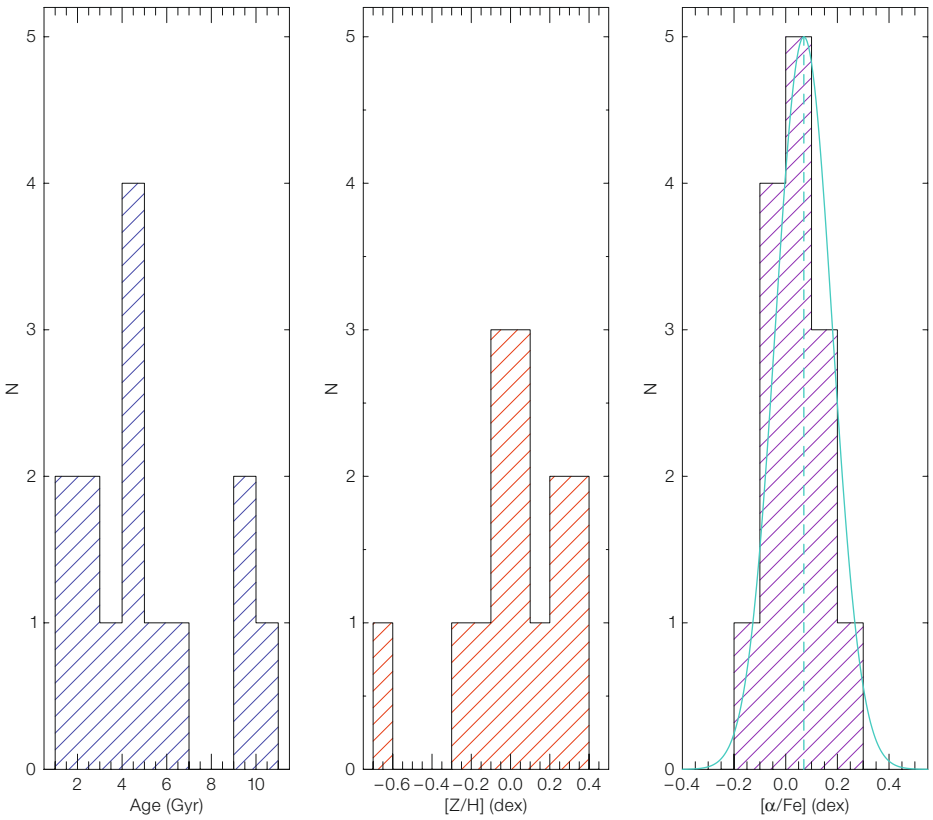

Figure 4. Distribution of age (left panel), metallicity (central panel) and α/Fe enhancement (right panel) for the central regions of the sample galaxies. The solid line in the right panel represents a Gaussian centred at the median value [α/Fe] = 0.07 dex of the distribution. Its width, σ = 0.11, is approximated by the value containing 68 per cent of the objects of the distribution.

Age is mildly correlated with velocity dispersion, and α/Fe enhancement. We conclude that the more massive bulges of our sample galaxies are older, more metal-rich and characterised by rapid star formation.

Age, metallicity and α/Fe enhancement: gradients

Different formation scenarios predict different radial trends of age, metallicity, and α/Fe enhancement. Therefore the radial gradients of the properties of the stellar populations of bulges are a key piece of information to understand the processes of their formation and evolution. In the monolithic collapse scenario, gas dissipation towards the galaxy centre, with subsequent occurrence of star formation and galactic winds, produce a steep metallicity gradient. A strong gradient in α/Fe enhancement is expected too. The predictions for bulges forming through long time-scale processes, such as dissipationless secular evolution, are more contradictory. In the latter scenario the bulge is formed by redistribution of disc stars. The gradients possibly present in the progenitor disc could be either amplified, since the resulting bulge has a smaller scalelength than the progenitor, or erased as a consequence of disc heating (Moorthy & Holtzman, 2006).

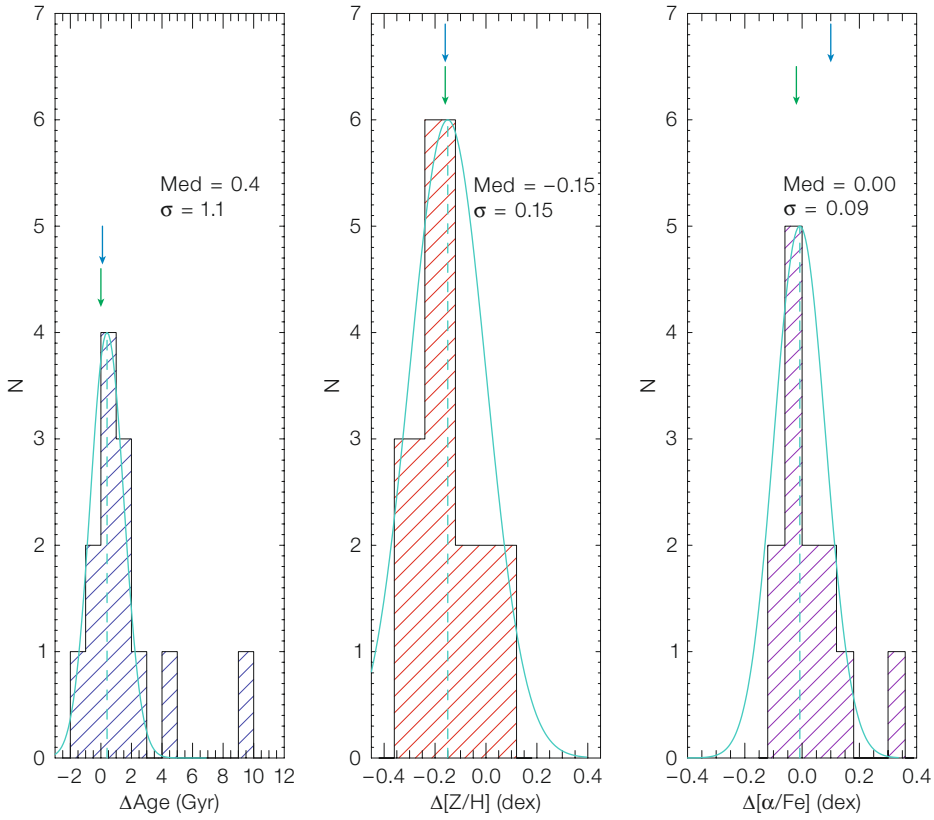

Figure 5. Distribution of the gradients of age (left panel), metallicity (central panel) and α/Fe enhancement (right panel) within radius r_{bd} at which bulge and disc give equal brightness contributions for the sample galaxies. Dashed line represents the median of the distribution and its value is listed. Solid line represents a Gaussian centred at the median value of the distribution. The width of the distributions, σ, are approximated by the value containing 68 per cent of the objects and are also listed. The green and blue arrows show the average gradient found for early-type galaxies and bulges by Mehlert et al. (2003) and Jablonka et al. (2007), respectively.

An issue in measuring the gradients of age, metallicity, and [α/Fe] in bulges could be the contamination of their stellar population by the light coming from the underlying disc stellar component. This effect is negligible in the galaxy centre but it could increase going to the outer regions of the bulge, where the light starts to be dominated by the disc component. In order to reduce the impact of disc contamination and extend as much as possible the region in which gradients were derived, we mapped them inside r_{bd}, the radius where the bulge and disc give the same contribution to the total surface brightness. For each galaxy, we derived the Mg_2, H_β , and <Fe> line-strength indices at the radius r_{bd}. The gradients were set as the difference between the values at centre and r_{bd}, and their corresponding errors were calculated through Monte Carlo simulations. The indices were converted into gradients of age, metallicity, and α/Fe enhancement following Thomas et al. (2003) and are shown in Figure 5.

Most of the sample galaxies show no gradient in age with the median of the distribution at 0.4 Gyr. Negative gradients of metallicity were observed and the number distribution shows a clear peak at [Z/H] = −0.15 dex. The presence of a negative gradient in the metallicity radial profile favours a scenario with bulge formation via dissipative collapse. Dissipative collapse implies strong inside-out formation that should give rise to a negative gradient in the α/Fe enhancement too. But no gradient was measured in the [α/Fe] radial profiles for almost all the galaxies. All the deviations from the median values of the other objects can be explained by their errors alone. No correlation is found between the central value and gradient of α/Fe enhancement, while the central value and gradient of metallicity are correlated. All these hints suggest that a pure dissipative collapse is not able to explain formation of bulges and that other phenomena like mergers or acquisition events need to be invoked.

Pseudo-bulges

Classical bulges are similar to low-luminosity ellipticals and are thought to be formed by mergers and rapid collapse. Pseudo-bulges are disc or bar components which were slowly assembled by acquired material, efficiently transferred to the galaxy centre where it formed stars. Pseudo-bulges can be identified according to their morphological, photometric, and kinematic properties following the list of characteristics compiled by

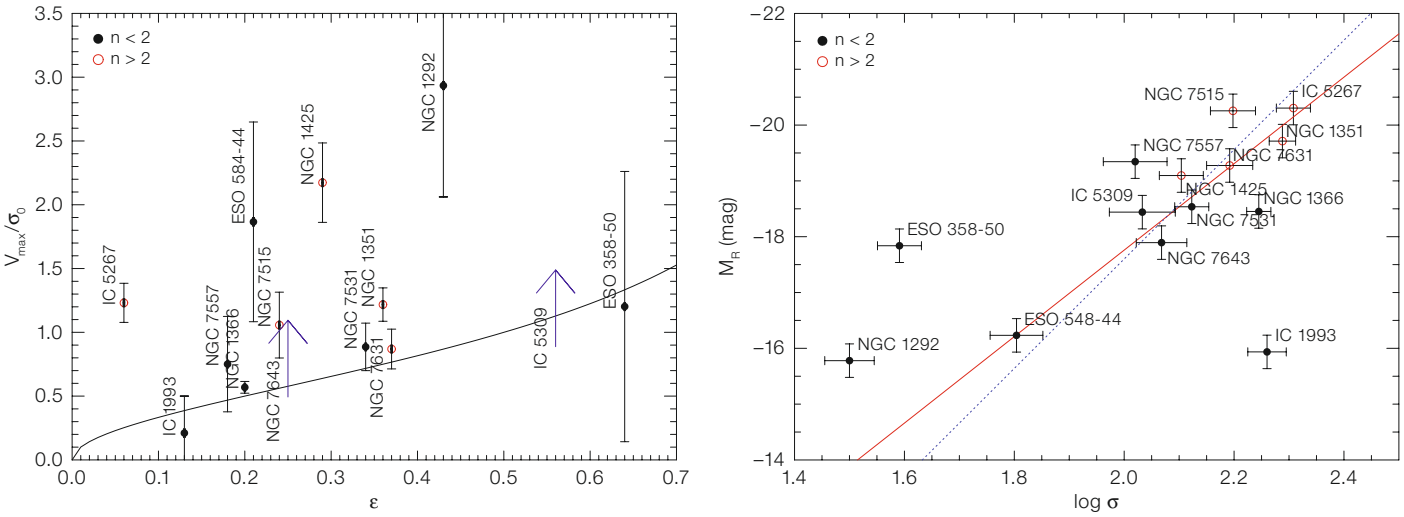

Figure 6. The location (left panel) of the sample bulges in the (V_{max}/σ_0, ε) plane. Filled and open circles correspond to bulges with Sèrsic index n ≤ 2 and n > 2, respectively. The continuous line corresponds to oblate-spheroidal systems that have isotropic velocity dispersions and that are flattened only by rotation. The location (right panel) of the sample bulges with respect to the Faber-Jackson relation by Forbes & Ponman (1999, blue dashed line). Filled and open circles correspond to bulges with Sèrsic index n ≤ 2 and n > 2, respectively and the linear fit is shown (red continuous line).

Kormendy & Kennicutt (2004). The more characteristics applied, the safer the classification becomes. Pseudo-bulges are expected to be more rotation-dominated than classical bulges, which are more rotation-dominated than giant elliptical galaxies. We measured the maximum rotation velocity V_{max} within r_{bd} from the stellar velocity curve and the central velocity dispersion σ_0 from the velocity dispersion profile. For each galaxy we derived the ratio V_{max}/σ_0. In Figure 6 (left panel) we compare it to the value predicted for an oblate spheroid with an isotropic velocity dispersion and the same observed ellipticity (Binney & Tremaine, 1987).

Another defining characteristic of pseudo bulges are their position on the Faber-Jackson relation. The pseudo-bulges fall above the Faber-Jackson correlation between the luminosity of the elliptical galaxies and early-type bulges and their central velocity dispersion (Kormendy & Kennicutt, 2004). Sample bulges, except for ESO 358-50 and NGC 1292, are consistent with the *R*-band Faber-Jackson relation we built from Forbes & Ponman (1999, $L \propto \sigma^{3.92}$). They are characterised by a lower velocity dispersion, or equivalently a higher luminosity, with respect to their early-type counterparts (Figure 6, right panel). According to the prescriptions by Kormendy & Kennicutt (2004), the bulge of NGC 1292 is the most reliable pseudo-bulge in our sample. Information about its stellar population gives more constraints on its nature and formation process. In fact, the NGC 1292 bulge population has an intermediate age and low metal content. The α/Fe enhancement is the lowest in our sample suggesting a prolonged star-formation history. The presence of emission lines in the spectrum shows that star formation is still ongoing. These properties are consistent with a slow build-up of the bulge of NGC 1292 within a scenario of secular evolution.

References

Aguerri, J. A. L., Balcells, M. & Peletier, R. F. 2001, A&A, 367, 428

Bender, R., Saglia, R. P. & Gerhard, O. E. 1994, MNRAS, 269, 785

Binney, J. & Tremaine, S. 1987, *Galactic Dynamics*, (Princeton, New Jersey: Princeton University Press), 747

Forbes, D. A. & Ponman, T. J. 1999, MNRAS, 309, 623

Gilmore, G. & Wyse, R. F. G. 1998, AJ, 116, 748

Jablonka, P., Gorgas, J. & Goudfrooij, P. 2007, A&A, 474, 763

Kormendy, J. & Kennicutt, R. C. 2004, ARA&A, 42, 603

Mehlert, D., et al. 2003, A&A, 407, 423

Méndez-Abreu, J., et al. 2008, A&A, 478, 353

Moorthy, B. K. & Holtzman, J. A. 2006, MNRAS, 371, 583

Thomas, D., Maraston, C. & Bender, R. 2003, MNRAS, 339, 897

Mid-infrared Interferometry of Active Galactic Nuclei: an Outstanding Scientific Success of the VLTI

Klaus Meisenheimer[1]
David Raban[2]
Konrad Tristram[1,3]
Marc Schartmann[1,4,5]
Walter Jaffe[2]
Huub Röttgering[2]
Leonard Burtscher[1]

[1] Max-Planck-Institut für Astronomie, Heidelberg, Germany
[2] Sterrewacht Leiden, the Netherlands
[3] Max-Planck-Institut für Radioastronomie, Bonn, Germany
[4] Max-Planck-Institut für Extraterrestrische Physik, Garching, Germany
[5] Universitäts-Sternwarte, München, Germany

Active Galactic Nuclei (AGN) are powered by accretion onto a supermassive black hole. The unified scheme for strongly accreting AGN postulates that the central engine is enshrouded by a doughnut-shaped structure of gas and dust – the so-called torus. We report observations with the MID-Infrared Interferometric Instrument (MIDI) at the VLT Interferometer, which resolve the tori in the nearest Seyfert 2 galaxies, and suggest a complex structure, consisting of a compact inner disc embedded in a patchy or filamentary outer torus. The prominent nearby radio galaxy Centaurus A, however, shows little sign of a torus. Instead, its mid-infrared emission is dominated by non-thermal radiation from the base of the radio jet. Thus, not all classes of AGN contain a thick torus.

The *unified scheme* for Active Galactic Nuclei (AGN) explains various types of AGN by a line-of-sight effect: it postulates that the central engine – an accreting supermassive black hole – is embedded in a doughnut-shaped torus of gas and dust. Thus, the hot accretion disc and the surrounding Broad Line Region (BLR) is only visible when looking along the torus axis. This is the case in Seyfert 1 galaxies, the optical spectra of which are characterised by a blue continuum and broad emission lines. In an edge-on case, however, the direct view onto the core is blocked by the dusty torus and only narrow emission lines from regions above and below the torus are visible. The object then appears as a Seyfert 2 galaxy. Spectropolarimetric observations of Seyfert 2 galaxies, showing broad lines in scattered light, support this idea (see review by Antonucci, 1993). The UV-optical light which is trapped by dust in the torus should heat the dust to a few hundred Kelvin, and the dust should re-radiate in the mid-infrared. Indeed, the Spectral Energy Distributions (SEDs) of both Seyfert 1 and Seyfert 2 galaxies display signatures of AGN heated dust between $\lambda \simeq 3$ and 30 μm. It is an open issue whether dust obscuration plays a similar role in radio galaxies.

Before the advent of the VLT Interferometer (VLTI), the size, shape and internal structure of the torus remained unknown, although the mid-infrared spectra located the dust within a few parsec of the core. Single 8-m-class telescopes cannot resolve mid-infrared structures of this size. Even in the *L*-band (3.6 μm) a diffraction-limited 8-m telescope is limited to 93 mas resolution (Full Width at Half Maximum, FWHM). At the distance of nearby Seyfert galaxies, such as NGC 1068 and NGC 4151 (14 Mpc), this corresponds to 6.5 parsec.

The situation changed dramatically in December 2002, when MIDI, the MID-Infrared Interferometric Instrument, became operational at the VLTI. MIDI observes in the *N*-band (wavelengths 8 to 13 μm). Using the widest telescope separation (UT1–UT4) of 125 m, the width of the point-spread function at 8 μm is only 7 mas, or 0.5 parsec at the distance of NGC 1068. But at the start of MIDI's operations two major questions remained: first, would MIDI be sensitive enough to reach extragalactic targets? Second, would observations with a handful of baselines allow us to reconstruct the dust distribution in the torus and thus provide scientifically meaningful insights? This article demonstrates that today both questions can be answered unequivocally: yes!

Mid-infrared interferometry with MIDI

MIDI operates as classical stellar interferometer of the Michelson type. It combines the beams of two telescopes at a time (Leinert et al., 2003). The sensitivity required for most AGN observations (correlated flux $F_{corr} \leq 1$ Jy in the *N*-band) can only be reached by the combination of two Unit Telescopes (UTs) of the VLTI. The highest sensitivity for detecting and tracking the interferometric *fringes* is obtained by inserting a prism into the interferometric beams, that spectrally disperses the *N*-band light with a spectral resolution $\simeq 25$. For brighter objects a grism with a higher resolution of 250 can be used. In both cases MIDI delivers two spectra (phase-shifted by 180 degrees) onto its detector, containing spectral and interferometric information at the same time. A special analysis pipeline is needed to extract this information. We use the *Expert Work Station* (EWS) pipeline developed in Leiden by Walter Jaffe.

Observations of the scientific target have to be complemented by standard star observations obtained with an identical instrumental set-up. The essential result of the pipeline analysis is a spectrum of the (calibrated) correlated flux $F_{corr}(\lambda)$ in the range 7.8 to 13.2 μm (see Figure 1b, c, d). $F_{corr}(\lambda)$ corresponds to the *Fourier Transform* of the source emission evaluated at a coordinate (called '*uv*-point' or 'baseline') given by the projected separation between the telescopes as viewed from the source. Spatial information about the source structure can be obtained comparing $F_{corr}(\lambda)$ at different *uv*-points. To the actually measured *uv*-points can be added the total flux $F_{tot}(\lambda)$ registered by a single telescope, essentially equivalent to an observation with zero baseline (see Figure 1a). Different baselines can either be realised by using different telescope combinations or by observing the target during its movement across the sky with a fixed telescope combination.

As evident from Figure 1, the AGN spectra between 8.5 and 12.5 μm are often dominated by a broad absorption trough, caused by silicate dust grains. The exact profile of this 'silicate feature' depends on the chemical composition, size and crystalline structure of the grains. Thus the *N*-band interferometry of an AGN not only resolves the spatial structure of the nuclear dust but also can give insight into the dust properties within the inner few parsecs.

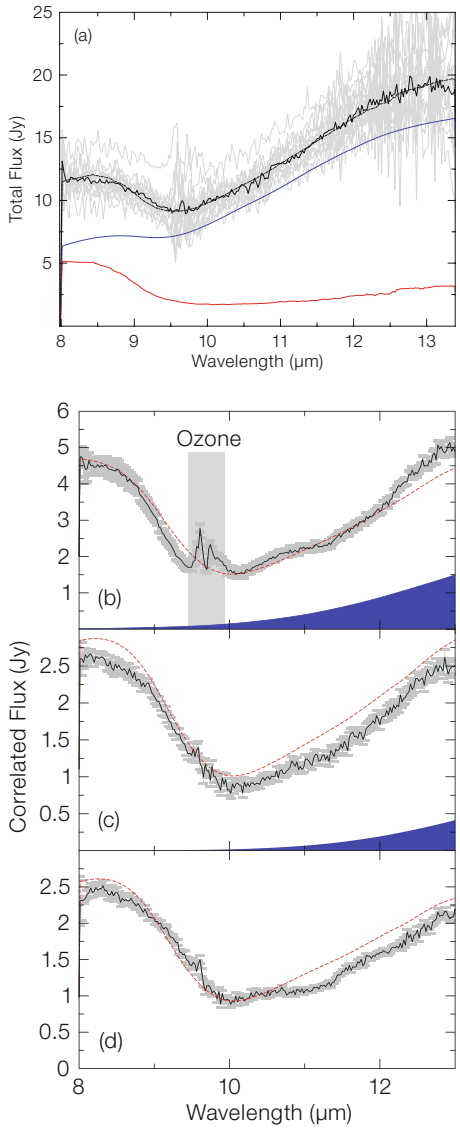

Figure 1. Results of MIDI observations of NGC 1068. (a) Total flux $F_{tot}(\lambda)$: the contribution of the hot component is shown in red, that of the extended component in blue. (b) Correlated flux $F_{corr}(\lambda)$ obtained with a 40-m baseline orientated along position angle P. A. = 36°. The red dotted line gives the model fit and the blue shaded area shows the contribution of the extended component. (c) $F_{corr}(\lambda)$ for 52 m baseline along P. A. = 112°. (d) $F_{corr}(\lambda)$ for 97 m baseline along P. A. = 36°. The comparison between (b) and (c) shows that the hot component is more extended (better resolved) in SE–NW direction.

The dust torus in NGC 1068

The first AGN observed with MIDI was the prototypical Seyfert 2 galaxy NGC 1068. It is the brightest extragalactic *N*-band source in the southern sky. At its distance of 14.4 Mpc, one parsec corresponds to an angular scale of 14 mas, i.e. parsec-scale structures can just be resolved with MIDI at the VLTI.

The earliest MIDI observations of NGC 1068 were obtained half a year after MIDI became operational, during VLTI *Science Demonstration Time* (SDT). Jaffe et al. (2004) demonstrated for the first time that a compact, geometrically thick dust structure – as expected for the dust torus – indeed exists in Seyfert 2 galaxies. Essentially only two visibility points were observed at that time. The correlated fluxes were best modelled by two components, a small, relatively hot one ($T > 800$ K, diameter about 1 pc), embedded in a larger component of 320 K and about 3.5 pc diameter.

New observations with MIDI (Raban et al., 2008b) cover the *uv*-plane much better: 15 visibility points were obtained with the telescope combinations UT1–UT3, UT1–UT4, and UT2–UT3. An additional measurement with the orthogonal baseline UT3–UT4 proved essential for the following results. To study the details of the silicate absorption profile, the higher ($R \simeq 230$) resolution grism was used.

Even with this more complete *uv*-coverage, direct image reconstruction is not possible because MIDI observes only two telescopes at a time and rapid atmospheric phase shifts cannot be recovered by *phase closure* techniques. The measured $F_{corr}(\lambda)$ spectra for different baselines still have to be interpreted by simple models. Remarkably, a model of two components with Gaussian brightness distribution and black-body spectrum describes the correlated flux data reasonably well. With the inclusion of the longest VLTI baselines UT1–UT3 and UT1–UT4, the measurements perfectly constrain the size, shape and orientation of the hot, inner component of the dust torus: major axis 20 mas (1.4 pc FWHM), oriented along P. A. = 138°. It is rather elongated, with an axis ratio of 0.25, indicating a geometrically thin (disc-like?) structure. Only a lower limit, $T > 800$ K, can be set to its temperature. The lack of short baselines, < 50 m in the East-West direction makes the determination of the overall size and shape of the more extended 'torus component' uncertain. Its diameter is about 3.5 pc, but its exact shape remains to be determined by shorter baselines along the East-West direction.[1]

The major axis of the hot component is perfectly aligned with a spur of water masers extending about 20 mas towards NW from the (radio-)core, although the relative astrometric position cannot be determined. Surprisingly, the orientation of its minor axis (P. A. = 48°), which might mark the symmetry axis of an inclined disc, does not fit well to the source axis as determined from outflow phenomena. The inner radio jet points almost exactly North (P. A. = 2°), while the ionisation cone opens between P. A. ≃ −5 – −30°. For the standard torus scenario this is a puzzle: the open funnel which allows the ionising UV-photons to escape should be caused by the angular momentum barrier and thus be aligned with the rotation axis of the gas distribution. How could a tilted disc form out of this gas? Perhaps the hot inner component is not a rotationally supported structure (disc) but rather a filament or hot channel.

Further insight into the dust properties can be inferred from the depth of the silicate feature. In the total flux, which is

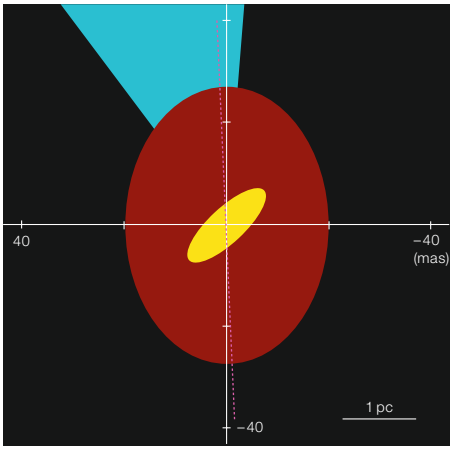

Figure 2. Observational model of the dust torus in NGC 1068. A hot component (yellow) is embedded in an extended cooler component (brown). The orientation of the radio axis is indicated by a purple dotted line and the blue wedge gives the opening angle of the ionisation cone, observed on 100-pc scales.

[1] Such baselines are provided by the Auxiliary Telescopes (ATs). A MIDI observation programme with the ATs is under way and has already detected fringes from NGC 1068.

dominated by the outer component (Figure 1a), the absorption optical depth at 10 μm is moderate, ≃ 0.4, whereas the depth towards the inner component is almost five times larger at ≃ 1.9 (Figure 1b, c, d). Obviously, most of the dust column is located in the outer component.

The dust torus in the Circinus galaxy

The Circinus galaxy at a distance of 4 Mpc is the closest Seyfert galaxy. It shows all signs of a classical Seyfert 2: narrow allowed and forbidden emission lines, strong silicate absorption and a heavily absorbed X-ray spectrum. An extended cone of emission line gas and the presence of broad lines in the polarised optical flux (caused by scattering) provide direct evidence that the central engine is hidden from our direct view behind a substantial amount of dust. Circinus is a spiral galaxy seen almost edge on. Thus, several magnitudes of visual extinction might be caused by the dust lanes in the spiral disc, behind which the nuclear region is located.

The high southern declination of Circinus ($\delta = -65^{\circ}$) makes it an almost ideal target for the VLTI: it can be observed for up to 12 hours during long winter nights, thus allowing the projected baseline orientation between each of two UTs to swing by up to 180° due to the earth's rotation. In five observing runs during the MIDI *guaranteed time observation* programme, we have been able to collect 21 visibility points, most of them with the shortest VLTI baselines UT2–UT3 and UT3–UT4 (Tristram et al., 2007). They provide the most complete *uv*-coverage obtained for any extragalactic target so far.

As in NGC 1068, at least two components with Gaussian brightness distribution are required to model the correlated fluxes: a compact component (major axis 0.4 pc and axis ratio 0.2); and an almost round extended component (FWHM 1.9 pc, see Figure 3). Contrary to the case of NGC 1068, the colour temperatures of the inner and outer components both lie around 300 K, differing by less than 50 K. However, the outer component does not seem to be smoothly filled with dust at a constant temperature. Comparing its average surface brightness with that of a black body leads to a covering factor of only 20 %. Moreover, the observed correlated flux values are poorly reproduced by the smooth Gaussian model, but rather seem to 'wiggle' around it when plotting them as function of baseline orientation. In order to test whether a patchy brightness distribution could improve the fit, we modified the smooth Gaussian distribution by a foreground screen of randomly distributed variations in transmission. A thousand different screens were realised, the images were Fourier-transformed, and compared with the observed correlated fluxes. Indeed, we found several patchy screens which reproduce the observations much better than the smooth model. The best-fitting model is displayed in the right panel of Figure 3. Interestingly enough, it shows a bright patch on the axis of the ionisation cone. We regard this as evidence that our interferometric data contain hints for the existence of hotter dust close to an open funnel which confines the ionising radiation.

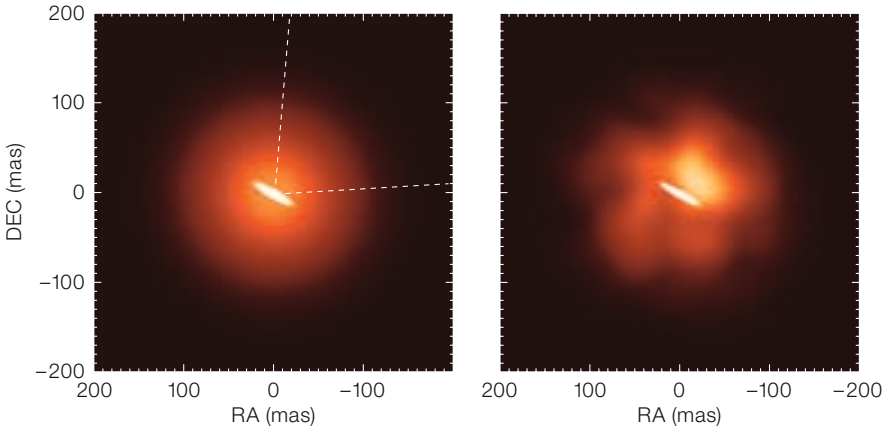

Figure 3. The dust torus in the Circinus galaxy. The left panel shows the smooth model (composed of two Gaussian brightness distributions, the right panel visualises the best-fitting patchy model. Dashed lines indicate the opening angle of the ionisation cone.

The size and orientation of the inner, disc-like component again fit very well to the known disc of water masers which show a Keplerian rotation pattern (Figure 4). Although the location of the dust emission with respect to the maser disc cannot be determined by our MIDI observations, it is very likely that both discs are co-spatial: in this case the inner dust component would also have to be interpreted as a rotationally supported disc.

It is worth noticing that the depth of the silicate absorption towards the dust components in Circinus shows a different behaviour than that observed in NGC 1068. In Circinus the depth of the silicate feature towards the inner component is shallower than towards the outer component. Obviously the dust column through the outer dust component is not very high and the absorption trough is partly filled by silicate *emission* from the dust disc.

The radio galaxy Centaurus A

The radio galaxy Centaurus A (= NGC 5128) plays a key role in extragalactic astronomy: at a distance of only 3.8 Mpc it is the closest large *elliptical galaxy*, the closest *galaxy merger* and the closest

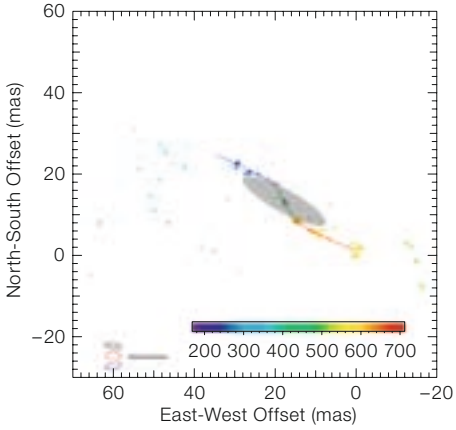

Figure 4. Overlay of the compact dust component in Circinus over the location of the (warped) disc of water masers (from Gallimore et al., 2004).

violent AGN. At its distance, 1 pc corresponds to 53 mas. The radio source can be traced over seven orders of magnitude in angular scales, from the VLBI jets (a few mas) to the outer lobes (several degrees). Extinction in the dust lane of the merging spiral galaxy severely obscures our view towards the nucleus of Centaurus A. Thus observations at infrared wavelengths are mandatory (see Meisenheimer et al., 2007, and references therein for more details).

Centaurus A was observed in 2005 with MIDI using two telescope combinations: UT3–UT4 and UT2–UT3. With both combinations two visibility points were obtained, separated by about two hours. The projected baseline with UT3–UT4 was orientated roughly perpendicular to the parsec scale radio jet, while UT2–UT3 was aligned with it (Figure 5). We found that the mid-infrared emission is marginally resolved perpendicular to the jet axis with a 60-m projected baseline, whereas it remains unresolved along the jet axis. Accordingly, we conclude that the 8 to 13 μm emission from the core of Centaurus A is dominated by an unresolved point source (FWHM < 6 mas), which contributes between 50 % and 80 % of the total flux at 13 μm and 8 μm, respectively. The extended component is tiny (FWHM ≃ 30 mas), and seems elongated perpendicular to the radio axis (see sketch in Figure 5). However, a better *uv*-coverage (including longer baselines) will be required to constrain the size, shape and orientation of this extended component more accurately. We interpret the extended component as dust emission from a small, inclined disc (diameter about 0.6 pc). The unresolved component is identified with the non-thermal 'synchrotron core' of Centaurus A, since we find that – after correcting for the foreground extinction of $A_V = 14$ mag (derived from the depth of the silicate absorption) – its flux level and spectrum lies perfectly on the extrapolation of the power-law spectrum observed at millimetre wavelengths. Together with photometry at shorter wavelengths (from HST and the AO camera NACO at the VLTI) the flux of the unresolved point source fits perfectly to a canonical synchrotron spectrum: it is characterised by a rather flat power-law $F_\nu \propto \nu^{-0.36}$, cutting off exponentially at a frequency $\nu_c = 8 \times 10^{13}$ Hz. We interpret

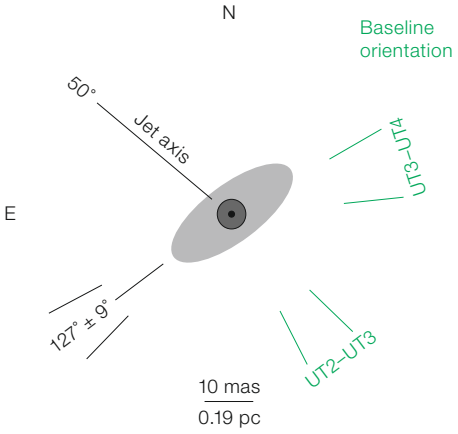

Figure 5. Sketch of our model for the *N*-band emission from the central parsec of Centaurus A. An unresolved point source is surrounded by a faint dust disc.

this 'synchrotron core' as the base of the radio jet (for details see Meisenheimer et al., 2007). Our interferometric results on Centaurus A demonstrate that mid-infrared radiation processes are not restricted to thermal dust emission.

The thermal dust emission from the core of Centaurus A is very feeble, more than 20 times weaker than that of the Circinus galaxy at the same distance. We think that *both* a lack of dust in the inner parsec and the absence of a sufficiently strong heating source are responsible for this. Certainly, Centaurus A neither contains a torus which severely blocks our line of sight nor a UV-optically bright central accretion disc. Most likely, the accretion onto its black hole happens via an *advection dominated accretion flow* (ADAF), which is very inefficient in converting accretion power $\dot{m}c^2$ into radiation.

Models of the torus

The concept of a doughnut-shaped 'torus', continuously filled with gas and dust, is an oversimplified geometrical picture. Already 20 years ago, Krolik & Begelman (1988) pointed out that it must consist of a large number of individual clouds orbiting around the AGN core. However, frequent cloud–cloud collisions would make such a system very unstable: within a few orbital timescales it should settle into a geometrically thin disc. Other arguments for a clumpy sub-structure of the torus include the widely spread and continuous distribution in X-ray absorbing hydrogen column densities between Seyfert 1 and Seyfert 2 galaxies and several cases in which an AGN changed its broad line spectrum, indicating a change in central obscuration. Radiative transfer calculations of 'clumpy' torus models showed that another problem of the continuous torus models – namely their prediction of a strong silicate emission in Seyfert 1 galaxies, which is rarely observed – can be solved by shadowing effects in a clumpy structure (Nenkova et al., 2002). In a recent study we demonstrate by fully 3D radiative transfer calculations (Schartmann et al., 2008) that a wide variety of cloud distributions is able to reproduce the observed mid-infrared spectra. Moreover, when simulating interferometric observations of such a clumpy torus, we find similar 'wiggles' in the correlated fluxes to those observed in Circinus.

Despite the success of radiative transfer models in explaining the infrared SEDs of AGN, they cannot solve the stability problem pointed out by Krolik & Begelman: how could the geometrically thick distribution of clouds be maintained? To address this question a hydrodynamical model is required that simulates a realistic mass injection into the torus and follows the evolution of the gas clouds. We are currently developing a torus model for Seyfert galaxies that starts from a number of assumptions. The centre of the galaxy harbours a massive young stellar cluster (age between 40 and 100 million years). Stellar mass loss via planetary nebulae and stellar winds injects gas and dust into the system, while frequent supernova explosions stir up the gas. Locally the gas gets compressed and the subsequent cooling instability leads to the formation of dense and cool filaments (see Figure 6). In between the filaments cavities of very hot plasma form overpressured regions, which expand radially along the density gradient. Thus the cool filaments also become radially stretched. The cool gas and dust streams inwards along the filaments and accumulates in a very dense turbulent disc with a few parsec radius.

In a second step, the radiative transfer through the simulated density distribution

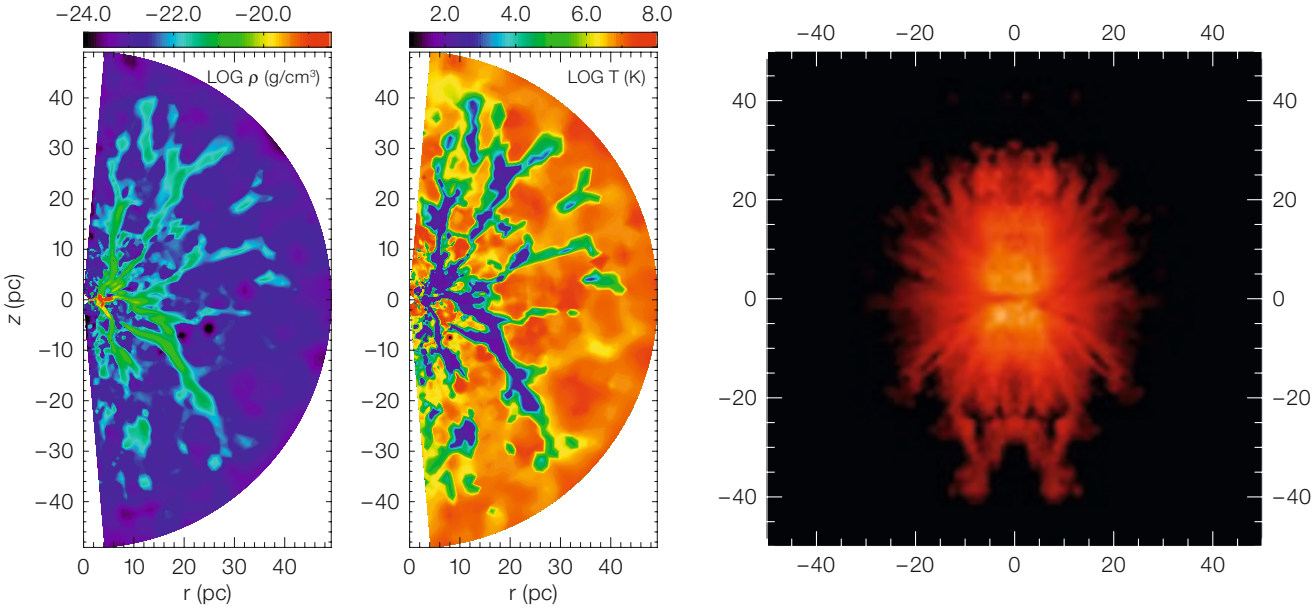

Figure 6. Hydrodynamical torus model. The left and middle panels show the gas density and temperature in a meridional slice. The right panel displays the image at 12 μm which would be observed from an edge-on view onto this torus. The simulations refer to an AGN that is about five times more luminous than NGC 1068.

is calculated (assuming a standard gas-to-dust ratio in all cells below sublimation temperature). The emerging mid-infrared images (right panel in Figure 6) reproduce the filamentary density structure. They can explain the 'patchy' outer torus observed in Circinus rather nicely. It should be noted, however, that the central turbulent dust disc appears *dark* in our simulations. A set of torus models is generated by varying the mass injection and supernova rates. Observing those under various aspect angles can well account for the wide spread in hydrogen column in Seyfert galaxies (over three orders of magnitude) while the change in silicate depth (from absorption to moderate emission) remains limited.

MIDI observations of distant AGN

In addition to the detailed studies described above, we carried out an AGN snapshot survey during the *guaranteed time observations* of the MIDI consortium. The survey tried to identify all those AGN, which are bright enough in the *N*-band to be observed with MIDI. The preliminary target list was selected from AGN with known *N*-band flux > 1 Jy. Since most of the available *N*-band photometry was obtained in large apertures, it was necessary to observe all targets with TIMMI2 at the 3.6-m telescope (beam size 0.7″) to get the core flux at λ = 12 μm. The final target list (Table 1) contains all southern AGN with S_N(core) > 300 mJy (Raban et al., 2008). 13 of the targets have been observed during the snapshot survey, two more were tried by other observers. From 11 of these 15 targets, MIDI could detect interferometric fringes (column 6 in Table 1). Three of the sources, for which MIDI observations were attempted, could not be observed since their nuclei were too faint for the adaptive optics system MACAO. Only one source, the star burst nucleus in NGC 253, seems too extended to show an interferometric signal.

Most targets have been observed only with the shortest baseline UT2–UT3, and remain unresolved within the errors (which are dominated by the measurement of the total flux F_{tot}). Additional observations with longer baselines will be required to determine the size and flux of their dust tori (if present). Despite its northern declination (+40°), we recently managed to observe the nearest Seyfert 1 galaxy, NGC 4151 with the VLTI. It is clearly resolved at 10 μm with a 60-m baseline.

But seen from the VLT, the *uv*-coverage of this Seyfert 1 galaxy will always remain very limited. The closest southern Seyfert 1 galaxy which is bright enough for MIDI observations, NGC 3783, is three times more distant than NGC 4151. In order to obtain a direct comparison, more distant (and luminous) Seyfert 2 galaxies have to be studied as well.

Synthesis

At the first sight, our results for the dust structures in the Seyfert 2 galaxies NGC 1068 and Circinus look quite similar: they both contain an elongated inner component which is embedded in a larger dust distribution, heated to about 300 K. The observed difference in torus size is expected from the fact that NGC 1068 is about 10 times more luminous than Circinus. In both sources the inner component is aligned with the location of water masers.

On the other hand, one might argue that the differences between both objects are even more significant: only in NGC 1068 do we find dust heated to almost the sublimation temperature, while in Circinus any strong temperature gradient between the innermost dust and outer parts of the torus is absent. Moreover, the elongation of the hot dust component in NGC 1068 appears significantly tilted with

Name	Type	z	Scale [mas/pc]	S_N (core) [mJy]	MIDI	Remarks
*NGC 1068	S2	0.00379	14.0	15 000	X	well observed (16 visibility points), see text
NGC 1365	S1.8	0.00546	11.0	610	X	marginally resolved in snapshot survey
IRAS 05189-2524	S2	0.0425	1.0	550		AO correction with MACAO failed
MCG-5-23-16	S1.9	0.00827	5.7	650	X	done in snapshot survey
Mrk 123	S1	0.0199	2.5	640	X	done in snapshot survey
NGC 3281	S2	0.01067	4.4	620		AO failed on nucleus, nearby star not used
*NGC 3783	S1	0.00973	5.0	590	X	observed by Beckert et al. (in prep.)
NGC 4151	S1	0.00182	14.0	1400	X	resolved in snapshot survey
Centaurus A	RG	0.00332	53.0	1220	X	first results with short baselines, see text
IC 4329A	S1	0.01605	3.1	420	x	fringes detected
*Mrk 463	S1	0.0504	1.0	340		not yet tried
Circinus	S2	0.00145	50.0	9 700	X	well observed (21 visibility points), see text
NGC 5506	S2	0.00618	8.0	910		AO correction with MACAO failed
NGC 7469	S1	0.01631	3.1	410	x	fringes detected
NGC 7582	S2	0.00539	9.0	320		not yet tried
3C 273	QSR	0.1583	0.3	350v	X	two interferometric measurements
NGC 253 core	LE	0.00080	57.3	1100	–	no fringes detected (Hönig, priv. comm.)

Table 1. Target list and results of the AGN snapshot survey carried out during MIDI guaranteed time observations (GTO). Targets marked by * were released from the GTO list early. A cross in the column 'MIDI' indicates successful MIDI observations (X: complete interferometric measurement, x: fringes detected, but unstable weather conditions prohibited complete observation).

respect to the source axis as defined by the radio jet and the ionisation cone, whereas the dust disc in Circinus seems to fit perfectly into an axisymmetric torus model. The outer torus in Circinus appears patchy or filamentary as predicted by hydrodynamical models. The low absorption depth in the silicate feature towards the inner component indicates that our line of sight onto the dust disc is not severely blocked by the outer structure and most of the large hydrogen column towards the X-ray core must be located *within* a radius ≃ 0.2 pc. In contrast, NGC 1068 exhibits a huge dust column towards the hot component. Here most of the absorbing gas and dust is located *outside* a radius of ~ 1 pc.

From these differences it seems evident that the torus in the Circinus galaxy is not just a scaled-down version of that in NGC 1068. Thus the question arises: is there such a thing as the standard torus in Seyfert galaxies? In any case, the 'torus' possesses a complex structure, which not only *appears* different (due to line-of-sight effects) but may *differ intrinsically* between individual AGN. This is not necessarily in conflict with the essential assumption of the unified scheme: it is still possible that Seyfert 1s and Seyfert 2s are intrinsically the same class of objects. In order to verify this generic assumption, one has to prove that similar tori, as in NGC 1068 and Circinus, also exist in Seyfert 1 galaxies. The detection of an extended component in NGC 4151 with MIDI marks a promising first step in this direction. Finally, our results on Centaurus A demonstrate that the absence of broad emission lines cannot always be explained by an obscuring torus. Intrinsic properties of the accretion flow onto the black hole might be equally important.

References

Antonucci, R. 1993, ARA&A, 31, 473
Gallimore, J. F., Baum, S. A. & O'Dea, C. P. 2004, ApJ, 613, 794
Jaffe, W., Meisenheimer, K., Röttgering, H., et al. 2004, Nature, 429, 47
Krolik, J. H. & Begelman, M. C. 1988, ApJ, 329, 702
Leinert, C., Graser, U., Richichi, A., et al. 2003, The Messenger, 112, 13
Meisenheimer, K., Tristram, K. R. W., Jaffe, W., et al. 2007, A&A, 471, 453
Nenkowa, M., Ivezi, Z. & Eliitzur, M. 2002, ApJL, 570, L9
Raban, D., Heijligers, B., Röttgering, H., et al. 2008a, A&A, in press (arXiv:0804.2395)
Raban, D., Jaffe, W., Röttgering, H., et al. 2008b, MNRAS, in press
Schartmann, M., Meisenheimer, K., Camenzind, M., et al. 2008, A&A, in press (arXiv:0802.2604)
Tristram, K. R. W., Meisenheimer, K., Jaffe, W., et al. 2007, A&A, 474, 837

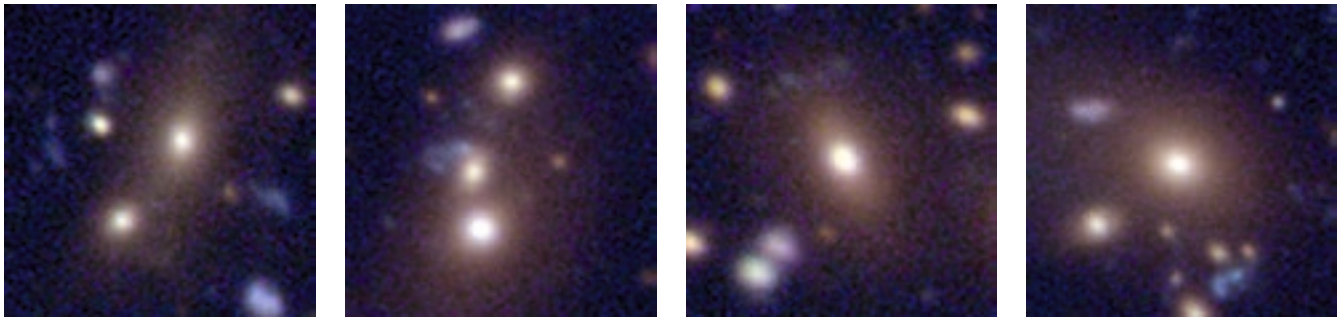

Colour images of the brightest galaxies in four galaxy groups at redshift ~ 0.36, formed by combining VIMOS *B*, *V* and *R* band images (20″ × 20″ sections shown). The galaxies are ordered from left to right in increasing stellar mass, i.e. a rough time sequence. The brightest galaxies in the left two images have gravitationally bound bright companions. See ESO Science Release 24/08 for more details.

The Supernova Legacy Survey

Mark Sullivan[1]
Christophe Balland[2]

[1] Department of Physics, University of Oxford, United Kingdom
[2] Laboratoire de Physique Nucléaire et des Hautes Énergies (LPNHE), Centre National de la Recherche Scientifique (CNRS) – Institut Nationale de Physique Nucléaire et de Physique des Particules (IN2P3), Universités Paris VI and Paris VII, France*

The accelerating Universe was one of the most surprising discoveries of 20th century science. The 'dark energy' that drives it lacks a compelling theoretical explanation, and has sparked an intense observational effort to understand its nature. Over the past five years, the Supernova Legacy Survey (SNLS) has made a concerted effort to gather 500 distant Type Ia Supernovae (SNe Ia), a sample of standard candles with the power to make a 5 % statistical measurement of the dark energy's equation of state. The SNLS sample also provides one of the most uniform sets of SNe Ia available, with a photometric and spectroscopic coverage allowing new insights into the physical nature of SN Ia progenitors. With the survey recently completed, we report on the latest science analysis, and the vital role that the ESO VLT has played in measuring these distant cosmic explosions.

Type Ia Supernovae as cosmological tools

Type Ia Supernovae (SNe Ia) are a violent endpoint of stellar evolution, the result of the thermonuclear destruction of an accreting carbon-oxygen white dwarf star approaching the Chandrasekhar mass limit. As the white dwarf star gains material from a binary companion, the core temperature of the star increases, leading to a runaway fusion of the nuclei in the white dwarf's interior. The kinetic energy release from this nuclear burning – some 10^{44} J – is sufficient to dramatically unbind the star. The resulting violent explosion and shock wave appears billions of times brighter than our Sun, comfortably out-shining the galaxy in which the white dwarf resided.

SN Ia explosions are observed to explode with approximately the same intrinsic luminosity to within a factor of two, presumably due to the similarity of the triggering white dwarf mass and, consequently, the amount of nuclear fuel available to burn. These raw luminosities can be standardised further using simple empirical corrections between their luminosity, light-curve shape and colour – intrinsically brighter SNe Ia typically have wider (slower) light curves and a bluer optical colour than their fainter counterparts (e.g. Phillips, 1993). The combination of extreme brightness, uniformity, and a convenient month-long duration, makes SNe Ia observationally attractive as calibrateable standard candles; objects to which a distance can be inferred from only a measurement of their apparent brightness on the sky. Applying the various calibrating relationships to SN Ia measurements provides distance estimates precise to ~ 7 %, which can be used via the redshift-magnitude relation (or Hubble Diagram) to determine cosmological models.

For many years following the realisation of the cosmological potential of SNe Ia, finding distant events in the numbers required for meaningful constraints was a considerable logistical and technological challenge. Years of searching were required to discover only a handful of SNe Ia (e.g. Perlmutter et al., 1997). The field only matured with the advent of large-format CCD cameras capable of efficiently scanning large areas of sky, and the simultaneous development of sophisticated image processing routines and powerful computers capable of rapidly analysing the volume of data produced. The substantial search effort culminated in the late 1990s when two independent surveys for distant SNe Ia made the same remarkable discovery: the high-redshift SNe Ia appeared about 40 % fainter – more distant – than expected in a flat, matter-dominated Universe (Riess et al., 1998; Perlmutter et al., 1999), providing astonishing evidence for an accelerating Universe. When these observations were combined with analyses of the cosmic microwave background, a consistent picture emerged of a spatially flat Universe dominated by a dark energy responsible for ~ 70–75 % of its energy, opposing the slowing effect of gravity and accelerating the Universe's rate of expansion.

This incredible discovery sparked an intense observational effort: at first to confirm the seemingly bizarre and unpredicted result, and later to place the tightest possible observational constraints on dark energy, in the hope that a theoretical understanding could follow. Many hundreds of SNe Ia have now been discovered out to a redshift of 1.5 in an effort to map the Universe's expansion history, and alternative cosmological probes have been developed and matured: understanding dark energy has become a key goal of modern science.

The Supernova Legacy Survey

The five-year Canada-France-Hawaii Telescope (CFHT) Supernova Legacy Survey (SNLS) started in mid-2003 with the ambitious goal of discovering, confirming and photometrically monitoring around 500 SNe Ia to determine the nature of dark energy. The development of the square-degree imager MegaCam on the 3.6-m CFHT, and the efficiency with which it could survey large volumes of sky, meant that SNe Ia out to $z = 1$ could be discovered routinely and essentially on demand. The multi-band optical data (Figure 1) comes from the Deep component of the CFHT Legacy Survey (CFHT-LS), observing each of four fields every three or four days during dark time in a rolling search for around six lunations per year. As optical transient events are discovered, the repeated imaging automatically builds up high-quality light curves which can be used to measure the SN peak brightnesses, light-curve

* The full SNLS core collaboration is: Pierre Astier (LPNHE, CNRS-IN2P3), Dave Balam (University of Victoria), Christophe Balland (LPNHE, CNRS-IN2P3), Stephane Basa (LAM), Ray Carlberg (University of Toronto), Alex Conley (University of Toronto), Dominique Fouchez (CPPM), Julien Guy (LPNHE, CNRS-IN2P3), Delphin Hardin (LPNHE, CNRS-IN2P3), Isobel M. Hook (University of Oxford), Andy Howell (University of Toronto), Reynald Pain (LPNHE, CNRS-IN2P3), Kathy Perrett (University of Toronto), Chris J. Pritchet (University of Victoria), Nicolas Regnault (LPNHE, CNRS-IN2P3), Jim Rich (CEA-Saclay), Mark Sullivan (University of Oxford).

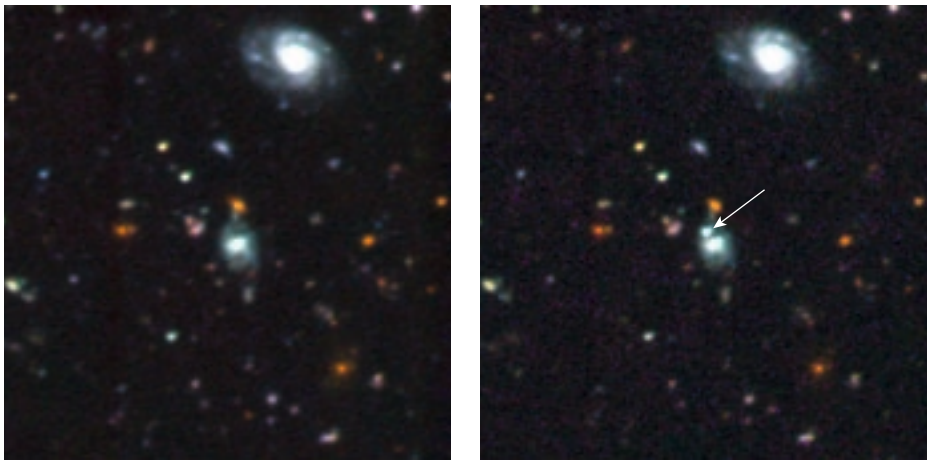

Figure 1. The point of light marked on the right image is a distant Type Ia Supernova, nearly four billion light-years away at a redshift of 0.31. This false-colour image is generated from *g′*, *r′* and *i′* data taken using MegaCam at the 3.6-m Canada-France-Hawaii Telescope on Mauna Kea. Once these transient events have been located, they can be spectroscopically confirmed by 8-m-class telescopes such as the ESO VLT.

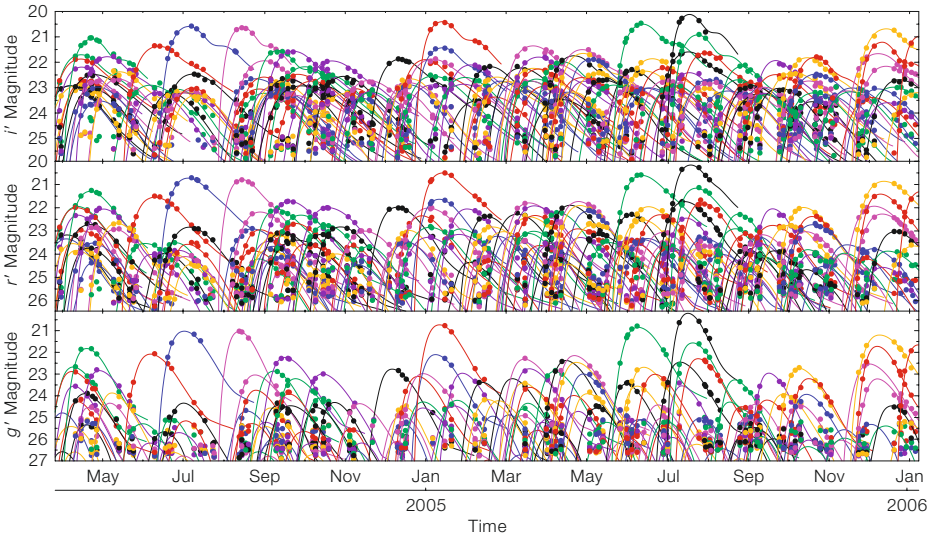

Figure 2. The light curves of more than 150 SNe Ia, discovered and photometrically monitored by CFHT. Each point represents a single MegaCam observation (several SNe are observed simultaneously due to that instrument's wide field of view). The solid curves are light-curve template fits to each SN and are used to interpolate the brightness at maximum light for the subsequent cosmological analyses (e.g. Astier et al., 2006). The three panels show data taken in the *i′* filter (upper), *r′* (middle) and *g′* (lower). *z′* data is also taken but is not shown. The multi-band data is essential for both accurate *k*-corrections to the rest-frame, and for measurement of the optical colour of the SN at maximum light.

widths, and colours required for the cosmological analysis (Figure 2). In addition, a vast database of deep and accurate photometry yielding well-sampled multi-colour light curves for all classes of optical transients is available.

The role of the VLT

A critical component of any SN survey is spectroscopic follow-up of candidate events, confirming their nature and measuring the redshifts essential for placement on a Hubble Diagram. The SNLS is no exception. Being optically faint – fainter than 24th magnitude at a redshift of one – distant SN spectroscopy requires the light-collecting power of 8-m-class telescopes, such as the ESO VLT. As with all transient events a rapid response is essential while the SN Ia candidate remains optically bright. Our ESO/VLT real-time follow-up (Basa et al., in prep.) has used ToO mode with FORS1 and FORS2 (Appenzeller et al., 1998), the latter for the higher-redshift candidates where the sensitive red response becomes more critical. In general, FORS1 was operated in MOS mode with the moveable slits, observing not only the principal transient target, but the host galaxies of several other old variable events, the light from which has since faded. This multiplexing has resulted in a large number of redshifts of transients as well as spectra of the SNe Ia.

Over the duration of two ESO large programmes, we have followed up nearly 320 optically transient events, and with the last six months of data still being analysed, have confirmed 200 as SNe, and more than 160 as SNe Ia (see examples in Figure 3). When the analysis is complete, this number is expected to rise to more than 200, representing the largest number of SNe Ia confirmed with a single telescope. This will be a dataset with considerable legacy value, not only for studying dark energy, but also for learning about the physics of the SN explosions themselves.

VLT spectra represent a large fraction of the SNLS SNe Ia spectra, and considerable work has been done to produce a clean identification of their types and redshifts, necessary for their subsequent cosmological use. In particular, two new techniques have been developed for our VLT spectra. The first is a dedicated pipeline that makes use of photometric information during the spectral extraction phase (Balland et al., in prep.). Distant SNe Ia are often buried in their host gal-

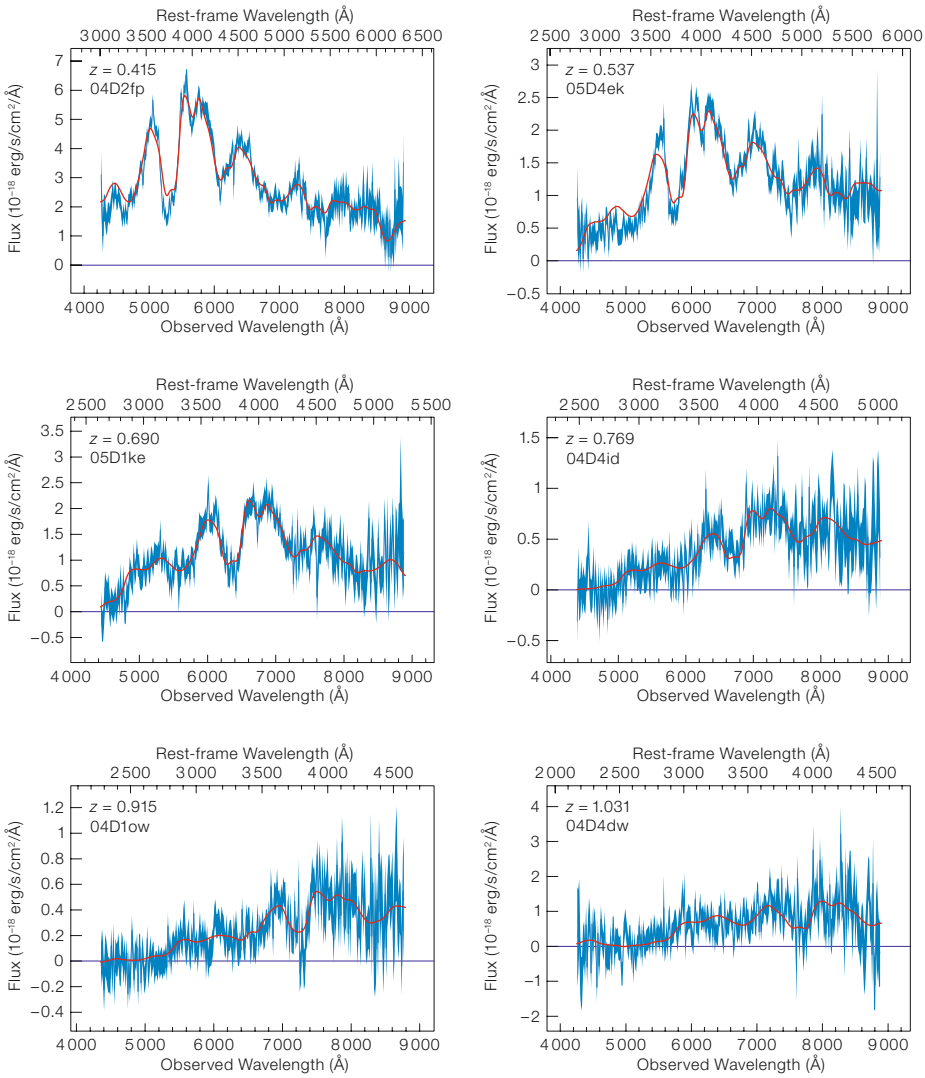

Figure 3. Example spectra of SNe Ia from the VLT/FORS follow-up campaign (Balland et al., in prep). Each panel shows a different SN Ia distributed over $z \simeq 0.4$ to $z \simeq 1$. In each case the blue line is the observed FORS spectrum, and the red the model template fit. The characteristic Ia features allow robust SN classifications, and in the spectra with a higher signal-to-noise, the chemical features can also be used to study the redshift evolution of SN Ia properties.

axes, with light from the continuum of the galaxy drowning out signal from the SN, making the task of SN identification difficult (Figure 4). The spatial profile of the host galaxy is measured from MegaCam images in several photometric bands projected along the slit and then matched to the spectral profiles from FORS at the corresponding wavelengths. This technique allows a precise estimate of the host contamination at the SN position, optimally recovering the spectra of both the SN and its host. If the SN is too close to its host galaxy centre for a separate extraction, the combined spectrum is extracted and fit to a two-component model comprising a spectral model of the SN Ia and a galaxy model drawn from a large set of template spectra spanning the Hubble sequence. The left panel of Figure 4 shows an example of such a fit, with the spectrum of this distant SN well measured despite its location in the core of its host.

The second technique concerns the spectral identification. This uses a spectrophotometric model of SNe Ia constructed from a sample of both nearby and distant SNe covering a wide range of epochs. Each new SN candidate spectrum is fit to this model, and the best-fit parameters are compared on a case-by-case basis to the average properties of the SN Ia model sample. Differences are interpreted as the signature of peculiar or non SNe Ia spectra. Although the final identification relies on human judgement, this procedure limits the subjectivity usually entering SN classification.

The resulting clean, host-subtracted SN Ia spectra can be used to analyse any evolution in the strength of the SN chemical features with redshift, placing constraints on the degree to which the SNe themselves change with cosmic time. This is one of the most direct methods available for probing any changing composition of the SN Ia progenitors.

Cosmological measurements

The key measurement made by the SNLS is the determination of the equation of state of the dark energy, *w*, the ratio of its pressure to energy density. Dark energy must have a strong negative pressure to explain the observed cosmic acceleration and hence have a negative *w*. The sim-

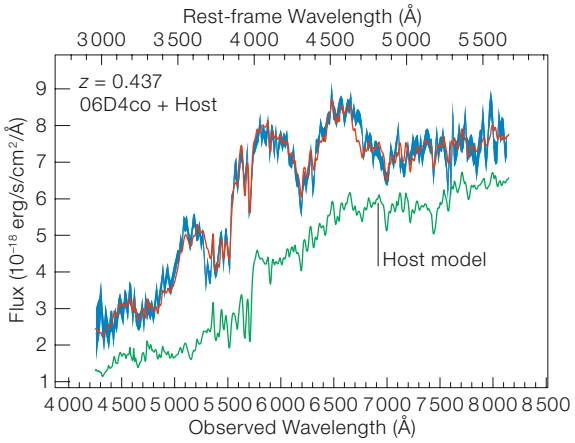

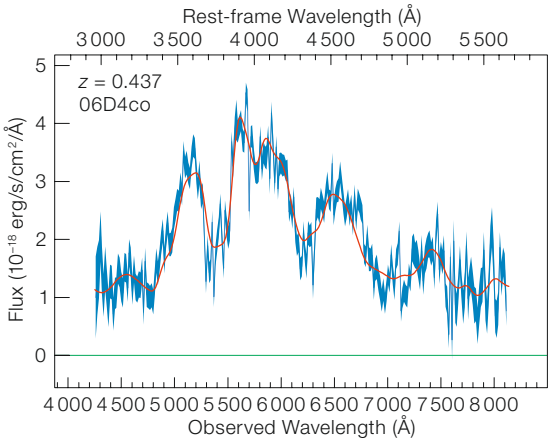

Figure 4. An example of host galaxy subtraction techniques developed for analysing VLT/FORS spectra of SNLS SNe Ia. The left panel shows the raw spectrum (blue) and model fit (red), together with the best-fitting host galaxy spectrum (green). Once the host galaxy is subtracted (right panel), the spectrum is ready for both classification and science analysis.

plest explanation is a Cosmological Constant, an intrinsic and non-evolving property of empty space with a negative pressure equal to its energy density such that $w = -1$. Other ideas include the broad family of quintessence models, which predict a dynamic and varying form of dark energy field generally with $w \neq -1$, and phantom energy, a form of dark energy with $w < -1$ that would ultimately tear apart all gravitationally bound structures in a 'big rip' (for a detailed review of the different possibilities see Copeland et al., 2006). An alternative considered by some theorists is that the cosmologist's fundamental tool, General Relativity, may simply fail on very large scales.

SNe Ia are used to measure cosmological parameters by comparing their standard candle distances (derived from their apparent brightnesses and a knowledge of the SN Ia absolute luminosities) with luminosity distances calculated from their redshifts together with a set of cosmological parameters and the equations of General Relativity. As the cosmological parameters are, in principle, the only unknowns in this analysis, constraints can be placed on their values with a sufficient number of SNe Ia.

This apparently simple concept has several non-apparent difficulties. Measuring departures in dark energy from $w = -1$ requires an extremely precise experiment: a 10 % difference in w from –1 is equivalent to a change in SN Ia brightness at $z = 0.6$ of only 0.04 magnitudes, an absolute precision perhaps not routinely achieved in astronomy. The challenge of photometrically calibrating the physical SN fluxes, as well as empirically controlling the various light-curve width and colour relations, is therefore considerable. Furthermore, the values of the other cosmological parameters that enter the luminosity distance calculation, such as the matter density or amount of curvature in the Universe, are not perfectly known. Other complementary observations must be used in conjunction with SNe Ia (see Figure 5) which place constraints, or priors, on the matter density (e.g, observations of large-scale structure) or spatial flatness (e.g., observations of the Cosmic Microwave Background). Finally, the absolute luminosity of a SN Ia is not known precisely and cannot be used a priori. The SN Ia method critically relies on sets of local SNe at $0.015 < z < 0.10$, where the effect of varying the cosmological parameters is small, and which essentially anchor the analysis and allow relative distances to the more distant events to be measured.

The cosmological analysis of the first year SNLS dataset (SNLS1) is published in Astier et al., 2006; the key results are shown in Figure 5. The result, $\langle w \rangle = -1.023 \pm 0.090$ (statistical error), is consistent with a cosmological constant (i.e., $w = -1$) to a better than 9 % precision. Analyses of SNLS3, the third-year sam-

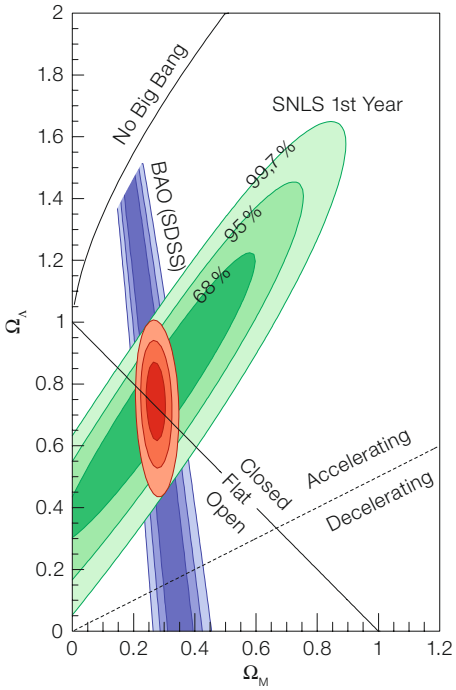

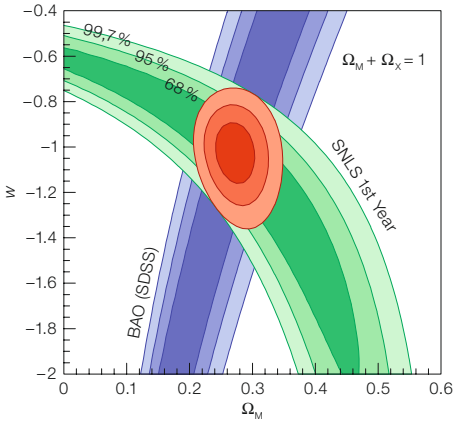

Figure 5. Cosmological constraints from SNLS1. On the left are the cosmological constraints in Ω_M versus Ω_Λ (assuming $\langle w \rangle = -1$), and on the right the constraints in Ω_M versus $\langle w \rangle$ (assuming a flat Universe and a constant equation of state w). The best-fitting result was $\Omega_M = 0.263 \pm 0.042$ for a flat ΛCDM model, and $\langle w \rangle = -1.023 \pm 0.090$ for a flat cosmology with a constant w. The statistical error in $\langle w \rangle$ of 9 % will improve to better than 6 % in the upcoming SNLS3 papers.

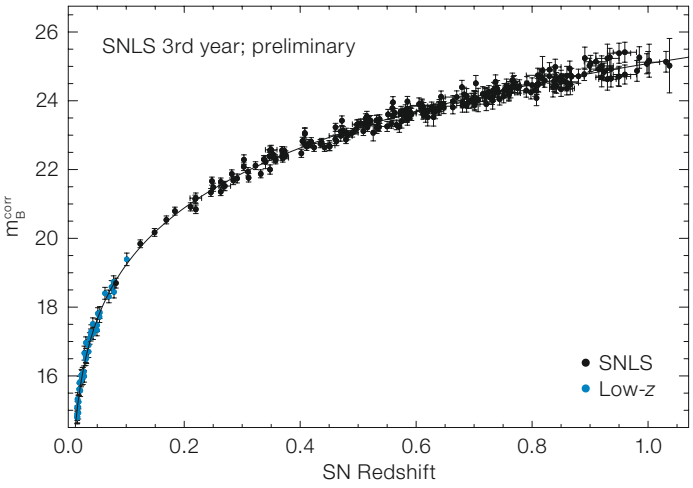

Figure 6. The preliminary Hubble Diagram from the SNLS3 analysis. Each black filled circle represents a SN detected and monitored at the CFHT, and spectroscopically confirmed using 8–10-m class facilities such as the ESO/VLT. The blue circles are the lower-redshift comparison sample which anchor the Hubble diagram analysis.

ple, are now nearing completion (a preliminary Hubble Diagram can be found in Figure 6). With a sample size three times larger than SNLS1, the analysis provides not only a step forward in the statistical precision, but in the understanding of SNe Ia as astrophysical events, and will lead to a better than 6 % constraint on $\langle w \rangle$. A ~ 5 % measurement of $\langle w \rangle$ is expected from the final SNLS sample, as well as the first detailed measurements of the degree to which w changes out to $z = 1$.

Supernova astrophysics

Taken at face value, the simplicity of the SN Ia technique – comparing the relative brightnesses of events at different distances – suggests the ultimate accuracy of their use may only be limited by the extent to which relative calibrations of their fluxes can be performed. This may, however, be an over-simplification, and would ignore the considerable uncertainty that exists over the underlying physics governing SN Ia explosions. For example, the configuration of the progenitor system prior to explosion is very uncertain. Both single degenerate systems (a white dwarf star together with a main-sequence or red-giant companion) or double degenerate systems (two white dwarf stars) could theoretically result in a SN Ia explosion. There are also open questions as to how the metallicity or age of the progenitor star may influence the observed properties of the SN explosion, leading to possible biases as the demographics of the SN Ia population shifts slightly with look-back time.

The SNLS has provided some new insight into these issues. The homogeneous nature of the CFHT-LS data provides not only precise SN light curves, but also extremely deep image stacks from which SN Ia host galaxy information can be obtained (Sullivan et al., 2006). Analyses of these data allow the measurement of galaxy properties such as stellar mass, star formation activity and mean age, and subsequent studies of how SN Ia properties relate to these different variables.

In particular, the classical view that most SNe Ia result from old, evolved stellar populations appears incorrect. Although some SNe Ia do occur in passive systems with little or no recent star formation activity, consistent with a long delay time from stellar birth to SN explosion, most seem to occur in actively star-forming galaxies, suggesting a short delay time (Figure 7; see also Sullivan et al., 2006). These prompt and delayed SNe Ia possess different light curves: prompt SNe Ia appear brighter with broader light curves, while the delayed component SNe are fainter with fast light curves. By virtue of the evolving mix of quiescent and star-forming galaxies with redshift, a subtle redshift evolution in SN Ia population demographics is predicted (Figure 7) and has now been observed in SNLS data (Howell et al., 2007). Although such shifts do not affect cosmological conclusions if the SN Ia calibrating relationships remain universally applicable, further analysis of the SNLS dataset is required to test this assumption.

The most straightforward interpretation of this environmentally-dependent SN Ia rate is a wide range of delay times, but the exact physical implications are un-

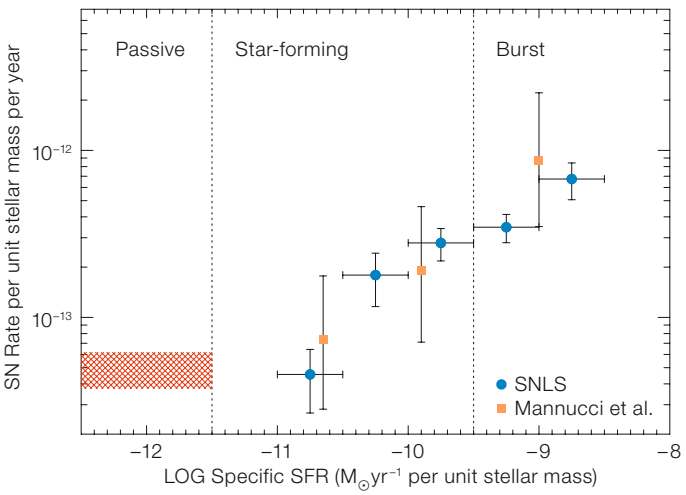

Figure 7. SNLS has provided evidence that SN Ia properties are dependent on the age of the progenitor system. The SN Ia rate per unit stellar mass *versus* host star-formation rate per unit stellar mass (Sullivan et al., 2006). Blue points refer to SNLS data, orange points to local estimates. The red area indicates the SNLS SN Ia rate in passive, or zero star-formation rate, galaxies. A SN Ia population with a wide range of delay times is supported: simplistically, a delayed population in quiescent galaxies together with a prompt population whose rate correlates with recent star formation.

clear. The SNLS relation between SN Ia rate and star-formation rate (Figure 8) implies that around 1 % of all white dwarfs end their lives as SNe Ia (Pritchet et al., 2008), independent of their initial mass. As the single degenerate model typically has lower conversion efficiencies at lower masses, this suggests that some other mechanism is responsible for the production of at least some SNe Ia. However, the precise implication for the progenitor systems must await the construction of a more detailed delay-time distribution.

Future perspectives

The upcoming analysis of the SNLS third year dataset will provide the most precise measurement yet of the nature of the dark energy driving the accelerating cosmic expansion. While these cosmological results will inevitably draw most attention, SNLS has also allowed new insights into the astrophysics governing SN Ia progenitors and their explosions. To date, no effect has been uncovered that challenges the conclusions that have been drawn from using SNe Ia in cosmological applications, but some open questions remain. Why are the brightest SNe Ia associated with short delay times and the youngest galaxies? How well do SNe Ia from different environments inter-calibrate in a cosmological analysis? A tantalising possibility is the existence of *more than one progenitor mechanism* (e.g. Mannucci et al., 2006). The key to making progress is to pinpoint any fundamental environmental differences between delayed and prompt events. For example, metallicity is predicted to affect SN Ia luminosities and rates. Timmes et al. (2003) predict that higher metallicity progenitors produce white dwarfs richer in ^{22}Ne, with an increased neutronisation during nuclear burning producing stable ^{58}Ni at the expense of the ^{56}Ni that powers the light curves. As a result, a ≤ 25 % difference in luminosity is expected between high and low metallicity environments. Recent observational results hint at these effects (Gallagher et al., 2008), but urgently need confirmation with detailed spectroscopy of the host galaxies of larger, complete and homogeneous samples, such as the SNLS. Such a programme will soon commence using the VLT.

As with any experiment, the final precision of the SNLS results is governed by both statistical and systematic uncertainties. As more SNe Ia are used in the analysis and the statistical error decreases, the contribution of systematic errors becomes increasingly important. Ultimately, the challenge of controlling systematics in SN cosmology is two-fold. The first is photometric calibration. The SNLS calibration is accurate to about 0.01–0.015 magnitudes; future, planned experiments will require a calibration of better than 1 % in both the distant and nearby sample – as much effort is required for the local sample as was needed for the higher-redshift SNLS dataset. The second challenge is understanding the limitations of SN Ia by investigating their astrophysical properties and controlling any subtle evolutionary effects. SNLS is providing the essential stepping stone for both efforts.

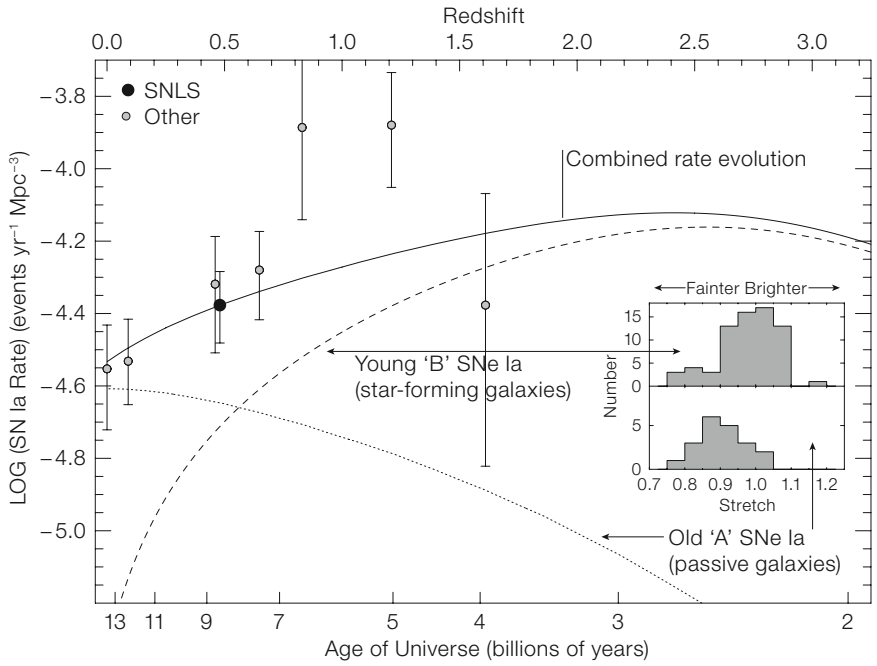

Figure 8. The volumetric SN Ia rate redshift evolution derived from the SNLS SN Ia properties. The relative mix of the two components will evolve with redshift (main panel). As SN light curve width ('stretch') correlates with star-formation activity in the host (inset histograms), a mild evolution in mean SN Ia light-curve width with redshift is implied as the relative mix of the two components changes. This effect has been detected in SNLS data (Howell et al., 2007), and must be carefully controlled in Hubble diagram analyses.

References

Appenzeller, I., et al. 1998, The Messenger, 94, 1
Astier, P., et al. 2006, A&A, 447, 31
Copeland, E. J., Sami, M. & Tsujikawa, S. 2006, International Journal of Modern Physics D, 15, 1753
Gallagher, J. S., et al. 2008, arXiv:0805.4360
Howell, D. A., et al. 2007, ApJL, 667, L37
Mannucci, F., Della Valle, M. & Panagia, N. 2006, MNRAS, 370, 773
Perlmutter, S., et al. 1997, ApJ, 483, 565
Perlmutter, S., et al. 1999, ApJ, 517, 565
Phillips, M. M. 1993, ApJL, 413, L105
Pritchet, C. J., Howell, D. A. & Sullivan, M. 2008, arXiv:0806.3729
Riess, A. G., et al. 1998, AJ, 116, 1009
Sullivan, M., et al. 2006, ApJ, 648, 868
Timmes, F. X., Brown, E. F. & Truran, J. W. 2003, ApJL, 590, L83

Some of the participants of a recent media training workshop which took place at the ESO Vitacura office (see page 60).

Inauguration of the scale model of the Solar System in the school yard of Garching's Grundschule Ost (see page 58).

Photos: (Upper) M. San Martin; (Lower) U. Baumgart

Scientific Approach for Optimising Performance, Health and Safety in High-Altitude Observatories

Michael Böcker[1]
Joachim Vogt[2]
Tanja Nolle-Gösser[3]

[1] ESO
[2] Deutsche Flugsicherung GmbH, Germany
[3] Technical University of Dortmund, Germany

The ESO coordinated study "Optimising Performance, Health and Safety in High-Altitude Observatories" is based on a psychological approach using a questionnaire for data collection and assessment of high-altitude effects. During 2007 and 2008, data from 28 staff and visitors involved in APEX and ALMA were collected and analysed and the first results of the study are summarised. While there is a lot of information about biomedical changes at high altitude, relatively few studies have focussed on psychological changes, for example with respect to performance of mental tasks, safety consciousness and emotions. Both, biomedical and psychological changes are relevant factors in occupational safety and health. The results of the questionnaire on safety, health and performance issues demonstrate that the working conditions at high altitude are less detrimental than expected.

Environmental influences at high altitude

High-altitude environments are exposed to increased radiation, low humidity, thunderstorms, wind chills, and temperature variation. These environmental influences need to be considered when studying human behaviour at high altitude. Sakamoto et al. (2003) studied the cosmic radiation exposure for workers at the Chajnantor site. Cosmic rays are enhanced to a level that even the effects on very-large-scale integration electronic instruments, such as correlators, may not be negligible. The measured annual gamma ray dose rate (including ~ 0.45 mSv per year contribution of terrestrial gamma rays) was 3.14 mSv at Pampa La Bola, 1.70 mSv at San Pedro de Atacama, and 0.99 mSv at Santiago, respectively. As for the neutron component, altitude dependence is more severe: the measured neutron dose rates were 0.80 mSv at Pampa La Bola, and 0.25 mSv per year at San Pedro de Atacama, whereas it was 0.01 mSv per year at Santiago. After correction for the effects of solar activity and indoor shielding, Sakamoto et al. (2003) estimate the occupational exposure of an 8–6 shift employee to be 2.0 mSv per year, which exceeds that of a typical worker engaged in nuclear fuel cycle processing. Nevertheless the measured data is within the thresholds for health effects recommended by Euratom (Vogt, 2002).

In addition to the effects of radiation, workers at high altitude are also confronted with a variety of weather effects. Thunderstorms, lightning and lightning electromagnetic pulses occur during the entire year, but especially during winter time. Thunderstorms over the Chajnantor Plateau are usually strong with lightning frequency of 1.6 flashes per minute. Measurements between April 1995 and June 2003 demonstrated that the temperature is usually in the range between –20˚C and +20˚C at the Chajnantor site. At the APEX station in Sequitor and the ALMA Operations Support Facility (OSF) site, the ambient air pressure is 750 mbar ± 100 mbar, which corresponds to an air density of 0.96 kg/m^3 and a temperature range between –10˚C and +30˚C is expected. Hence, humans and materials must cope with the environmental high-altitude constraints, for example with a temperature shock from indoors to outdoors, and vice versa, of up to 30˚C.

The ALMA and APEX high sites are exposed to an environment of 0 to 30 per cent relative humidity and the annual precipitation on the site is in the range of 100 to 300 mm. Most of this falls as snow but thunderstorms with rain (and without) do occur. Heavy rain and hail may occur. From around 2 000 m up to about 3 000 m altitude, the expected relative humidity is 5 to 30 per cent with maximum rainfall of 20 mm/h. No hail precipitation is expected. Whereas the expected wind speed has a maximum of 65 m/s at the very high-altitude site, the wind speed at the Array Operations Site (AOS) and Sequitor will not exceed 40 m/s. The wind chill strongly affects people working at Chajnantor.

The above-mentioned data demonstrate that the environmental conditions are a continuous challenge for all humans working at very high altitudes. In particular the outdoor ALMA construction work requires strict rules and regulations as well as sustainable processes to allow people to adequately cope with the environmental demands. Several information campaigns have emphasised the danger of too rapid ascent to the high sites and the importance of the acclimatisation and adaptation of human behaviour to the environmental conditions. The recommended break times at the ALMA OSF as well as the mandatory safety instructions for staff members, for example, are effective occupational safety and health (OSH) enablers. Measures to improve work conditions, organisation, human behaviour, safety, and health awareness must be developed under strong medical supervision for all staff working at the high-altitude site.

Rationale of the study: behavioural and organisational issues

The environmental conditions mentioned above have an impact on technical equipment but also on the human physiology, well-being and behaviour. In addition to the directly related high-altitude disease symptoms, there are a number of minor symptoms when working at high altitude (West, 2003), for example:

(1) loss of appetite;
(2) loss of body weight (mainly related to 1);
(3) bright flashing arcs of light in the peripheral vision when blinking, possibly due to dehydration of the eye caused by stretching of the retina;
(4) fingernails separating from the skin further down the nail than usual and the tops of the nails becoming very white;
(5) constipation.

High-altitude workplaces are defined as workplaces at a level of 3 000 m and above. A recently published article in the Scientific American, entitled "Into Thin Air: Mountain Climbing Kills Brain Cells" (Fields, 2008) caused uncertainty among

astronomers about OSH at high-altitude observatories. The article described a study of a small sample of eight Aconcagua climbers who all suffered from a reduction of brain cortex ('cortical atrophy') detected in brain scans. Mountain climbing is physically very strenuous and requires much more oxygen compared to the typical work of most astronomers and technical staff at high-altitude sites. However the ESO internal medical statistics demonstrate that there are several cases of minor high-altitude sickness per week and preventive OSH measures should be in place at all high-altitude observatory sites. Although mountain climbing, as mentioned above, is in a different category, the negative influence of high altitude should by no means be underestimated and it is always present at ESO's APEX and ALMA sites at 5 050 m on the Altiplano de Chajnantor.

Workers whose itineraries take them above an altitude of about 2 400 m must be aware of the risk of altitude illness and potentially impaired mental performance. While the individual response to high altitude can vary, all people are at risk of altitude illness above about 3 000 m. The current internal ESO statistics of those working at the ESO ALMA and APEX high sites and the ALMA OSF do not suggest that certain demographics like age, sex or physical condition correlate with the susceptibility to altitude sickness. Wu et al. (2007) found some contra-indications for going to high-altitude sites based on a sample of 14 050 workers with an average age of 29.5 ± 7.4 years. But finally, there is no clear indication who will suffer from high-altitude illness. Wu et al. (2007) suggest that neither taking a rather permissive stance nor setting rigid rules of contra-indication are appropriate to decide who should ascend or not. On the one hand, one may put some persons at undue risk, but, on the other hand, one may exclude too many people from ascending. Obviously, poor physical condition (chronic obstructive pulmonary disease with notable arterial desaturation, cardiac infarction, heart failure, obesity with sleep apnea, or severe hypertension) at sea level will worsen at high altitude.

Conditions at the very high-altitude sites affect nearly all biological processes, particularly rhythms, including sleep. Due to the reduced adjustment of the body at high altitude, the person concerned has to work against bodily demands. Finally, the low oxygen (hypoxic) stress of altitude can impair work efficiency, performance and best practice, mainly due to maladaptive behaviour, distorted consciousness, impaired biomedical functioning and reduced sleep quality.

West (2004) attributes all medical effects of high altitude to the low partial pressure of oxygen in the inspired air, and so the most effective way of improving human performance is to add supplementary oxygen. Recent technical advances allow this to be done very efficiently by oxygen enrichment of room air or outdoors through use of small movable oxygen bottles with pulsatile nasal oxygen supply. However, an interface risk assessment must be performed, too. In case of indoor oxygen supplement, other OSH risks, such as an increased risk of fire, must be considered (West, 1997). Today's movable respiration systems for people working outdoors, or inside the ALMA antennas, are very comfortable, practicable and usable even in narrow spaces. Nevertheless, the system might hinder people from safely performing their work if it is not properly secured or if the environment is not properly designed for these processes. Hence, additional protective measures have been implemented at the site and to the technical equipment. There is, for example, the special operator seat in the ALMA antenna transporter which allows the driver to use the oxygen bottles during operation. However, a general use of oxygen might slow down the acclimatisation process of people at very high-altitude sites.

While there is a lot of knowledge about biomedical changes at high altitude and under low oxygen conditions, changes in behaviour, cognition, and emotion have rarely been systematically investigated. The study presented here, which was introduced in the earlier article by Böcker & Vogt (2007), bridges this gap using an elaborate questionnaire. Moreover, issues of work and organisation beyond the individual visitor and worker, such as planning of work and team performance, are addressed. Previous studies were often conducted on mountaineers with only a few persons taking part, and are thus not representative of the situation at an observatory. Therefore, people working or visiting the ALMA and APEX high-altitude observatory sites have been invited to fill in the questionnaire. The project aims to provide more systematic information on potential high-altitude induced hazards at the individual and work process level in order to better protect staff from negative effects and accidents, and to prevent damage to expensive scientific instruments. Changes in ability at the individual level have an impact on actual work behaviour at the process level as, for example, driving a car or planning of work. Finally, the project also considers potential performance losses such as performed capacity or meeting client demands, as well as problems in decision making during commissioning or operation of complex astronomical systems. These can be relevant for organisational performance, which is explicitly considered in the scope of this project.

Method

To systematically develop adequate recommendations, a questionnaire has been developed in English and Spanish to obtain the subjective impressions of visitors and employees (subsequently visitors/workers) when staying at high altitude. It was made available to all visitors/workers at the ALMA and APEX sites and returned by 28.

The first part of the questionnaire obtains work-related biographical data. The participants are asked how often they spend time at high altitude and how they prepare for the missions. They may also describe any unusual event at altitude workplaces and if they felt any limitations with respect to their work which may have been due to altitude (e.g. "Have you experienced limitations in planning and coordination"?). This is the introductory question concerning potential hazard areas, which are further elaborated in the second section of part one of the questionnaire. Here, 17 physical and psychological complaints are listed and the participants report to what extent they experienced complaints on a scale from 1 = extremely to 5 = not at all (e.g. emotions such as anger, irritability).

In the third section of the first part of the questionnaire the participants are asked to rate the change of abilities, work behaviour, and work performance at high altitude. The scale ranges from 1 = strongly impaired, through 3 = not changed, to 5 = strongly improved at altitude (example ability item: “Perceptual speed: ability to perceive and compare information quickly and accurately”; example work behaviour item: “Driving a car”; example performance item: “Performed capacity”). This final section of part one of the questionnaire was designed to draw conclusions on potentially impaired performance at high altitude.

The second part of the questionnaire refers to OSH programmes and their perceived benefit. In the first section of part two of the questionnaire the participant is asked to list all safety-related information he used and any other support (e.g. “Briefing by Supervisor”) used to become knowledgeable and fit for high-altitude workplaces. The participants are also asked to estimate the amount of time spent with each document/support as well as how beneficial they have been concerning work at high altitude. In the second section of part two of the questionnaire, the document/support with the highest perceived benefit is described and rated by the participant.

The third part contains a “Performance and Well-being Diary” consisting of three tables. The participant rates the average workload per day, before, during and after his mission, in the first table and how it was managed in the second table. The third table describes the well-being, before, during, and after the mission. Of the questionnaires returned so far, this final part was not well filled in. It will be covered in one of the following reports.

Study participants

28 questionnaires were returned. 86 per cent of the respondents were men. The largest age group was between 41 and 45 years old (32 per cent), however, all age groups, from less than 25 to older than 51, were represented in the sample. The majority of the participants were working as technicians or engineers (61 per cent). Roughly half of them were visitors at high altitude; the other half consisted of regular workers.

Results

Generally, the study participants did not report major problems at high altitude; the level of limitations, complaints, and difficulties was rather low, mostly not significantly different compared to normal altitude. The differences between visitors and workers show that – at this low-problem level – workers reported slightly more limitations, slightly more complaints, and slightly more difficulties; however, only very few differences were statistically significant. Figure 1 shows, for example, the average limitations of tasks at high altitude reported by visitors/workers.

The visitors reported only slight to no limitations of planning, team work, manual and other tasks (e.g. computer programming). The workers tended to report slightly more limitations heading towards 3 (moderately limited), but not statistically different from 4 (slightly limited). However, in most cases a significant difference to the rating 5 (“not at all limited”) was found, indicating that there are limitations under high-altitude conditions, although they are only moderate in the case of the worst-affected task (other tasks such as programming). Team work can have a social activation function, in that it reduces the fatigue and attention problems that might be induced by high-altitude conditions and travel jet lag. Workers tended to report more limitations than visitors; however, no group difference was statistically significant.

The experience of physical and psychological complaints at altitude workplaces ranged on average from slight to non-existent. Concentration problems, fatigue, reduction of usual activities, and shortness of breath were the only complaints from workers with means below 4 and – in case of shortness of breath – also for visitors. Fatigue and shortness of breath are the two symptoms, in which the deviation from rating 5 (not at all) to 4 (slightly) is statistically significant and not a mere variation by chance in both groups. For visitors, the experienced slight concentration problems and dizziness/vertigo are significantly different from rating 5 (= not at all). For workers, the reduction of normal activities is significantly different from 5. Most other complaints that have been reported by mountaineers were not experienced at all by the ESO site workers and visitors (e.g. isolation, nausea and vomiting). There was a slight tendency that visitors report fewer complaints than workers, however, no group difference reached statistical significance.

Work behaviour reported by workers and visitors was not significantly changed (average of 3 = not changed). This is not surprising because the underlying abilities were, if at all, only slightly impaired and humans can compensate for ability losses by increasing effort. This might lead to the conclusion that, for example, the influence of critical incidents (accidents, armed robbery or similar) on the compensation ability might be negatively affected for staff working at very high altitude. Vogt et al. (2004, 2007) reported up to 30 per cent loss of planning ability after critical incidents, if these critical incidents were not treated properly. It has been demonstrated that Critical Incident Stress Management (CISM) is a useful intervention tool. Untreated staff were straining harder and needed significantly longer recovery periods compared to their normal performance.

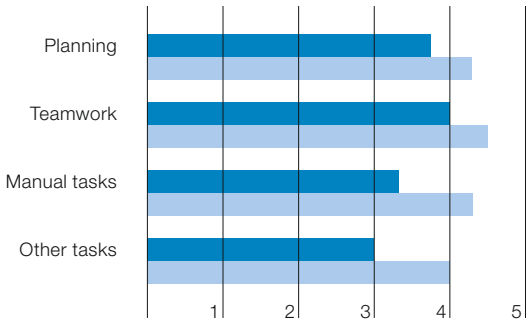

Figure 1. Histogram showing the breakdown of self-reported limitations of tasks in high-altitude work (1 = extremely limited; 2 = very; 3 = moderately; 4 = slightly; 5 = not at all limited).

Study conclusions

From the perspective of visitors/workers at high altitude, the results of this study document fewer problems than expected. The visitors/workers neither reported major psychosomatic complaints nor impairment of abilities, work behaviour or work performance. However, the data indicated some areas worthy of further study that bear potential improvement for OSH programmes, such as concentration/awareness problems, fatigue/under-arousal and reduced capacity. Although not statistically significant from the study so far, workers generally report slightly more problems at high altitude than visitors. However, cultural differences, for example, optimism of local workers *versus* critical view of visiting scientists, probably also play a role.

With respect to the preparations for high-altitude work and the benefits of OSH programmes, one result of this pilot study is that some participants did not report any preparation in matters of safety for their work at high altitude. The remaining visitors and workers, who reported on their preparations, mostly used more than one method. Some visitors have done more than expected. Additional information which exceeds that contained in the ALMA High Altitude Visitors Information packet and the site safety instruction by the site safety officer, was sometimes mentioned in the questionnaire returns. This diligence implies that high-altitude safety and health issues are seriously considered also by visitors – an indication that most of them were concerned about visiting a high-altitude site and, therefore, were interested in getting useful background information.

Although only a minority of participants did not report about preparations for ascent to high altitude, serious incidents may be more likely to happen to individual high-altitude visitors/workers with reduced safety consciousness. Thus, we need to find out how to convince everybody to adequately prepare for the work at very high altitude. This finding is in line with other studies, for example, with air traffic controllers, who in two thirds of cases concerning critical incidents had attended a stress management programme and in one third had not (Vogt et al., 2004; 2007). The latter third demonstrated a reduced performance for a longer period after an incident. The organisational culture and the safety attitude of supervisors play an important role in the decision of employees to use OSH programmes or not. With improved attractiveness and marketing of the materials/programmes on the one hand, and organisational culture and safety leadership on the other, we have the necessary tools to win over everyone to an appropriate preparation for and use of OSH materials/programmes.

References

Böcker, M. & Vogt, J. 2007, The Messenger, 127, 64
Fields, R. D. 2008, Scientific American, April/May 2008
Sakamoto, S., et al. 2003, ALMA Memo, 446
Vogt, J. 2002, in *Lehrbuch der Umweltmedizin*, ed. Dott, W., et al., (Stuttgart: Wissenschaftliche Verlagsgesellschaft mbH), 479
Vogt, J., et al. 2004, International Journal of Emergency Mental Health, 6, 185
Vogt, J., Pennig, S. & Leonhardt, J. 2007, Air Traffic Control Quarterly, 15, 127
West, J. B. 1997, Aviation Space and Environmental Medicine, 68, 162
West, J. B. 2003, ALMA Memo, 477
West, J. B. 2004, The Observatory, 124, 1
Wu, T., et al. 2007, High Altitude Medicine & Biology, 8, 88

Report on the ESO and Radionet Workshop on

Gas and Stars in Galaxies – A Multi-Wavelength 3D Perspective

held at ESO Garching, Germany, 10–13 June 2008

Matt Lehnert[1]
Carlos De Breuck[2]
Harald Kuntschner[2]
Martin Zwaan[2]

[1] Laboratoire d'Etudes des Galaxies, Etoiles, Physique et Instrumentation (GEPI), Observatoire de Paris-Meudon, France
[2] ESO

An overview of the ESO/Radionet workshop devoted to 3D optical/near-infrared and sub-mm/radio observations of gas and stars in galaxies is presented. There will be no published proceedings but presentations are available at *http://www.eso.org/sci/meetings/gal3D2008/program.html*.

The main aim of this ESO/Radionet workshop was to bring together the optical/near-IR and sub-mm/radio communities working on three-dimensional (3D) extragalactic data. The meeting was attended by more than 150 scientists. This article, due to space limitations, provides a, necessarily biased, overview of the meeting. We decided not to publish proceedings, but the presentations are available from the workshop homepage at *http://www.eso.org/sci/meetings/gal3D2008/program.html*. The names of speakers relevant to a topic are included here so that

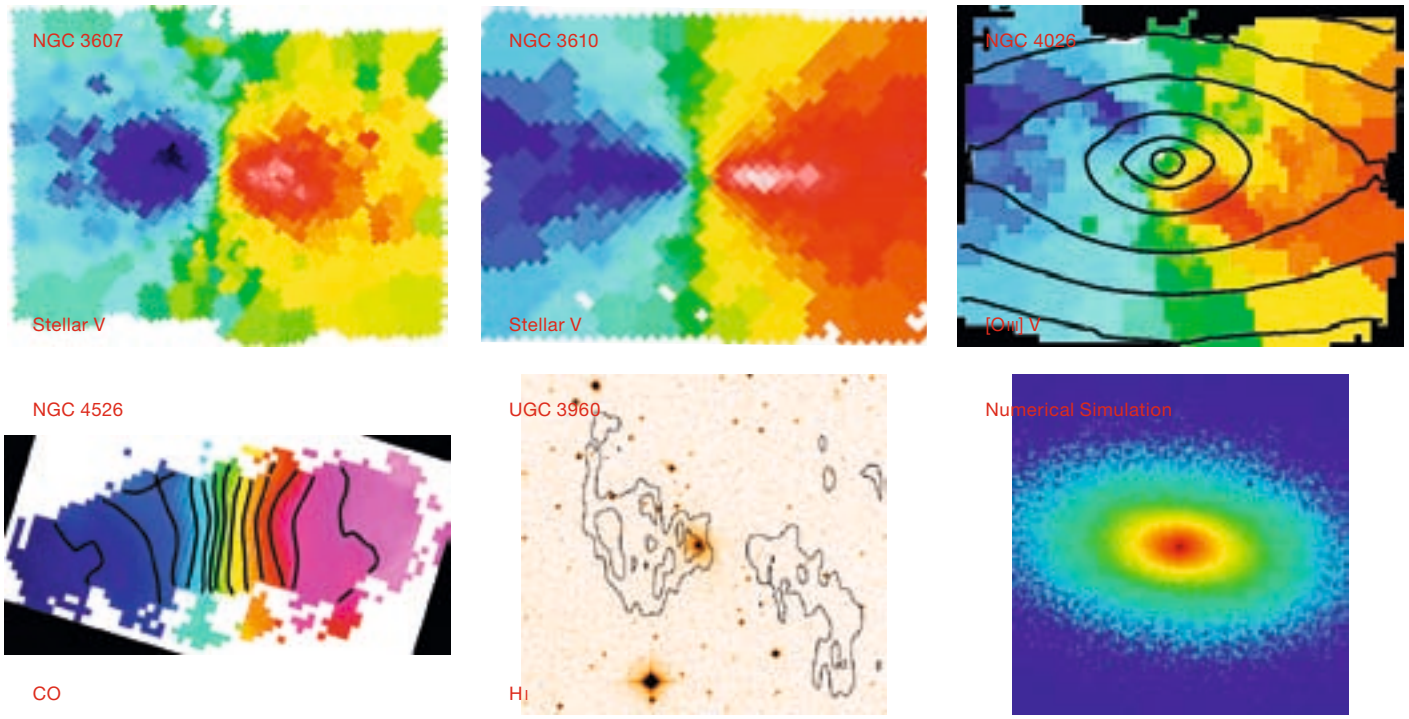

Figure 1. The Atlas^{3D} project *(http://www-astro.physics.ox.ac.uk/atlas3d)* includes a multi-wavelength coverage of a complete sample of nearby early-type galaxies, including optical IFU, CO and HI data combined with a specific effort on numerical simulations. Illustrations of the Atlas^{3D} datasets are shown, from top left to bottom right: stellar velocity maps of NGC 3607 and NGC 3610; ionised gas velocity map of NGC 4026; CO velocity map of NGC 4526; HI contours of UGC 3960; and a projected snapshot of a numerical simulation.

further reference to the presentations can be made through the web page.

The optical/near-IR community now has access to an increasing number of powerful Integral Field Units (IFUs; see presentation by Eric Emsellem) and the second-generation VLT instruments, as well as the proposed E-ELT instruments, will all have IFU units (Niranjan Thatte). These instruments will thus provide large data cubes sampling the stellar content and the warm/hot ionised gas.

Radio and millimetre interferometers have provided 3D information on gas in galaxies for decades (Thijs van der Hulst). ALMA will – by design – always provide high spatial and spectral resolution data cubes of the cold gas (Robert Laing), allowing the molecular and dust distribution to be traced in galaxies. Future radio facilities (Philip Diamond) will extend current studies of neutral hydrogen out to cosmological distances and will provide information on the cool gas in and around galaxies. All of these devices and techniques are necessary if we are ever going to understand the complex interaction between gas and stars in galaxies.

It was clear from the meeting that we are indeed learning a great deal about the detailed relationships between gas phases in galaxies, how star formation proceeds, and how the global environment within galaxies affects these relationships. Perhaps uniquely emphasised at this meeting was the important role that instrumentation, especially those that provide three-dimensional (spatial and spectral) information, can play in our overall understanding of star formation and galaxy evolution.

Early- and late-type galaxies

One of the most fascinating themes of the conference was the nature and continuing growth of early type galaxies. The paradigm that early-type galaxies always mean pressure-supported systems with no recent star formation, and certainly no accreted gas, has been consigned to historical novelty. It appears now through the Atlas^{3D} project with the SAURON imaging spectrograph (presentation by Michele Cappellari, see Figure 1) that early-type galaxies show a surprising amount of rotation. This was not apparent previously because of the narrow range of magnitudes and the limited number of the galaxies in earlier surveys. Less luminous, and more numerous early-type galaxies tend to show more rotational support than their more massive and rarer cousins. So most early-type galaxies are lenticulars and not ellipticals. These observations can plausibly be explained by mergers with a range of mass ratios that are typically 1:2 or 1:3 (Thorsten Naab). But of course, the final result depends on the initial orientations and amplitude of the various angular momentum vectors of the progenitors and the orbit (Maxime Bois). However, there were some puzzling, and perhaps alarming, comments that these merger models, while perhaps explaining the large-scale dynamics, cannot account for the orbit families within early-type galaxies. Obviously, the exquisite 3D data that we are able to produce is a real puzzle for modellers (Mathieu Puech).

It also appears that we can watch the growth of structure within early-type galaxies. By studying the CO and HI emis-

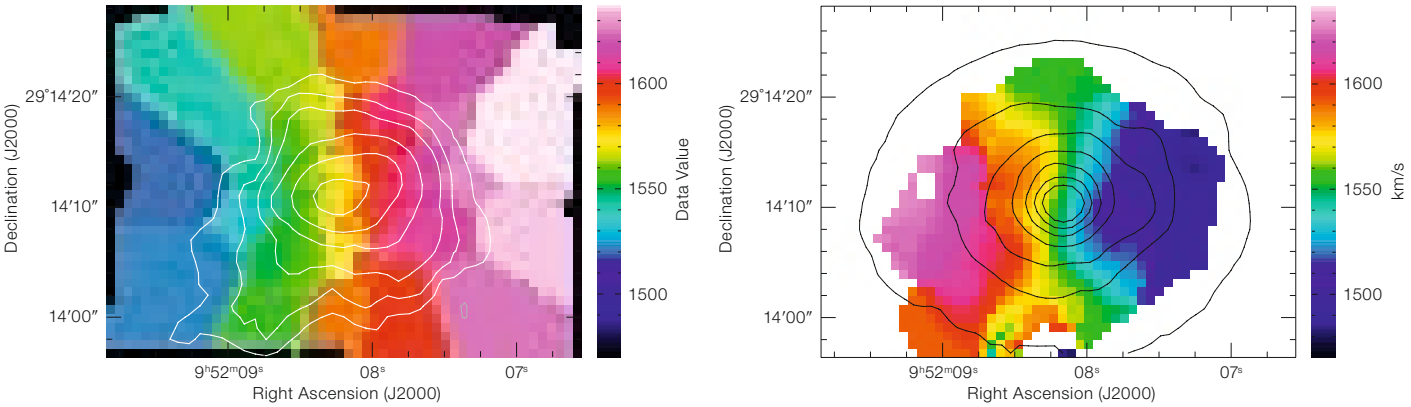

Figure 2. Comparison of CO and optical 3D data for NGC 3032. **Left:** Stellar mean velocity field, overlaid with contours from the integrated/total CO(1–0) map (Young et al., 2008). **Right:** CO mean velocity field, overlaid with the optical (roughly *V*-band) isophotes (Emsellem et al., 2004).

sion from early-type galaxies, it is possible to observe a relationship between gas content and the dynamical properties and ages of the stars in their circumnuclear regions. For example, even though this relation can only be measured for a relatively short time, due to rapid fading, ~ 20 % of early-type galaxies show evidence for young stars in their circumnuclear regions (Martin Bureau) and overall there appears to be a relationship between young ultraviolet bright discs, CO emission, and young stars and star formation (see Figure 2). In fact, it appears that such star-formation events follow the relation between the star-formation rate and the gas-surface density relation – the so-called Schmidt-Kennicutt relation (Martin Bureau). Even though such observations are just beginning, it is already clear that early-type galaxies can contain a significant amount of neutral hydrogen (10–15 % of which have 10^{9-10} solar masses of HI; Raffaella Morganti) with a hint that perhaps galaxies with centrally concentrated HI also have younger stars in their nuclei. These observations may also explain the dichotomy in 'kinematically decoupled cores' (KDCs), that is a core which has different kinematics to the surrounding galaxy. Large KDCs appear to have formed long ago, while smaller KDCs appear to have formed rather recently (results by the SAURON team, reported by Martin Bureau). This difference is likely to be related to recent gas accretion as seen in mm- and cm-wavelength observations.

Late-type star-forming galaxies in the local Universe are also full of surprises. There are several theories for explaining how star formation is driven on large scales – from gravitational instabilities, to such instabilities aided by magnetic fields, to large-scale convergent flows or density fluctuations in the gas. Recent multi-wavelength observations in the optical, HI and CO of star-forming galaxies indicate that molecular gas forms with fixed efficiency, that giant molecular cloud populations are universal, but that the formation of molecular clouds clearly depends on the large-scale environment (contribution by Adam Leroy, see Figure 3). This universality of molecular clouds was emphasised by comparing the clouds in our own Milky Way with those of other galaxies (Alberto Bolatto). These data seem to disfavour the primary role of magnetic fields in star formation, but are currently limited by the sensitivity of the tracer CO emission to optical depth effects. Obviously much more work needs to be done to constrain star-formation theories, which are so critical to our understanding of galaxies.

Active galactic nuclei and black holes

What is the role of active galactic nuclei (AGN) in galaxy formation and evolution? The relationship between the mass of the supermassive black holes and the mass of their surrounding spheroids is one of the most remarkable relationships in astrophysics and suggests an underlying connection between galaxies and black holes. However, is this relationship universal across all spheroid masses? The answer appears to be yes at the low-mass end of spheroid mass (talks by Roberto Saglia and Davor Krajnovic) but perhaps not at the high-mass end. Where does this relationship come from? It could be due to a self-limiting cycle of black hole growth, followed by kinetic energy from the AGN quenching both star formation and further accretion by the black hole. Active galaxies appear to have a greater incidence of streaming motions in the large-scale gas distributions (Gaelle Dumas), which then might reach the nucleus through torques on the gas (unlikely), but perhaps viscosity is a more likely mechanism, and finally

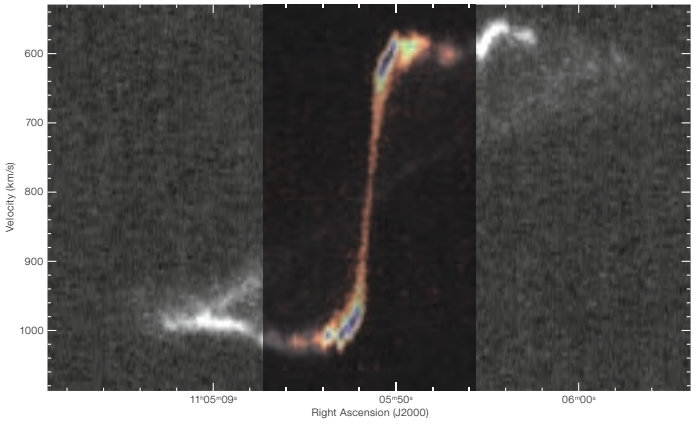

Figure 3. Major axis position-velocity diagram of NGC 3521. Greyscales are neutral hydrogen 21-cm emission from the THINGS project (Walter et al., 2008). The colours represent HERA CO emission (HERACLES, PI: Adam Leroy). Picture credit: Erwin de Blok.

this may lead to both star formation and accretion onto the black hole (Eva Schinnerer). But what comes first, the supermassive black hole or the galaxy? Dynamical masses derived from CO observations of very high-redshift powerful AGN (Figure 4) suggest that supermassive black holes become very massive before their galaxies have grown substantially. In fact, instead of being about 0.1 % of the total bulge mass, the black hole mass at $z \sim 6$ it is more like 3 % (Fabian Walter)! When they do get fuelled, the AGN, or at least the radio-loud AGN, can drive vigorous outflows of the type necessary to suppress further star formation and black hole growth (Nicole Nesvadba). But it also appears as if the halos of radio galaxies might have significant amounts of HI, up to $10^{11–12}$ solar masses, as probed by resonantly scattered Ly-alpha radiation (Joshua Adams).

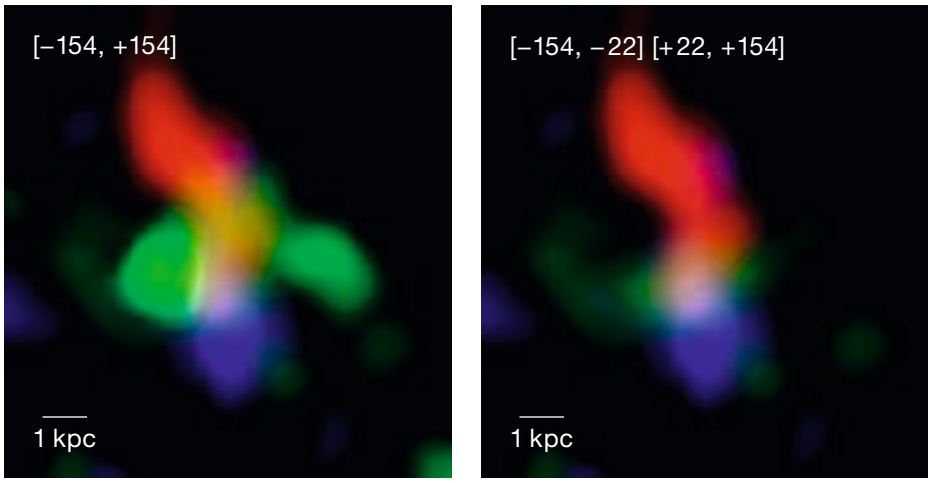

Figure 4. CO velocity field of the $z = 4.4$ interacting galaxy BRI 1335 (Riechers et al., 2008), with the velocity of the gas colour coded. The left panel shows the whole velocity range (indicated in the top), while in the right panel the contribution of gas around the systemic velocity of the galaxy is excluded, emphasising the outflows.

What processes drive the growth of mass in galaxies? What are the relative roles of gas accretion, from the dark matter halo and surroundings, versus merging with other galaxies as the driving force for the star-formation history of the Universe? This debate was joined in the meeting from several different directions. Direct observations of gas accretion in nearby galaxies are scant. The amount of HI seen in the halos of galaxies is relatively insignificant (talks by Filippo Fraternali, George Heald and Tobias Westmeier) and its origin is unclear (George Heald). Perhaps these are not the correct type of observations, and this accreting gas is in another phase yet to be probed. The role and nature of mergers in the local Universe is of course not disputed. The most actively star-forming galaxies in the local Universe are gas-rich mergers and provide an important testing ground for our theories of star formation in active environments (presentations by Christine Wilson and Susanne Aalto), even if we do not understand completely how they evolve (John Hibbard). In such environments, with their high optical depths, it is important to probe the gas in a number of molecular species, thus providing information about the physical conditions within the gas (talks by Susanne Aalto and Masatoshi Imanishi). Mergers may also play an important role in our understanding of the environments of galaxies. Tidal dwarfs, formed out of the tidal arms that are generated during the merger process, helping us to understand the properties of star formation in differing environments, can also provide important information about the nature of dark-matter halos (Pierre-Alain Duc). Three-dimensional observations of high-redshift galaxies ($z \sim 2$) in the rest-frame optical and mm, on the other hand, emphasised the role of gas accretion. Some participants suggested that these observations are apparently not consistent with a significant role of mergers (Kristen Shapiro), but rather with a simple settling of discs over many dynamical times (Natascha Förster Schreiber, see Figure 5). The star-formation rates in high-z galaxies appear to be consistent with gas accretion from hierarchical merging models, as well as the star-formation properties like local discs (talks by Nicolas Bouché, Helmut

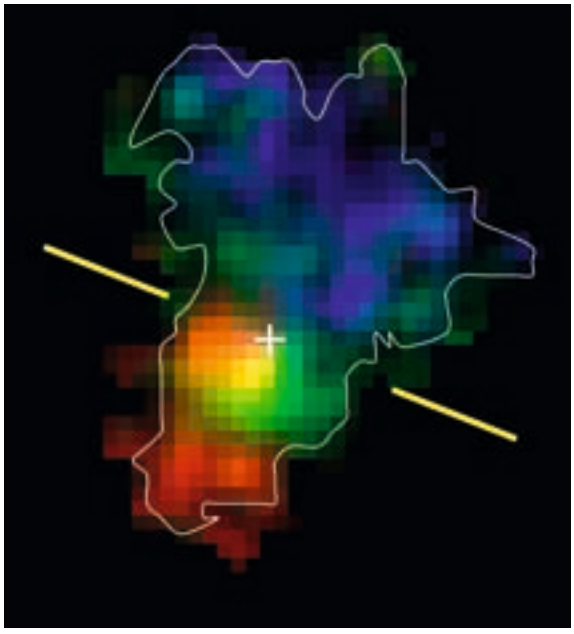

Figure 5. H-alpha velocity field of the $z = 2.38$ galaxy BzK-15504 obtained with SINONFI+AO (from Genzel et al., 2006).

Photo: H. H. Heyer, ESO

Figure 6. The conference participants group photograph taken just in front of the Max-Planck-Institut für Plasmaphysik lecture theatre.

Dannerbauer and Mark Swinbank). However, it also appears that there is a great deal of diversity in the observed molecular properties of high-redshift populations (Pierre Cox).

Of general concern with high-redshift galaxy studies is the low spatial resolution. At $z = 2$, the scale is about 8 kpc per arcsecond; thus with seeing-limited, or even adaptive-optics, observations the resolution is no better, and often much worse, than 1 kpc. Strongly lensed galaxies, however, offer the opportunity to obtain physical resolutions of ~ 100 pc and investigate the fine-scale relationships between the optical emission-line gas and the molecular gas (as exemplified in talks by Mark Swinbank and Andrew Bunker). As such, this is a powerful technique for studying the phenomenology of distant galaxies, such as their ability to drive winds, and investigating whether or not their star formation is similar to that in the local Universe. In the mm regime, ALMA will have a significant impact (talk by Robert Laing), as is already illustrated by the new extended baselines of the IRAM Plateau de Bure interferometer (Pierre Cox).

A very important component of this meeting, and one that perhaps makes it unique for a meeting of this kind, was the various talks on data reduction and visualisation techniques. Of course, mm- and cm-wave astronomers have been using 3D visualisation techniques for decades (Thijs van der Hulst) but these are still relatively new for optical and near-infrared astronomy (Giovanni Cresci). Particularly interesting are the techniques being used in medical imaging and diagnosis (described by Neb Duric). While often in a different regime (higher resolution and signal-to-noise), medicine is producing a number of powerful techniques to look for subtle relationships in three-dimensional (and four-dimensional!) data. The vast explosion in data rates in astronomy should also not be overlooked. How are we going to handle this flood of data? Visualisation should make more use of the computing power of modern Graphical Processing Units, developed for the computer game industry (Chris Fluke). Of course the *raison d'être* of the Virtual Observatory is to make this vast quantity of data, with all its complexity, available to the community (Igor Chilingarian).

In summary, it was clear from the myriad of physical processes, which must be understood in order to understand galaxies and star formation, that we have our work cut out for us. The amount of detail that the current generation of 3D facilities is revealing in galaxies is quickly advancing our knowledge. The next generation of observing facilities (e.g. ALMA and the second-generation VLT instruments) being planned or developed will only add to this happy state of affairs. However, what was also clear from the discussions during the meeting is that we need to develop our theoretical understanding and modelling techniques to be able to truly take advantage of our new observational abilities. While overall the meeting was optimistic about the future of research into gas and stars in galaxies, it was also obvious that we have a lot more to learn!

References

Emsellem, E., et al. 2004, MNRAS, 352, 721
Genzel, R., et al. 2006, Nature, 442, 786
Riechers, D., et al. 2008, ApJL, submitted
Walter, F., et al. 2008, ApJ, in press
Young, L. M., Bureau, M. & Cappellari, M. 2008, ApJ, 676, 317

ESO at SPIE – Astronomical Telescopes and Instruments in Marseille

Alan Moorwood
ESO, SPIE Symposium Chair

The latest in the series of bienniel SPIE meetings devoted to Astronomical Telescopes and Instruments, held alternately in the US and Europe now for more than a decade, took place in Marseille from 23 to 28 June 2008. Its theme was "Synergies between Ground and Space" and, with more than 2 000 participants and 1800 papers, came close to rivalling the, so far, largest meeting in Hawaii in 2002.

ESO was again a major presence contributing 140 participants and over 50 papers plus a Symposium Chair, 6 Conference Chairs, many Programme Committee members, a Plenary Speaker, plus the large stand shown in Figure 1 which proved to be one of the most popular meeting points. As overheard more than once, it provided a great opportunity for ESO Garching and Chile staff to meet!

The Technical Programme comprised
– three plenary talks: Fabio Favata on the ESA Programme; John Mather on the COBE satellite, his resulting Nobel prize and JWST; and Tim de Zeeuw on European Perspectives for Ground-based Astronomy;
– eight telescopes and systems conferences;
– four technology advancement conferences;
– continuous poster sessions;
– half-day plenary workshop of invited papers on the Early Universe;
– seven courses on optics, detectors and software;
– a student networking lunch;
– an extensive exhibition featuring many high-tech companies and ESO.

The social programme included
– welcome reception;
– conference dinner, in the spectacular setting of the palace built by Napoleon III overlooking the old port of Marseille and with an entertaining after dinner speech by Matt Mountain, Director of the Space Telescope Science Institute;
– visits to local facilities such as LAM, OAMP, OHP and SESO, largely organised by Jean-Gabriel Cuby.

Photo: E. Janssen, ESO

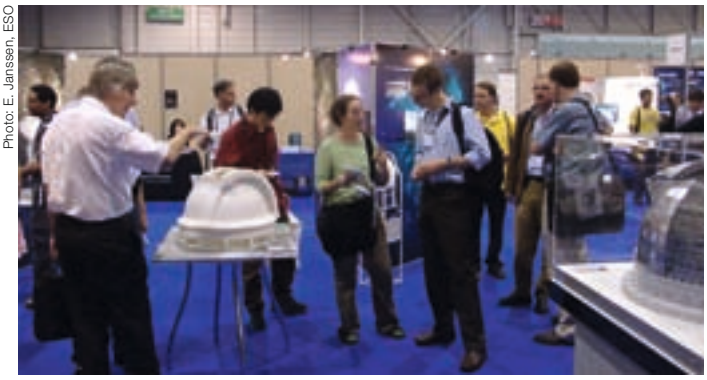

Figure 1. The ESO stand with models of a possible ELT dome and an ALMA antenna amongst other things – and some interested and engaged visitors.

As usual, this meeting covered essentially everything happening, or planned, astronomically on the ground and in space and placed considerable stress on individual participants to map out their own interests amongst the parallel sessions. I personally think one of the most useful products of these symposia is the Technical Programme, which provides an invaluable directory of astronomical projects and those involved. Given the weather, some opted simply to stay in the rooms with the best air conditioning. Fortunately, that was acceptable in the main auditorium where the plenary talks and the plenary conference were held. Having led the development of the ASTRONET Science Vision, Tim de Zeeuw (Figure 2) was in the unique position of being able to present both Europe's astronomical research priorities and those planned to be met with ESO's current and future facilities, while Nobel Laureate John Mather and the director of the Max-Planck Institute for Astrophysics, Garching, Simon White, reminded us of their goals to discover the unexpected.

One big attraction for me was the possibility of hearing overviews of the performance of most major facilities (all the 8–10-m observatories) and the status of future projects (ELT's, SKA, JWST) from those responsible, and all within the space of a few days. Others were probably more interested in more detailed technical aspects of optical and detector systems, mechanics, software, operations or system engineering and management (a big theme for synergy between ground and space) or discussing directly with the authors of posters over a glass of wine.

Despite the range and high quality of the programme itself, I would also not be surprised if most people still got more practically out of the numerous organised or impromptu side meetings and personal contacts which these symposia foster. A classic I attended myself was a meeting of the informal 8-m club, formed many years ago to facilitate exchanges of technical information and experience amongst the VLT, Gemini, Keck and SUBARU projects. Rather than telescopes, this time it was mostly second-generation instrumentation, adaptive optics and laser talk.

The next meeting in this series will be held in June 2010 in San Diego, California, which I am sure will again attract a substantial number of ESO staff.

Photo: H. Boffin, ESO

Figure 2. Tim de Zeeuw, Director General of ESO, delivering his plenary talk "European perspectives for ground-based astronomy".

In Memoriam Bengt Westerlund

John Danziger[1]
Jacques Breysacher[2]

[1] Osservatorio Astronomico di Trieste, Italy
[2] Saubion, France

Photo: E. Maurice, ESO Historical Picture Archive

Bengt Westerlund, pictured second from left, at a *despedida* (farewell party) at the Pelícano Camp in May 1970.

Bengt Westerlund, who died on 4 June, 2008 began his astronomical career in Sweden where he was born in 1921. He received his PhD in astronomy from the University of Uppsala in 1954 and spent most of the subsequent years, until 1967, at Mt. Stromlo Observatory, Australia, where he was first the Uppsala Schmidt Observer and an Honorary Fellow at the Australian National University (ANU), then becoming in 1958 Reader in Astronomy at the ANU. In 1967 he took a position as Professor of Astronomy at Steward Observatory where Bart J. Bok had become director. In 1969 he was appointed Director of ESO in Chile, which position he held until 1975 when he returned to Sweden to take up the position of the Professor of Astronomy at Uppsala Observatory, retiring in 1987.

His career was devoted to observational astronomy and his work on the structure of the Milky Way and the Magellanic Clouds earned respect and appreciation amongst his colleagues. Within those broad categories he contributed significantly to studies of clusters, stellar populations, carbon stars, planetary nebulae, WR stars, diffuse interstellar bands, luminous stars, stellar classification, and supernova remnants. Beyond these he also published papers on dwarf spheroidals, emission-line galaxies and radio galaxies. In this work, at Mt. Stromlo, Steward Observatory and at ESO in Chile, he was always successful in engaging the interest and participation of students, a number of whom produced high-quality theses under his supervision. Also Bengt was always a keen organiser and participant in international meetings.

The years in Chile were not always easy because of the political turmoil culminating in the violent military coup in 1973. Bengt Westerlund handled these matters in his usual quiet diplomatic manner, so that the life and functioning of ESO Chile was scarcely affected by the surrounding events. The growth of ESO Chile during his time also created additional managerial responsibilities which Bengt handled in his customary calm manner. After his departure from ESO he served for eight years on the OPC, four years of which were as chairman of that important committee.

In whatever ambience Bengt Westerlund worked, he was known for his unfailing courtesy, gentleness, consideration and generosity. People at all levels in ESO and elsewhere remember and still appreciate these characteristics. He was not only sociable but above all a gentleman's gentleman. Bengt Westerlund is survived by his wife Vivi, a constant companion, and his two children Carl Gunnar and Gunilla Margareta.

Do you know your Solar System? Children in Garching do!

Florian Kerber, Reinhard Hanuschik, Harald Kuntschner
ESO

Complaints about real and perceived shortcomings of the educational system are commonplace. There is also no shortage of well-intentioned suggestions and ideas from all parties involved. But what about some hands-on action? What do you do if you want to try out something new now? The Grundschule Ost (East Junior School) in Garching felt they wanted to dip their toes into astronomy for their project days this year. They decided to contact an expert resource nearby and do this jointly with ESO. Or as the school's choir put it:

"Wie kann man über den Weltraum was lernen?
Danke, danke, das sagen wir heut'!
Zum Glück gibt's die ESO und die hilft uns dabei gerne!
Danke, danke, das sagen wir heut'!"

"How can we learn more about space?
Thanks, thanks we're saying today.
Fortunately ESO's ready to help.
Thanks, thanks we're saying today."

This process was simplified by the fact that there is an overlap between ESO staff and the school's parents and parents council, but this is by no means essential. It is essential though to set a clear and agreed goal for the project. The ESO team was formed by the ESO scientists Reinhard Hanuschik, Florian Kerber and Harald Kuntschner. Katjuscha Lockhart from ESO Human Resources coordinated all activities with the school. We took the children on a tour of the Solar System with a series of talks – one for each grade – and then let the school take over to build a scale model of the Solar System's planets for the school yard.

Photo: E. Janssen, ESO

Figure 1. Presentation by Florian Kerber from ESO to schoolchildren at the Grundschule Ost in Garching.

The four presentations (see Figure 1) given by us featured a trip with a 'pedestrian rocket' indicating that an effort of mind is needed to make this phantasy journey covering the sun and planets, including an express return to Earth using a comet. We set out to convey some of the fundamental concepts: where do light and warmth come from; why do we have day, night and year; why are some planets rocky and some gaseous; but tried to stay clear of too many numbers. Some numbers though can be brought to life in an intriguing way. The distance between Sun and Earth is often made more tangible by giving the light travel time of 8.3 min. We learned that kids were a lot more excited about another comparison: a racing car at 300 km/h will take about 57 years (neglecting pit stops) to travel the distance, which means that its young driver will have reached grandparents age when he or she arrives. Some children were quick to point out that this doesn't work anyway because the sun is too hot. The talks contained plenty of nice pictures and a few animations but didn't try to compete with video games. It turns out it is still quite easy to focus children's attention for a full 60 minutes if you make sure to get them involved by asking plenty of questions – they'll respond with more and more – and repeating one or two key messages as a chorus: such as "What's the big difference between the sun and the planets? The Sun makes light of its own, the planets don't." About 75 pupils (three classes per grade) attended each talk in the school atrium. The presentations were meant to capture the children's attention and focus their enthusiasm towards the goal of learning more, and of jointly building the scale models of the planets.

Various activities in the classroom followed and then, under the able guidance of the handicraft teacher, the miniature Solar System became a reality. Two different scales were used – one for the distances from the sun and the other for the physical size of the planets. Here ESO scientists only provided the necessary factual information, but the actual implementation was fully in the hands of the school and they did a marvelous job. Everything came to fruition on 24 July when the Planetenweg was inaugurated in the school yard. Planet by planet it grew outward accompanied by songs and a verbal fact sheet presented by the children for each planet. A good crowd of parents, siblings and grandparents attended the event and the local media was present as well. A colour picture of two small children carrying Saturn to its slot graced the title page of the local section of the *Süddeutsche Zeitung*, the renowned south German newspaper. Another picture, this time documenting two of the authors carrying Jupiter (see the Astronomical News section page, lower image), highlighted the local *Garchinger Stadtanzeiger* (Garching town gazette).

The ESO 'godfathers' were honoured during the ceremony with a certificate, but the greatest reward clearly was to witness the enthusiasm of the children and the insight they have gained. It was very impressive to see what can be achieved when effort and creativity from various sources come together. It was gratifying that the pupils acted as teachers themselves when they presented the Solar System to kindergarden pupils the next day.

Still concerned about the school system and the education of our children? If you want to try something different in school next year why not contact your expert resource near-by.

Acknowledgements

We thank all children, teachers and parents who made this project a success. Special thanks go to Frau Streidl (head), Frau Werner (deputy head), Frau Suffa-Hänsel (handicrafts teacher) and Frau Gehring (choir leader). Financial support (material for planets) by ESO's Outreach Department is also gratefully acknowledged.

Lights, Camera, Astronomers! Media training at ESO Chile

Gonzalo Argandoña, Michael West
ESO

Photo: G. Argandoña, ESO

Figure 1. ESO Chile Fellow Ezequiel Treister (centre), is interviewed by Chilean journalists Valeria Foncea (left) and Marie Claire Dablé (right) as part of the media training workshop held at ESO offices in Santiago.

Communicating astronomy with the public is an important part of ESO's mission. The Office for Outreach plays a leading role in this endeavour, bringing many exciting discoveries in frontline research to a worldwide audience. ESO astronomers are also a key component of this collective effort: they are the faces behind the discoveries, and often eloquent spokespersons for astronomy.

Almost every week, a wide range of journalists visit ESO sites in Chile to produce stories that inform the public in Europe and beyond, reaching millions of people through television, film documentaries, written media and the internet. Naturally, many of these stories feature ESO staff in action.

Yet most astronomers have had little or no training on how to communicate effectively with the public through the media. Consequently, many are uncomfortable giving interviews, or talk in a way that is difficult for non-scientists to understand.

To help ESO Chile astronomers become better science communicators, the Office for Outreach in Chile and the Office for Science in Chile have organised several media training workshops for staff astronomers and fellows in Santiago. These day-long workshops, which are voluntary, were led by Marie Claire Dablé, a journalist from the Pontificia Universidad Católica de Chile and director of a local multimedia company, and the prize-winning television reporter Valeria Foncea from Chile's TVN, as well as ESO Chile's public outreach team. Nicolas Luco, science editor of El Mercurio, Chile's largest newspaper, also joined the participants for lunch to provide insights into what makes a good science story.

The training workshops begin with a short introduction to the media, presenting practical tips on how to handle interviews, followed by a look at some real examples of astronomers interacting with journalists, extracted from recent news reports and documentaries. There is a strong emphasis on television, given the popularity of this medium. According to the special Eurobarometer survey conducted in 2007, the most trusted source of information on scientific research for citizens in the European Union is still television (68 %), followed by newspapers (41 %), radio (26 %) and internet (23 %).

The second part of the workshop is entirely practical. Astronomers put themselves in front of the camera and under the lights to practise a series of basic interview skills: strategies to stay focused on their main message; bridging techniques to come back to their 'comfort zone'; the avoidance of jargon; and the use of analogies and metaphors to connect with the audience (see Figure 1). These interviews are filmed and reviewed afterwards by the participants, which allows for rich group discussion.

ESO Chile astronomers and fellows who participated in the media training workshops (see the Astronomical News section page, upper image) offered to date have been unanimous in their opinion that it was a very informative and fun experience. As one staff astronomer said after completing the workshop: "That was fantastic! I learned a lot and feel more confident dealing with journalists."

The response from ESO Chile astronomers has been so enthusiastic that additional workshops are being organised for those who were unable to take part in the first sessions. More advanced media training will also be offered in the future, touching on such topics as non-verbal communication, how to deal with anxiety when speaking in public, and strategies for effective presentations.

"It is the responsibility of every practising astronomer to play some role in explaining the interest and value of science to our real employers, the taxpayers of the world."

IAU Division XII, Commission 55 on "Communicating Astronomy with the Public"

Social Engagement at ESO

Michael Böcker
ESO

In 2007 a presentation was made to the Lebenshilfe Freising e.V. *(www.lebenshilfe-fs.de)* on the scientific, as well as technical, challenges facing staff working at the ESO observatories in Chile. The non-profit organisation Lebenshilfe e.V. is a social establishment with the organisational goal to promote the development of people with disabilities. This year seven students and two lecturers from the Lebenshilfe e.V. were invited to a presentation at ESO headquarters about the Solar System given by Martin Kümmel (from ST-ECF). As a practical highlight for the students, Gerardo Avila from the ESO Instrumentation Division offered a view of the Sun through the telescope of the AGAPE amateur astronomer's association at ESO headquarters. The young adults, pictured in the figure above, very much appreciated the informative and interesting afternoon organised by ESO for the end of their school education.

Photo: E. Janssen, ESO

A group of young people from the Lebenshilfe Freising e.V., together with Michael Böcker and Martin Kümmel from ESO, in front of the AGAPE telescope in Garching.

New Staff at ESO

Antoine Mérand

I grew up in France, where clouds and light pollution rule the sky. My native region (Vendée) in the west, by the Atlantic Ocean, is no exception. I was led to astronomy at a young age by an uncle who always dreamt about being an astronomer. I received books from him and I clearly remember not seeing Halley's comet through his telescope, in 1986. I was seven years old.

Nevertheless, I bought a telescope as a teenager, and enjoyed too few clear nights, star hopping for the brightest celestial wonders. As a result of the cloudy skies, I started to develop a strong interest in the telescope itself: how it works, how it forms an image, how to align it in order to get the nicest image. I ended up mostly using my telescope to look at non-celestial sources (including street lights).

After high school, I mostly studied mathematics, theoretical physics and computer science. What I enjoyed most were optics and computer science classes, and whatever in maths and physics that related to optics and computers. I moved to Paris, to attend the physics school *École Normale Supérieure* (ENS). There, I had my first astronomy class, taught at that time by the renowned astrophysicist Pierre Léna. Part of the curriculum at the ENS involved a research project lasting six months. Mine was suggested by Pierre Léna: to work with Steve Ridgway in Tucson (Arizona) on the interpretation of optical interferometry observations of Mira stars. That was my first contact with astronomy, and I was hooked. Everything was enchanting: optical interferometry is complicated and intricate, but I was working first-hand on data very few understood, and the people I worked with were kind, stimulating and challenged me like never before. Arizona was also one of the best places for astronomy and for an amateur the skies were splendid. Using binoculars I saw more globular

clusters or galaxies than I ever saw with my 15-cm telescope in France.

The next step was my PhD project. During my stay in Arizona, I visited an optical interferometer with Steve, the CHARA Array, atop Mount Wilson, in California. My project was to install at CHARA a fibre-fed optical beam combiner named FLUOR, developed at Paris Observatory by Vincent Coudé du Foresto and Guy Perrin. Between 2002 and 2005, I indeed installed the beam combiner (which had previously been at the IOTA interferometer in Arizona) and observed Cepheid variable stars in order to measure their diameter change during pulsation. Using the parallax of pulsation method, I was able to obtain one of the most precise distances to a Cepheid (to about 1 %). In 2006 I moved from Paris to Pasadena, California, to work full time at the CHARA Array, as a research associate. There, I supported FLUOR observations and participated in the instrumental developments. In particular, with Michael Ireland (from Caltech, now at Sydney University in Australia), we built a three-telescope visible beam combiner, PAVO. I also continued my observations of Cepheids, and extended my interests to the close environments of stars, to stellar companions and rotation.

Always in search of challenges (and new horizons), I joined ESO in 2008, as an operations astronomer for the VLTI, the interferometric mode of the VLT. I am very excited by the VLT, whose level of organisation and efficiency are entirely new to me. I have already started to get deeply involved with the VLTI, taking the freshly vacant AMBER instrument scientist position. I am looking forward to developing the VLTI, especially the forthcoming astrometric mode (using PRIMA) and the second-generation instruments, which will offer possibilities never seen before in interferometry.

Martin Zwaan

Not entirely new to ESO, I took up my position as astronomer in the ALMA Regional Centre (ARC) in February this year. As a fellow I had been enjoying working at ESO for several years already. During that time I got involved in ALMA and saw the project developing from the ground-breaking in late 2003 to construction being well underway now, with nine antennas in Chile. I am very pleased to continue working on ALMA, as one of the first staff in the ARC.

The ARC is part of the Data Management and Operations division and therefore builds on ESO's long history of operating large facilities. In many ways, our tasks are comparable to those of the User Support Department, with the important difference that ALMA is not yet a fully functioning telescope. In the near future my tasks will concentrate on maximising the scientific return of ALMA. In practice, this will entail helping ALMA users with their proposal preparation and the execution of their projects, and assisting with their data reduction. In the operations stage I will also travel to Chile on a regular basis to serve as astronomer on duty. Of course, all ARC tasks will be executed in collaboration with our colleagues in the US, East Asia and Chile. While only a small department at present, the ARC will continue to grow consistently over the next few years.

At present, in the pre-operations stage, we are not just waiting idly for ALMA to start working. One of our main tasks is ensuring the user software will be ready for ALMA operations. For example, the software package CASA, which will be the data reduction system for all ALMA data and will also form the backbone of ALMA's data reduction pipeline, is currently being extensively tested. To build up experience and identify missing functionality, I have also been using CASA for my personal research, reducing data from different radio telescopes. As of next year, I will be spending time at the ALMA site in northern Chile helping with commissioning and science verification.

My personal research concentrates on the role of gas in galaxy evolution. I am interested in studying how the Universe's neutral gas content evolves over time. Specifically, I try to reconcile what we know from radio emission in the present-day Universe with results from absorption lines originating in the much younger Universe. Of course, ALMA will produce data allowing tremendous advances in the study of neutral gas in galaxies at high- and low-redshifts, and I am very much looking forward to seeing the instrument delivering these data.

Fellows at ESO

Vincenzo Mainieri

I did my undergraduate studies in physics at the University of Rome and at that time I was not particularly interested in astronomy, but more in particle physics. I finally got interested in those shining objects up there when a friend showed me Jupiter using a small amateur telescope from the balcony of a flat in Rome, trying to find some clear sky between the buildings.

When I started a PhD in physics in Rome in 2000, I wanted to spend a period abroad and came to ESO for a short visit of two months. It was the right move at the right time. Thanks to my supervisor, Piero Rosati, I was introduced to the X-ray survey community and at that time the deep X-ray surveys with Chandra and XMM-Newton were starting and new science was available. I was able, during my thesis, to study, with unprecedented photon statistics, the X-ray spectral properties of active galactic nuclei (AGN).

I found the ESO environment and the campus in Garching a very stimulating place to work. So much so that after my PhD I decided not to move far, but simply to cross the street to the Max-Planck-Institut für Extraterrestrische Physik. There I was part of the X-ray group led by Günther Hasinger. I participated in the multi-wavelength follow-up studies of several of the major X-ray surveys, trying to understand the evolution, as a function of redshift and environment, of the properties of AGN. In the last few years I have been widening my interests – moving to the optical, infrared, submillimetre, and finally radio, bands. I was quite happy in September 2006 to cross the street once more and come back to ESO as a Fellow. During these two years of the fellowship I have been studying how the luminosity of an AGN affects its geometry and how these properties are connected with the host galaxy.

For my functional duties, I am following-up the science cases for a multi-IFU spectrograph for the E-ELT and am also participating in the preparations for the X-shooter commissioning.

After two very enjoyable and useful years as a fellow, I am looking forward to the next step – as an Assistant Astronomer in the User Support Department, where I will start working in October.

Suzanna Randall

According to my parents, my fascination with astronomy started when I was just a toddler, and would not stop staring at the Moon. My own first astronomical recollection is seeing photos of Mars' moons taken by some satellite – I was about seven years old and completely fascinated by the notion that a camera could have left Earth, let alone send back pictures of what to me seemed the most exotic and remote place imaginable. For years I collected pretty pictures of galaxies, nebulae and planets and occasionally braved the cold to observe stars in our back garden with my binoculars, only to all but forget about astronomy as a teenager.

However, upon finishing school I remembered my childhood passion and decided to move from small-town Germany to the bustling metropolis of London to study Astronomy at UCL. During my studies I had the opportunity to observe at several different observatories, and was hooked on both astronomy and travelling. I was then accepted for a PhD at the University of Montreal, apparently on the premises that my supervisor had "never had a student from the UK before". Focusing on the asteroseismology of pulsating subdwarf B stars, I had more than my fair share of observing, spending five weeks at a time at the 1.5-m on Mt. Bigelow in Arizona.

Eager to move to bigger telescopes, I applied to ESO as a Fellow, and with perfect timing received an offer the day before defending my thesis in Montreal. While I am stationed in Garching, my functional duties regularly take me to Paranal, where I work as a support astronomer at the VLT. For me, this is one of the most exciting aspects of my job, as I feel that I am at the forefront of astronomical research, and work with people from around the world in a unique and dynamic environment.

Announcement of the Joint ESO, CTIO, ALMA/NRAO and Universidad Valparaíso Workshop

The Interferometric View on Hot Stars

2–6 March 2009, Viña del Mar, Chile

One of the research fields in which interferometry excels has turned out to be hot star astrophysics. New results have often been quickly adopted by the community, providing important quantitative constraints in frontline research topics:
– Several hot stars have been shown to be very rapidly rotating, in a regime where geometric deformation and gravity darkening become important.
– Stellar winds have been resolved, like those of η Carinae and Wolf-Rayet stars.
– Circumstellar discs have been observed across a wide range of phenomena, such as gaseous accretion discs around young Herbig stars, decretion discs around Be stars, and dusty discs around B[e], and also Herbig, stars.

While some of these results, like the critical rotation of Achernar and other stars, were a complete surprise, others, like the prolate wind of η Carinae, have been anticipated by theoretical research, but were hardly expected in the clear and unambiguous form in which they were finally observed.

The meeting aims at bringing together both hot star and interferometry expertise, both observationally and theoretically, to review the progress made, as well as to outline current problems in hot star research that are expected to benefit most from interferometric observations.

Oral sessions during the meeting will be held on:
– High angular resolution techniques;
– The stars (including Cepheids);
– Stellar winds;
– Circumstellar discs;
– Hot binaries;
– Explosive stars;
and a poster session is foreseen.

Confirmed speakers include: Alex Carciofi, Olivier Chesneau, Asif ud-Doula, William Hartkopf, Stefan Kraus, Ronald Mennickent, Antoine Mérand, Georges Meynet, Florentin Millour, Coralie Neiner, Stan Owocki, Jayadev Rajagopal, Markus Schöller, Nathan Smith and Christopher Tycner.

On the Thursday and Friday before the meeting (26–27 February 2009), an interferometry primer will be held, mainly intended for students, but open to all workshop participants, provided there is enough space. The scope of the primer is to enable attendants without experience in interferometry to develop the first steps at judging the results presented during the meeting and thus develop ideas for discussion at the meeting. This primer will take place at ESO's premises in Vitacura, Santiago, and confirmed lecturers include: Andreas Quirrenbach, Olivier Chesneau, Markus Schöller, Antoine Mérand, Carla Gil, and Jean Baptiste Le Bouquin.

The workshop will take place in Viña del Mar, on the Pacific coast of Chile, about 100 km west of Santiago. Viña is famous as a holiday resort well beyond Chile. Since the meeting will take place just after the end of the Chilean holiday season, most of the tourist crowds will have returned home, but pleasant coastal weather is expected. Located just south of Viña del Mar across the city border is Valparaíso, one of Chile's most important harbours and a UNESCO world heritage site for its historical importance, natural beauty, and unique architecture.

For further information on the workshop, please refer to *http://www.eso.org/sci/meetings/IHOT09/* or contact *ihot09@eso.org*.

The registration deadline is 17 December 2008.

The Scientific Organising Committee consists of: Olivier Chesneau, Michel Curé, Doug Gies, Christian Hummel, Stan Owocki, Andreas Quirrenbach, Thomas Rivinius, Markus Schöller and Gerd Weigelt.

Paranal observatory by moonlight.

Photo: T. Rivinius, ESO

Announcement of the ESO Workshop on

ALMA and ELTs: A Deeper, Finer View of the Universe

24–27 March 2009, ESO Headquarters, Garching, Germany

The next two decades of ground-based astronomy will be dominated by the Atacama Large Millimetre/submillimetre Array (ALMA) and the advent of giant optical/near-infrared telescopes: the Giant Magellan Telescope (GMT); the US Thirty Meter Telescope (TMT); and the European Extremely Large Telescope (E-ELT).

The main goal of the workshop is to bring together the ALMA and ELT communities, to identify the common science cases and to outline instrumentation/upgrade priorities for the ALMA and ELT facilities in order to support these programmes.

The product of the workshop will be a report (rather than proceedings). The report will, on the one hand, present the common science cases in the areas of:
– fundamental physics, cosmology, and relics of the early Universe;
– galaxy and ISM evolution;
– star formation from re-ionisation to the present;
– Solar Systems near and far.

On the other hand, the report will identify upgrade paths for ALMA and instrument priorities for the ELTs. The conclusions will be used as feedback to the ALMA science group investigating science with ALMA in the 2020 era, and to the instrumentation plans of the various ELTs.

The workshop is jointly organised with representatives of all ALMA partners and ELT projects. Thus, we believe that the workshop will become an international milestone for all projects concerned.

Science Advisory Committee:
Jose Afonso (Observatorio Astronomico de Lisboa/ALMA), Andrew Blain (Caltech/ALMA), Roberto Gilmozzi (ESO/E-ELT), Richard Hills (ESO/ALMA), Rolf Kudritzki (Institute for Astronomy, University of Hawaii/Giant Segmented Mirror Telescope (GSMT)), Patrick McCarthy (Carnegie Observatories/GMT), Koh-Ichiro Morita (National Radio Astronomy Observatory (NRAO)/ALMA), Stephen A. Shectman (Carnegie Observatories/GMT), David Silva (National Optical Astronomy Observatory (NOAO)/GSMT), Chuck Steidel (Caltech/TMT), Al Wootten (NRAO/ALMA).

Local Organising Committee:
Annalisa Calamida, Markus Kissler-Patig, Christina Stoffer, Leonardo Testi.

The deadline for registration is 15 December 2008.

More information can be found at *http://www.eso.org/almaelt2009*.

One of the two ALMA transporters (Lore) is shown being used to move one of the Vertex antennas from inside the assembly building to an outside pad within the contractor area at the Operations Support Facility (OSF). This photograph was taken in June 2008. The Vertex antenna is currently undergoing pre-acceptance tests.

Personnel Movements

Arrivals (1 July–30 September 2008)

Europe	
Aller Carpentier, Emmanuel (E)	Optical Engineer
Beniflah, Thierry (F)	Head of Information Technology
Blondin, Stéphane (F)	Fellow
Calamida, Annalisa (I)	Postdoctoral Researcher
Ciattaglia, Emanuela (I)	Mechanical Engineer
Feng, Lu (CN)	Student
Gladysz, Szymon (PL)	Postdoctoral Researcher
Heckel, Isabell (D)	Administrative Assistant/Secretary
Kammermaier, Katharina (D)	Human Resources Officer
Kolb, Johann (F)	Optical Engineer
Kupcu Yoldas, Aybuke (TR)	Postdoctoral Researcher
Michaleli, Anna (GR)	Human Resources Officer
Mysore, Sangeeta (USA)	Operations Support Scientist
Nunez Santelices, Carolina Andrea (RCH)	Student
Penuela, Tania Marcelo (CO)	Student
Petry, Dirk (D)	Data Analysis Software Developer
Ricci, Luca (I)	Student
Sirey, Rowena (GB)	Senior Advisor/Intern. Relations
Chile	
Al Momany, Yazan (I)	Operations Astronomer
Aranda, Ivan (RCH)	Data Handling Administrator
Arias, Pablo (RCH)	Telescope Instruments Operator
Campos, Marcela (RCH)	Accountant
Elao, Cristian (RCH)	Electronic Engineer
Gallardo, Javier (RCH)	Software Engineer
Gesswein, Rodrigo (RCH)	Data Handling Administrator
Gonzalez, Javier Andres (RCH)	Maintenance Mechanical Technician
Lucas, Robert (F)	Astronomer
Mauersberger, Rainer (D)	Astronomer
Molina, Faviola (VE)	Operations Astronomer
Parra, Rodrigo (RCH)	Operations Astronomer
Reyes, Claudia (RCH)	Telescope Instruments Operator
Tamblay, Richard (RCH)	Maintenance Mechanical Technician
Wieching, Gundolf (D)	Radio Frequency Engineer
Yegorova, Iryna (UA)	Fellow

Departures (1 July–30 September 2008)

Europe	
Alves de Oliveira, Catarina (P)	Student
Boutsia, Konstantina (GR)	Student
da Silva Marques, Nuno Alvaro (P)	Student
Di Cesare, Stéphane (F)	Software Engineer
Hötzl, Stefan (D)	Electronics Technician
van der Plas, Gerrit (NL)	Student
Chile	
Bendek, Eduardo (RCH)	Instrumentation Engineer
Carry, Benoît (F)	Student
Dierksmeier, Claus (D)	Civil Engineer
Lombardi, Gianluca (I)	Student
Lopez, Cristian (RCH)	Student
Lynam, Paul (GB)	Fellow
Marin, Pedro (RCH)	Driver
Rantakyrö, Fredrik (S)	VLTI Astronomer
Reveco, Johnny (RCH)	Software Engineer
Salazar, Daniel (RCH)	Software Engineer

Announcement of the Report by the ESA-ESO Working Group on

Galactic Populations, Chemistry and Dynamics

Authors:
Catherine Turon (Chair), Francesca Primas (Co-chair), James Binney, Cristina Chiappini, Janet Drew, Amina Helmi, Annie Robin, Sean Ryan.

Abstract:
Between the early 40s, when Baade showed the first evidence for the existence of two distinct stellar populations, and today, with our Galaxy surprising us with new substructures discovered almost on a monthly basis, it is clear that a remarkable progress has been achieved in our understanding of the Galaxy, of its structure and stellar populations, and of its chemical and dynamical signatures. Yet, some questions have remained open and have proven to be very challenging.

The main task of this Working Group has been to review the state-of-the-art knowledge of the Milky Way galaxy, to identify the future challenges, and to propose which tools (in terms of facilities, infrastructures, instruments, science policies) would be needed to successfully tackle and solve the remaining open questions. Considering the leadership position that Europe has reached in the field of Galactic astronomy (thanks to the Hipparcos mission and the Very Large Telescope) and looking at the (near-)future major initiatives it has undertaken (VISTA and VST survey telescopes, Gaia mission), this work clearly has been very timely.

It is of uttermost importance for European astronomy to keep and further consolidate its leading position. This Working Group has made recommendations that would allow dissecting our backyard laboratory, the Galaxy, even further. ESO survey telescopes about to become operational and the upcoming ESA Gaia mission are a guarantee for opening new horizons and making new discoveries. We, the astronomers, with the support of our funding agencies, are ready to fully commit to the best exploitation of the treasure that is ahead of us. The main recommendations this Working Group has made to ESA and ESO are to guarantee the expected tremendous capabilities of these new facilities, to vigourously organise their synergies and to jointly give ways to European astronomers to be leaders in the exploitation of their output data.

The report is available at *http://www.stecf.org/coordination/eso-esa/galpops.php.*

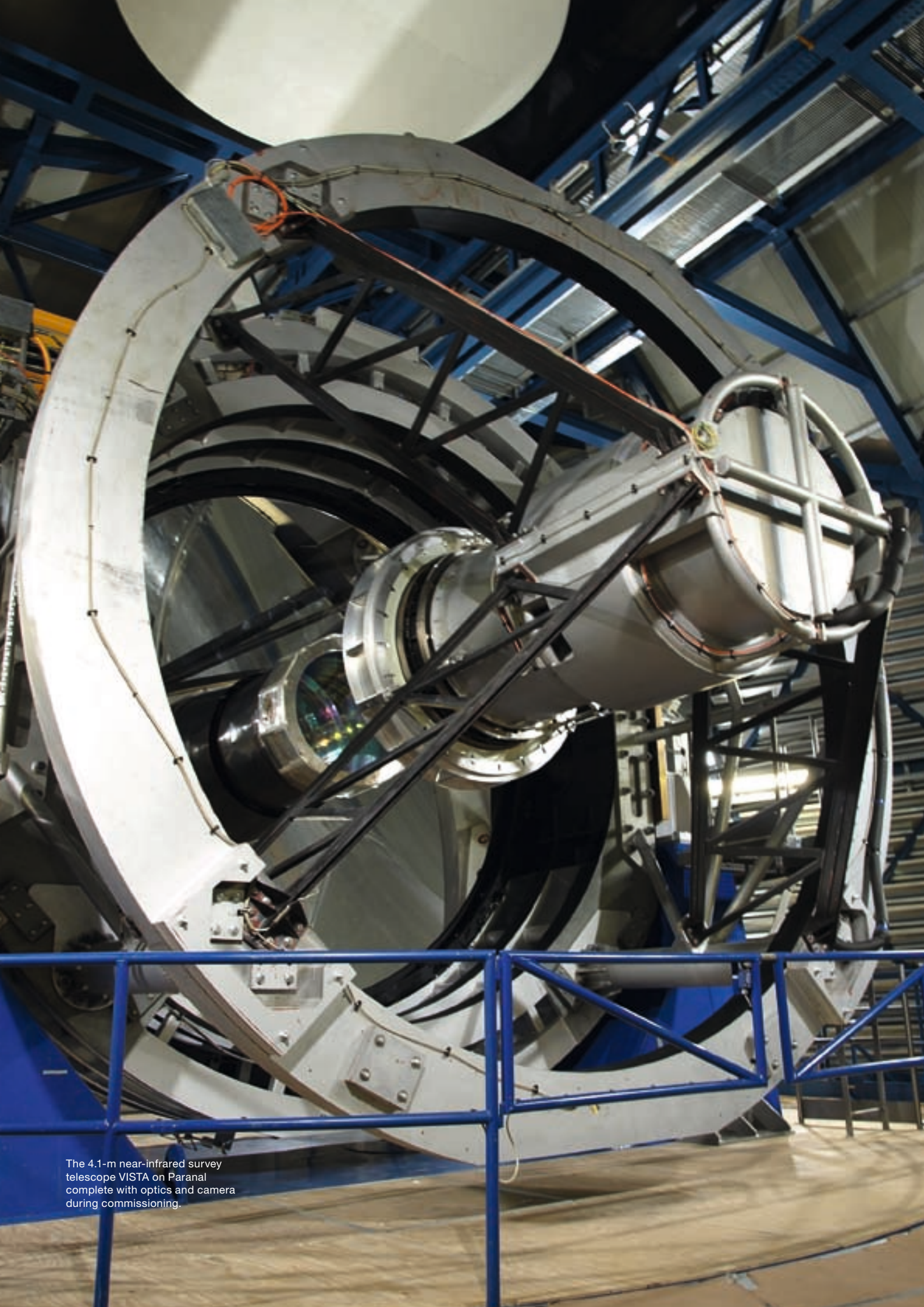

The 4.1-m near-infrared survey telescope VISTA on Paranal complete with optics and camera during commissioning.

ESO is the European Organisation for Astronomical Research in the Southern Hemisphere. Whilst the Headquarters (comprising the scientific, technical and administrative centre of the organisation) are located in Garching near Munich, Germany, ESO operates three observational sites in the Chilean Atacama desert. The Very Large Telescope (VLT), is located on Paranal, a 2 600 m high mountain south of Antofagasta. At La Silla, 600 km north of Santiago de Chile at 2 400 m altitude, ESO operates several medium-sized optical telescopes. The third site is the 5 000 m high Llano de Chajnantor, near San Pedro de Atacama. Here a new submillimetre telescope (APEX) is in operation, and a giant array of 12-m submillimetre antennas (ALMA) is under development. Over 2 000 proposals are made each year for the use of the ESO telescopes.

The ESO Messenger is published four times a year: normally in March, June, September and December. ESO also publishes Conference Proceedings and other material connected to its activities. Press Releases inform the media about particular events. For further information, contact the ESO Public Affairs Department at the following address:

ESO Headquarters
Karl-Schwarzschild-Straße 2
85748 Garching bei München
Germany
Phone +49 89 320 06-0
Fax +49 89 320 23 62
information@eso.org
www.eso.org

The ESO Messenger:
Editor: Jeremy R. Walsh
Technical editor: Jutta Boxheimer
Technical assistant: Mafalda Martins
www.eso.org/messenger/

Printed by
Peschke Druck
Schatzbogen 35
81805 München
Germany

ISSN 0722-6691

Contents

Front Cover Picture: Artist’s impression by Herbert Zodet of a possible design for the E-ELT dome. In order to house the 42-m telescope, the dome will be approximately 90 m in diameter and height.